Geochemistry and Petrogenesis of the McElroy and Larder Lake assemblages, Abitibi Greenstone Belt, Northeastern Ontario

by

Christopher T. Kimmerly, B.Sc.

A Thesis

submitted to the Department of Geological Sciences

in partial fulfillment of the requirements

for the degree of

Master of Science

September 1992

Brock University

St. Catharines, Ontario

Abstract

The McElroy and Larder Lake assemblages, located in the southern Abitibi Greenstone Belt are two late Archean metavolcanic sequences having markedly contrasting physical characteristics and are separated from one another by a regional fault. An assemblage is an informal term which describes stratified volcanic and/or sedimentary rock units built during a specific time period in a similar depositional or volcanic setting and are commonly bounded by faults, unconformities or intrusions. The petrology and petrogenesis of these assemblages have been investigated to determine if a genetic link exists between the two adjacent assemblages.

The McElroy assemblage is homoclinal sequence of evolved massive and pillowed flows, which except for the basal unit represents a progressively fractionated volcanic pile. From the base to the top of the assemblage the lithologies include Fe-tholeiitic, dendritic flows; komatiite basaltic, ultramafic flows; Mg-tholeiitic, leucogabbro; Mg-tholeiitic, massive flows and Fe-tholeiitic, pillowed flows. Massive flows range from coarse grained to aphanitic and are commonly plagioclase glomerophyric. The Larder Lake assemblage consists of komatiitic, Mg-rich and Fe-rich tholeiitic basalts, structurally disrupted by folds and faults. Tholeiitic rocks in the Larder Lake assemblage range from aphanitic to coarse grained massive and pillowed flows. Komatiitic flows contain both spinifex and massive textures.

Geochemical variability within both assemblages is attributed to different petrogenetic histories. The lithologies of the McElroy assemblage were derived by partial melting of a primitive mantle source followed by various degrees of crystal fractionation. Partial melting of a primitive mantle source generated the ultramafic flows and possibly other flows in the assemblage. Fractionation of ultramafic flows may have also produced the more evolved McElroy lithologies. The highly evolved, basal, dendritic flow may represent the upper unit

of a missing volcanic pile in which continued magmatism generated the remaining McElroy lithologies. Alternatively, the dendritic flows may represent a primary lava derived from a low degree (10-15%) partial melt of a primitive mantle source which was followed by continued partial melting to generate the ultramafic flows. The Larder Lake lithologies were derived by partial melting of a komatiitic source followed by gabbroic fractionation.

The tectonic environment for both assemblages is interpreted to be an oceanic arc setting. The McElroy assemblage lavas were generated in a mature back arc setting whereas the Larder Lake lithologies were produced during the early stages of komatiitc crust subduction. This setting is consistent with previous models involving plate tectonic processes for the generation of other metavolcanic assemblages in the Abitibi Greenstone Belt.

Ackowledgements

I would to thank Dr. Greg Finn for supervising, supporting and showing patience while this thesis developed. I benefited greatly from discussions and suggestions with Dr. Wayne Jolly and Dr. Frank Fueten.

Dr. Steve Jackson of the Ontario Geological Survey initially suggested that studying rocks in the Larder Lake area could be a good project (and he was right). His suggestions and discussions were also valuable. Lori Wilkinson, Seppo Kakko, Elaine Lau, in 1990, and Mike Johnston, in 1991, helped in the field and made bashing through the bush a little more bearable.

Dan Redmond, co-founder of the Precambrian Think-Tank, was a great office partner. Mike Lozon was very helpful when it came to advice in the generation of figures (especially with AutoCAD). Candy Kramer produced good thin sections. Geochemical analyses were conducted at the OGS Geoscience Laboratories and the Memorial University of Newfoundland.

Financial support from an Ontario Graduate Scholarship in 1991 and an N.S.E.R.C. scholarship in 1992 is greatfully acknowledged. A Lithoprobe grant supported field expenses in 1992.

Finally, many thanks go to my family for their support and understanding.

Table of Contents

List of Figures

List of Tables

List of Appendices

Chapter 1

Introduction

1.1 Introduction

Over 50 per cent of the Earths' history is represented by rocks which yield ages greater than 2.5 billion years. These Archean lithologies are exposed on all continents. They also act as basement rocks over which younger lithologies now lie. In addition, Archean rocks host many mining regions of both base and precious metals. Therefore, it is fruitful to understand Archean lithologies from a scientific and an economic view. This study compares the petrology and petrogenesis of two Late Archean metavolcanic assemblages in the Larder Lake area of the Abitibi Greenstone Belt.

1.2 Regional Geology

The Abitibi Subprovince is the largest granite-greenstone subprovince in the Superior Province of the Canadian Shield (Figure 1-1). It is approximately 800 km long by 240 km wide. The subprovince consists of several greenstone belts which contain low grade metavolcanic, metasedimentary and granitic rocks (Card 1990). The Abitibi Greenstone Belt is the largest greenstone belt and has been subdivided into northern and southern volcanic zones (Dimroth et al. 1982). The older northern volcanic zone consists of basaltic to andesitic calc-alkaline volcanic rocks which have generally been metamorphosed to higher metamorphic grades than the southern volcanic zone. The southern zone contains more tholeiitic to komatiitic rocks. Intrusive rocks in both volcanic zones include tonalite-trondhjemite-granodiorite, however the southern volcanic zone contains fewer intrusions. The northern zone has large gabbro anorthosite intrusions which are absent in the southern zone (Dimroth et al. 1983a).

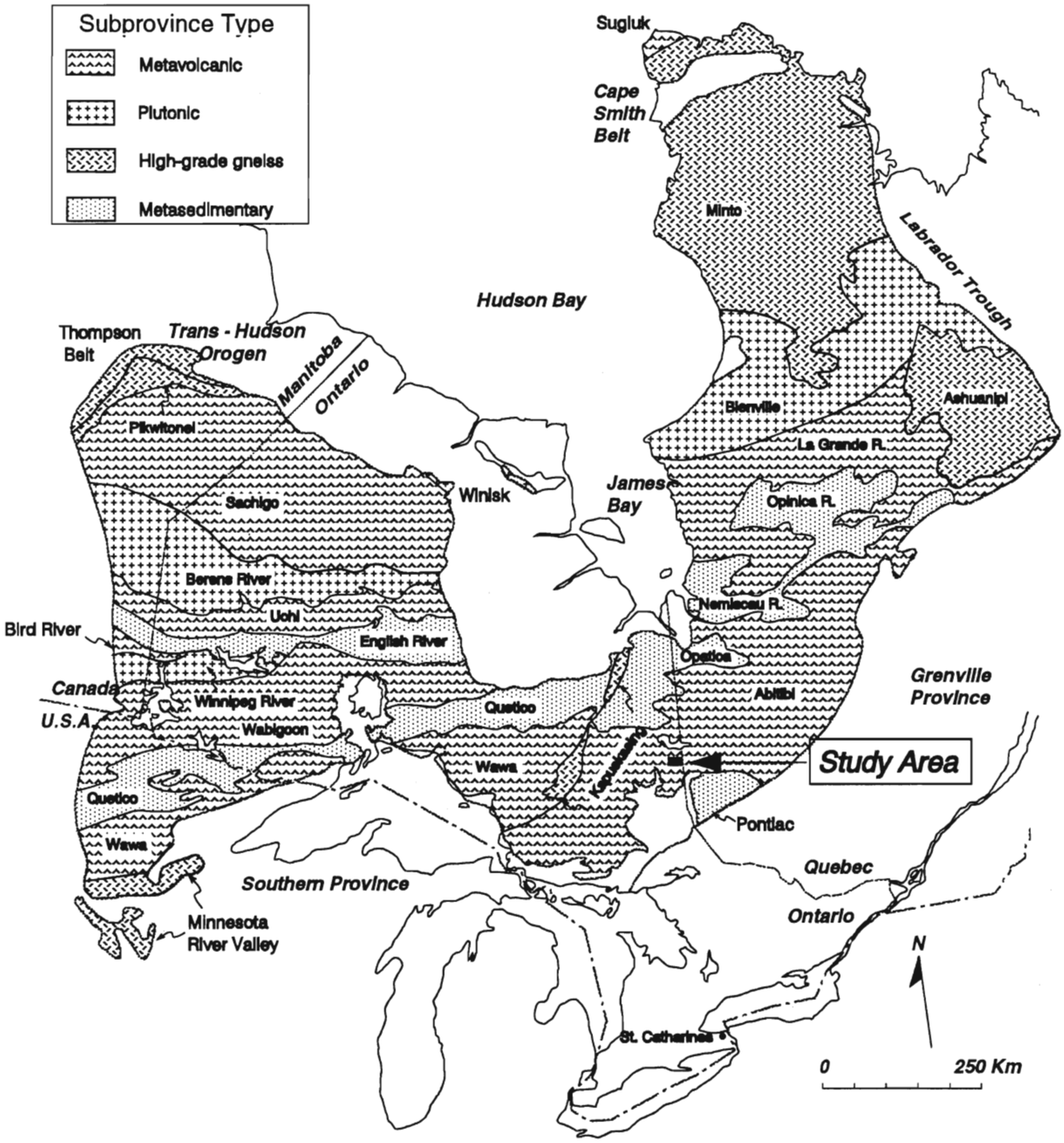

Figure 1-1: Subdivisions of the Superior Province with reference to the study area located in the central part of the Abitibi Subrovince (modified after Card and Cielsieski 1986).

In the southern volcanic zone, supracrustal rocks are preserved between the Lake Abitibi Batholith and the Round Lake Batholith (Jensen and Langford 1985) in a complicated structural pattern. Large scale east-west trending faults, the Destor-Porcupine and the Cadillac-Larder Shear Zone disect the region (MERQ-OGS 1983).

The volcanic rocks in the Kirkland Lake-Larder Lake area consist of komatiitic, tholeiitic, calc-alkalic and alkalic lavas. For the purposes of this study, the term assemblage is used. Assemblage refers to stratified volcanic and/or sedimentary rocks developed during a discrete interval of time in a common depositional or volcanic setting. They may share common structural, metamorphic, geochemical or geophysical features. Assemblages are typically bounded by faults, intrusions or unconformities (Thurston,1991). The term assemblage does not suggest genetic or stratigraphic implications. The nomenclature of Jensen (1985b) is presented in Table 1 for comparison.

Metavolcanic assemblages south of the Cadillac-Larder Shear Zone include the Pacaud Structural Complex, the komatiitic Wawbewawa assemblage, the tholeiitic Catharine and Boston assemblages, the calc-alkaline Skead assemblage and the komatiitic to tholeiitic McElroy and Larder Lake assemblages. Metavolcanic assemblages north of the Cadillac-Larder Shear Zone include the tholeiitic Kinojevis assemblage, the calc-alkaline Blake River assemblage and the alkalic Timiskaming assemblage (Figure 1-2).

It was originally thought that the geochemical variability of the metavolcanic assemblages in the Kirkland Lake region might represent a fractionated volcanic pile (Jensen 1985a). Recently, precise U-Pb zircon geochronological studies have shown that volcanism and sedimentation in the Larder Lake region occurred during a short time span (between 50-70 Ma) (Corfu et al. 1989) (Table 1). Komatiitic, tholeiitic and calc-alkaline metavolcanic and synvolcanic intrusions formed between 2750-2700 Ma. The tonalite-granodiorite-syenite

Table 1:Lithologic and Age Relations of Supracrustal Rocks in Kirkland Lake Region

Stratigraphic Unit[a]	Volcanic Type	Age (Ma)[a]	Jensen (1985)	
Timiskaming ass.	alkalic	≤ 2679[c]	Timiskaming Gp.	
				CLSZ*
Blake River ass.	calc-alkalic	2701 +/- 2[b]	Blake river Gp.	
Kinojevis ass.	tholeiitic	2701[c]	Kinojevis Gp.	
Hearst ass.	sediments			
Larder Lake ass	tholeiitic to komatiitic	2705 +3/-2[b]	Larder Lake Gp.	
				LNSZ**
McElroy ass..	tholeiitic to komatiitic			
				?
Skead ass.	calc-alkalic	2701 +/- 2[b]	Skead Gp.	
Catharine ass.	tholeiitic	?	Catharine Gp.	
Wawbewawa ass.	komatiitic	?	Wawbewawa Gp.	
Pacaud Structural Complex	calc-alkalic	2747 +/- 2	Pacaud Tuffs	

a: from Jackson and Fyon, 1991
b: from Corfu et al.,1989
c: from Corfu and Nobel, 1992

* Cadillac Larder Shear Zone

**Lincoln Nipissing Shear Zone

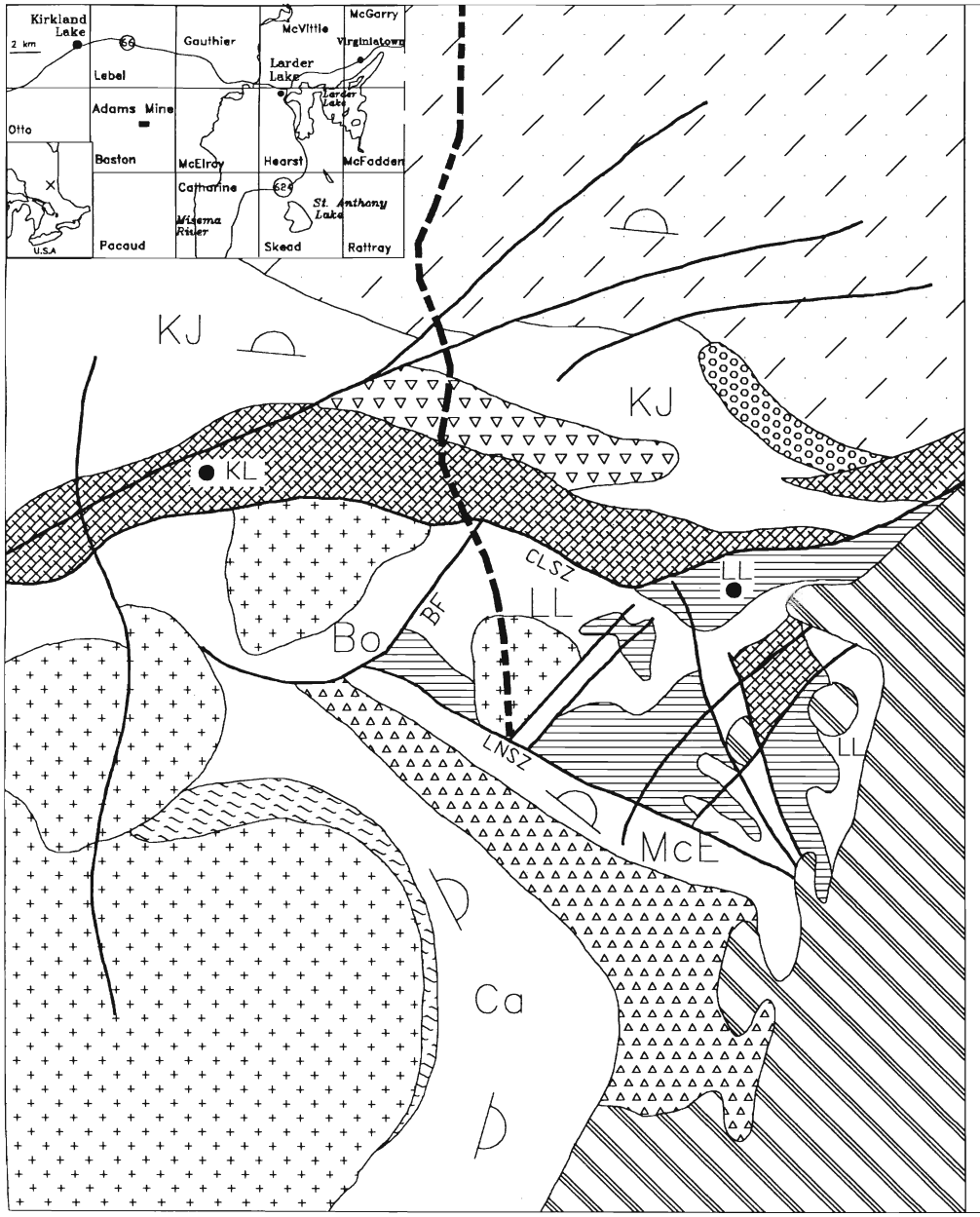

Figure 1–2: Regional geology of the Kirkland Lake area.

LEGEND

- Huronian sedimentary rocks
- Granitoid rocks
- Gabbro
- Timiskaming assemblage (≤2679 Ma)
- Blake River assemblage (2701 Ma)
- Hearst assemblage
- Gauthier assemblage
- Skead assemblage (2700 Ma)
- Tholeiitic Units/: (KJ) Kinojevis assemblage (2700 Ma)
  Komatiitic Units
  - (Ca) Catharine assemblage
  - (LL) Larder Lake assemblage (2705 Ma)
  - (McE) McElroy assemblage
  - (Bo) Boston assemblage
- Pacaud Structural Complex (2747 Ma)
- Faults : (CLSZ) Cadillac-Larder Shear Zone
  - (LNSZ) Lincoln Nipissing Shear Zone
  - (BF) Boston Creek Fault
- Lithoprobe Seismic Reflection Line 12

KL : Kirkland Lake
LL : Larder Lake

Facing indicator
Pillow lava

N

0 2.5 5.0 7.5 10
kilometres

intrusions formed between 2700-2680 Ma (Corfu et al. 1989). Alkalic Timiskaming metavolcanic and metasedimentary rocks formed after 2680 Ma (Corfu and Nobel 1992).

The oldest dated supracrustal rocks are found in the Pacaud Structural Complex (2747Ma) while the Skead assemblage has been dated at 2701 Ma and the Larder Lake assemblage at 2705 Ma (Corfu et al. 1989). Age relationships between adjacent metavolcanic assemblages (Table 1) are not consistent with an upward stratigraphic stacking of progressively more evolved rocks. It is possible that adjacent assemblages with similar ages and geochemical signatures were formed in different tectonic settings.

1.3 Larder Lake Group

Jensen (1985b) suggested that the Larder Lake, McElroy and Hearst assemblages consisted of volcanic and sedimentary rocks that were deposited on an unstable continental margin. The volcanic rocks comprise mainly komatiitic and tholeiitic lavas cut by numerous peridotitic dikes interpreted to represent feeders to the lavas. Calc-alkalic lavas are more common in the lower portions of the group. The sedimentary rocks consist of turbitidic clastic conglomerates, wackes, siltstones and mudstones and chemical chert and banded iron formation sedimentary rocks (Jensen 1985b).

The northwest trending Lincoln-Nipissing Shear Zone (LNSZ) and a thick ultramafic serpentinite separate the lower portion of the Larder Lake assemblage from the McElroy assemblage (Jackson et al. 1990). The LNSZ is a carbonatized shear zone (Figure 1-3) and separates the region into two areas of contrasting structural style (Jackson et al. 1990). South of the shear zone, metavolcanic rocks display simple anticlinal, homoclinal structure with a vertical dip, northwest strike and a northeastern facing direction. North of the LNSZ the lavas and sediments are complicated by folds and faults.

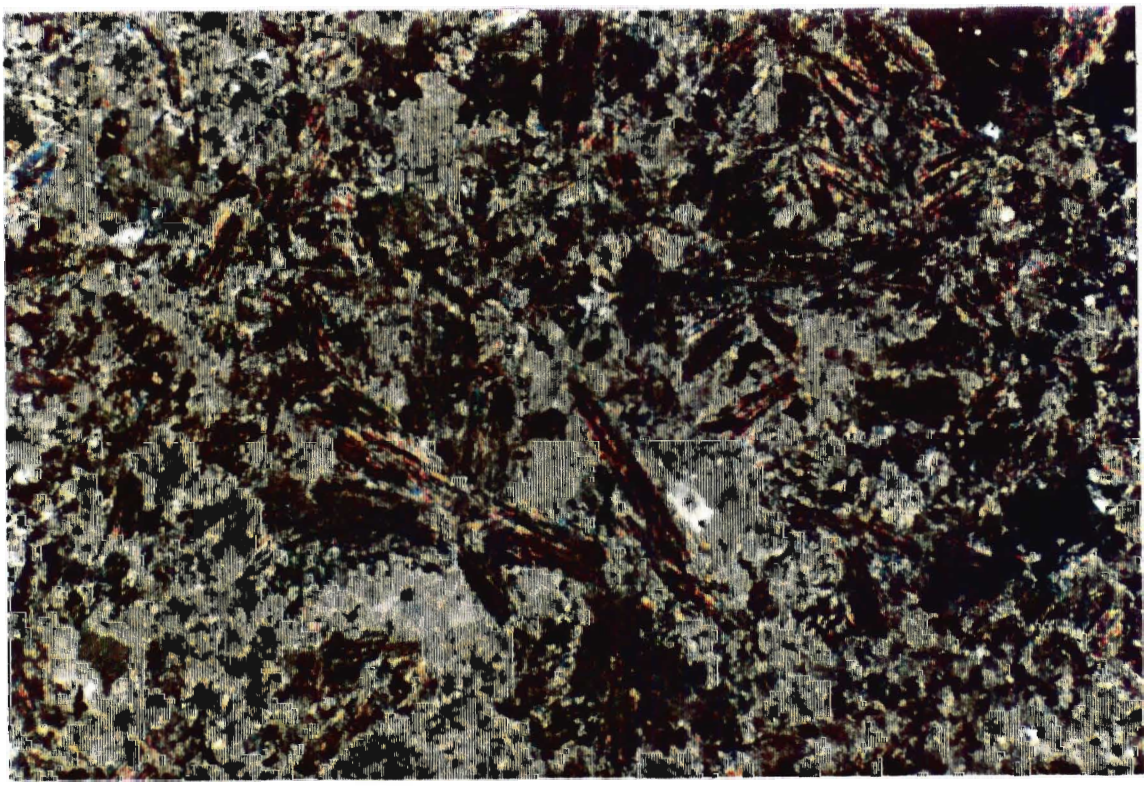

Figure 1-3: Photomicrograph of carbonatized rock within the Lincoln Nipissing Shear Zone. The rock does not display a fabric therefore carbonatization is post-shearing.

The difference between rocks separated by the LNSZ and the age reversals recorded between the Skead and Larder Lake assemblages suggest that the metavolcanic rocks in the Larder Lake region do not represent a chemostratigraphic continuum. Rather, packages of supracrustal rocks may have formed in a similar but not necessarily the same tectonic setting and were affected by similar but not identical magmatic processes.

1.4 Purpose of Study

The purpose of this study is to determine whether or not the McElroy and Larder Lake assemblages are related in terms field, petrographic and geochemical criteria. The methods used to address this problem were:

i) to subdivide and identify internal relationships within the McElroy assemblage;

ii) using field, petrographic and geochemical criteria, compare and contrast the McElroy and Larder Lake assemblages in order to identify whether a relationship exists between these two adjacent, metavolcanic units;

iii) to compare and contrast the McElroy assemblage with other metavolcanic units in the Abitibi Greenstone belt;

iv) using discriminant diagrams, developed for Phanerozoic tectonic settings, examine the tectonic setting of the McElroy and Larder Lake assemblages;

v) to determine the petrogenesis of the McElroy and Larder Lake assemblages.

1.5 Location and Access

The study area is located south of Larder Lake, Ontario. The area underlain by the McElroy and Larder Lake assemblages includes the northern part of Skead Township, northeast Catharine Township, southeast McElroy Township, a small portion of McFadden

Township and most of Hearst Township (inset Figure 1-2). Access is by numerous logging roads, trails and the Misema River. The northwest portion of the McElroy assemblage was accessed via mine roads of the Adam's Mine. Much of the Larder Lake assemblage is accessible along the shoreline of Larder Lake. Outcrop exposure is less than 5%.

1.6 Previous Work

1.6.1 Field Studies

Geological interest in the Kirkland Lake-Larder Lake region was initiated in the early 1900's with the discovery of gold. Many early surveys were in aid of the mining industry. Early surveys by Miller (1902), Parks (1904), Brock (1907), Bowen (1908) and Wilson (1910) grouped all supracrustal rocks as Keewatin and correlated these rocks with Keewatin rocks of the Lake of the Woods area (Lawson 1885). An unconformity separating Huronian sediments from the older Keewatin rocks was also identified by Brock (1907). Burrows and Hopkins (1914) recognized an unconformity at the top of the volcanic package and the base of the overlying Timiskaming sediments.

Within the study area townships marked on Figure 1-2 (inset) were mapped in detail (1:1200) by Thomson (1949), Abraham (1951) and Hewitt (1951). These studies identified that "Keewatin" metavolcanic rocks were unconformably overlain by "Timiskaming" metasediments (Thomson 1949, Hewitt 1951).

Jensen, in the 1970's and 1980's used geochemical criteria to further differentiate the volcanic rocks within the Kirkland and Larder Lake area. Recently, synoptic mapping in the study area has been completed by Jensen (1976,1977,1979,1985b), Mandzuik (1980), Jackson and Harrap (1989) and Jackson et al. (1990).

1.6.2 Petrogenetic Studies

Many petrogenetic studies of the Abitibi Greenstone Belt {Smith (1980), Dimroth et al. (1982,1983a,1983b), Gelinas and Ludden (1984), Hubert et al. (1984), Jensen and Langford (1985), Ludden et al. (1986), Hodgson and Hamilton (1989), Fowler and Jensen (1989), Barrie et al. (1991) and Blum and Crocket (1992)} resulting in several contrasting tectonic models have been proposed.

Dimroth et al. (1982,1983a,1983b) envisage an island arc-type setting for the generation of the Abitibi Greenstone Belt. An arc formed over a north dipping subduction zone produced the volcanic rocks. Sediments from the Pontiac Subprovince are interpreted by these authors to have formed an accretionary wedge to the south (Dimroth et al. 1982,1983a,1983b).

Jensen (1985a) suggested a megacauldron model in which volcanic rocks formed over a diapir. Gravitationally unstable thick mafic crust subsided and underwent partial melting to produce calc-alkaline lavas. Partial melting of calc-alkaline rocks produced trondhjemitic intrusions. Alkaline rocks were produced by the partial melting of sediments resulting from erosion of the plutons.

Ludden et al. (1986) suggest that the northern Abitibi formed in a volcanic arc setting and that the southern Abitibi formed by rifting of the northern arc. Collision terminated subduction and initiated sedimentation and thrusting.

Hodgson and Hamilton (1989) proposed that tholeiitic to komatiitic rocks formed in an extensional, oceanic environment while calc-alkaline rocks formed in an island arc environment and the sediments with interbedded komatiite formed in a passive margin. The oceanic, arc and continental margin settings were then tectonically stacked into their present configuration.

Blum and Crocket (1992) favour an active, extensional, fault-bounded environment for the eruption of the Larder Lake volcanics. Barrie et al. (1991) have also suggested a rift related setting for the metavolcanic rocks in the Timmins area.

Chapter 2

Local Geology

2.1 McElroy assemblage

2.1.1 Introduction

The McElroy assemblage is a northeast facing homoclinal sequence of mafic and ultramafic effusive and intermediate volcaniclastic rocks (Figure 2-1). The mafic rocks include aphanitic to fine-grained plagioclase glomerophyric pillowed basalts which grade into a spatially, dominating sequence of medium to coarse-grained massive flows. Leucogabbroic and dendritic textured, coarse flows represent a lesser proportion of the units. Minor amounts of fine-grained, polysutured ultramafic flows are also present. Less than 10% of the unit distribution consists of intermediate volcaniclastic rocks which range from ash tuff to tuff breccia. The lower most unit are the dendritic flows which are overlain by massive, ultramafic flows. Leucogabbroic and coarse-grained massive flows overlay the ultramafic flows. The coarse grained flows grade upward into finer-grained and pillowed flows, all of which contain the plagioclase glomerophyric texture (Figure 2-2). Contacts between units of the McElroy assemblage are generally unexposed. Contacts between the McElroy assemblage and other assemblages are equally uncommon.

The McElroy assemblage is bounded by the Lincoln-Nipissing Shear Zone to the north and the intermediate to felsic, fragmental, calc-alkalic Skead assemblage to the south. The lower contact with the Skead assemblage is not well exposed, however as the Skead assemblage is approached, the abundance of intermediate volcanic material in the McElroy assemblage increases. To the southeast the McElroy assemblage is overlain by Huronian sedimentary rocks of the Cobalt Group. To the northwest the McElroy assemblage is separated from the Boston assemblage by the Boston Creek Fault. The McElroy assemblage

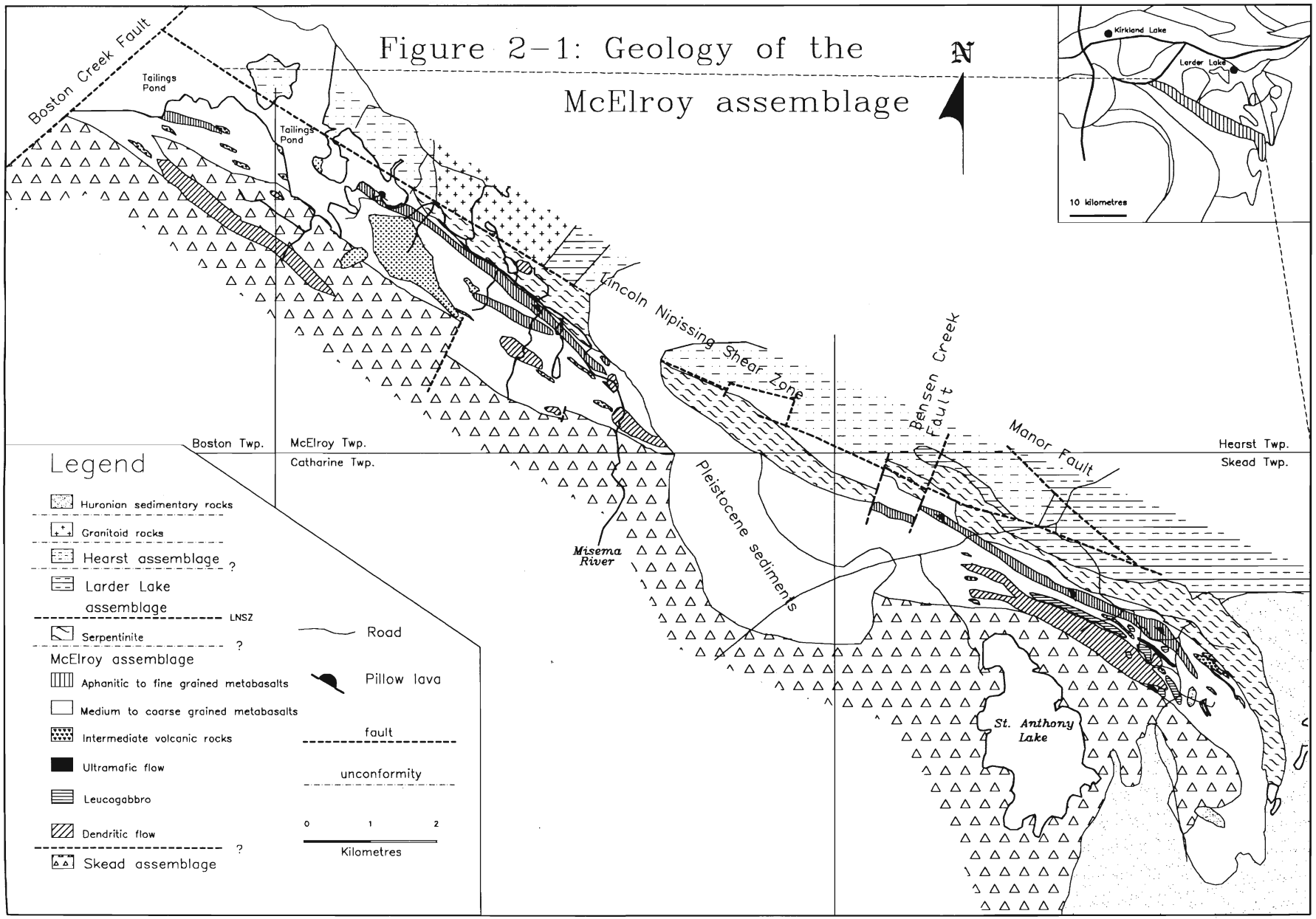
Figure 2-1: Geology of the McElroy assemblage
N
Kirkland Lake
Larder Lake
10 kilometres
Boston Creek Fault
Tailings Pond
Tailings Pond
Lincoln Nipissing Shear Zone
Benson Creek Fault
Manor Fault
Boston Twp.
McElroy Twp.
Catharine Twp.
Hearst Twp.
Skead Twp.
Misema River
Pleistocene sediments
St. Anthony Lake
Legend
Huronian sedimentary rocks
Granitoid rocks
Hearst assemblage ?
Larder Lake assemblage
LNSZ
Serpentinite ?
McElroy assemblage
Aphanitic to fine grained metabasalts
Medium to coarse grained metabasalts
Intermediate volcanic rocks
Ultramafic flow
Leucogabbro
Dendritic flow
?
Skead assemblage
Road
Pillow lava
fault
unconformity
0 1 2
Kilometres

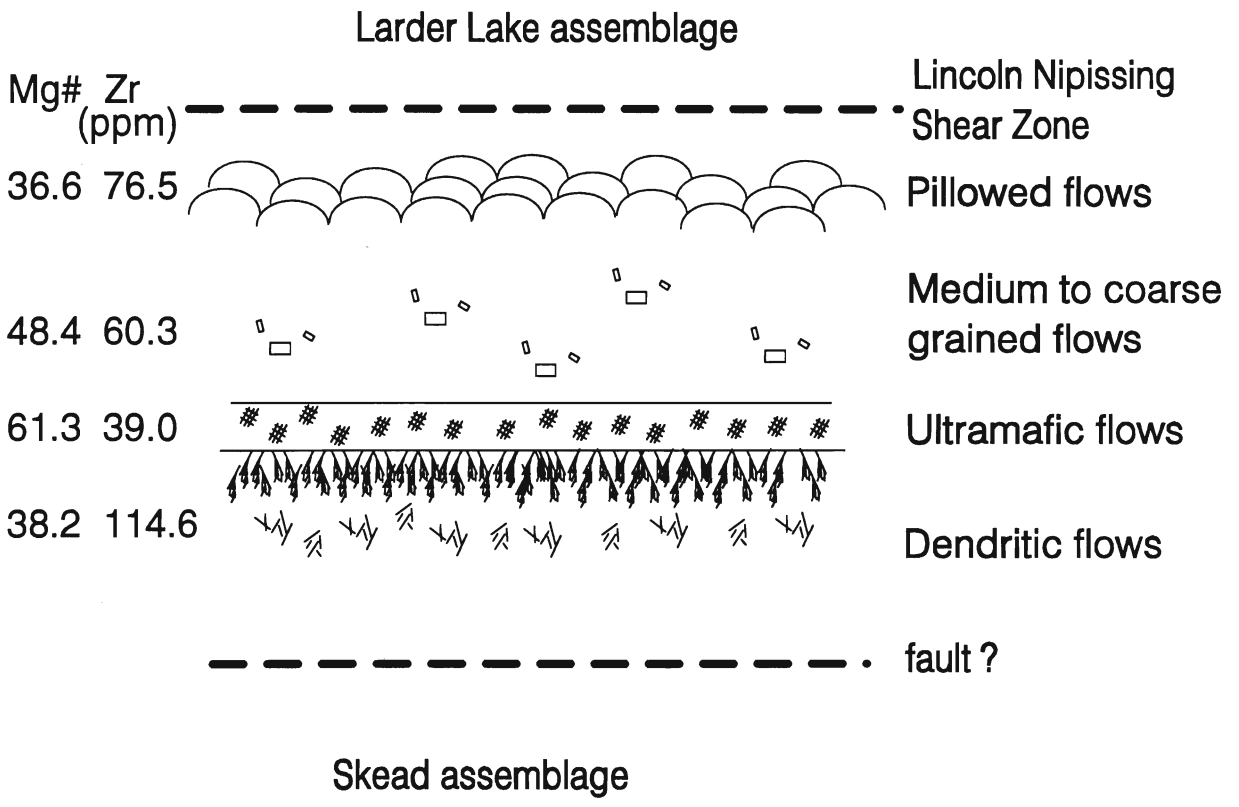

Figure 2-2: Simplified cross-section of the SW section of the McElroy assemblage. The Mg# and Zr values are the averages for the respective lithologies illustrating the progressive fractionated nature of the assemblage from the base to the top with the exception of the dendritic flows which do not follow this pattern.

covers an area of approximately 15 km^2 (Figure 2-1).

A major component of the McElroy assemblage is gabbroic textured rock consisting of either coarse, massive flows or intrusive equivalents. Limited exposure precludes distinguishing amongst the two alternatives.

2.1.2 Dendritic flows

At the base of the McElroy assemblage, there exists a gabbroic textured rock which has been informally called "hornblende" gabbro (Hewitt 1951). The unit is approximately 500 metres thick and has a strike length of approximately 7 km. The hornblende gabbro is a medium to coarse-grained rock which contains various gabbroic textures. At the top of the unit, it contains bladed amphibole in which actinolite pseudomorphs pyroxene. The crystals up to 3 cm long with a distinctive dendritic texture (Figure 2-3, 2-4). Actinolite needles typically have length to width ratios of 5:1. Anhedral to subhedral plagioclase is interstitial to the actinolite. Weathered surfaces show 35-40% black to dark green subhedral to euhedral amphibole crystals in a 60-65% milky white plagioclase rich groundmass. Fresh surfaces are characteristically black and exhibit good gabbroic textures. This phase of the unit can be traced along strike for over a 10 km in the southeastern section of the McElroy assemblage and is locally observed in the northwest portion of the assemblage. Zones of dendritic amphibole can be found in layers or isolated pods. Individual dendrites can be identified in the field and in thin section. The dendrites branch stratigraphically downwards for up to 10 centimetres until they gradually lose the preferred orientation and assume a more random gabbroic orientation (Figure 2-5).

Layered zones of dendritic amphibole occur in regions 2 m thick and at least 7 m wide (extent limited by outcrop exposure). The dendritic texture is separated by a sharp

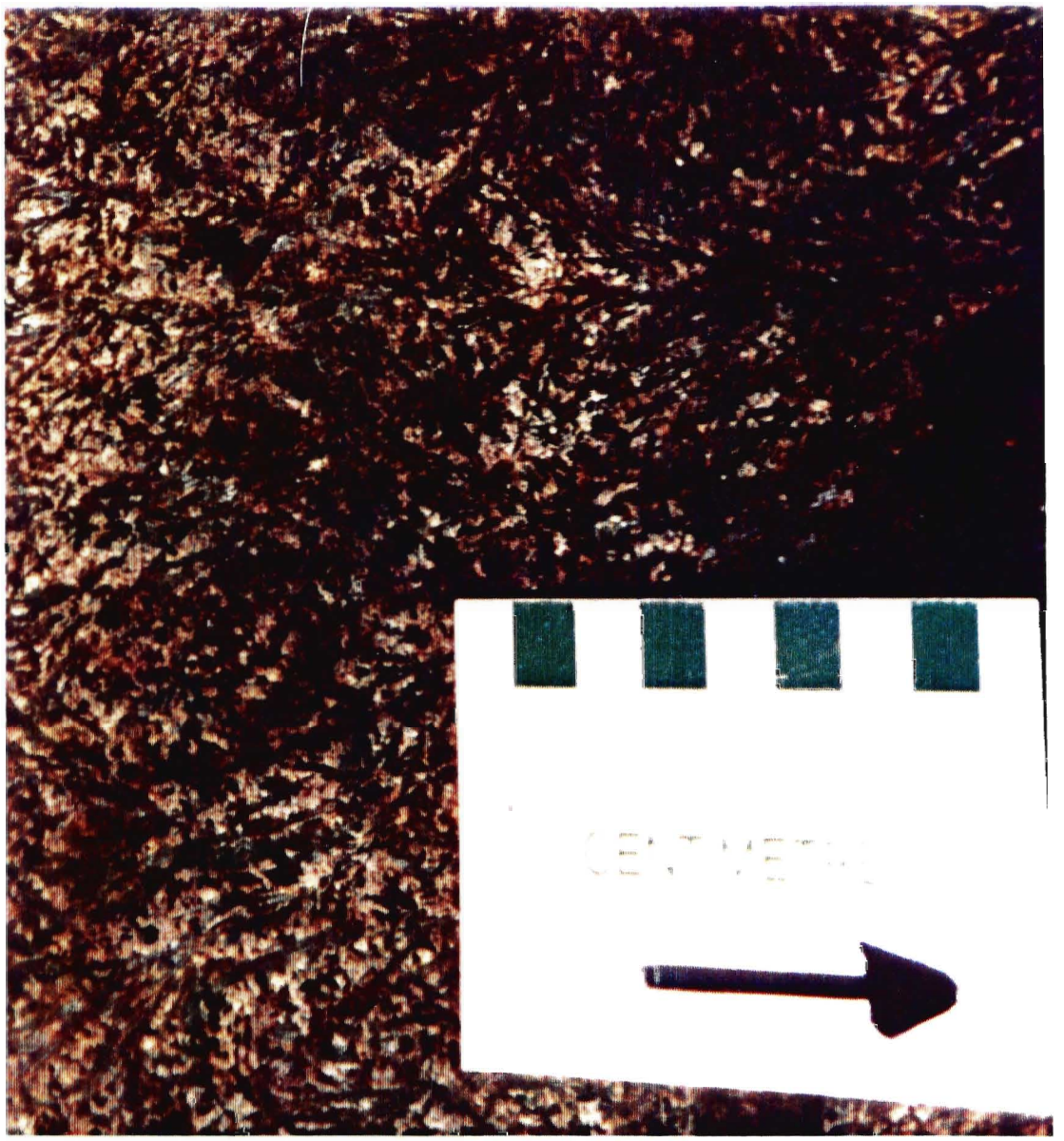

Figure 2-3: Outcrop photograph of spinifex-type texture within the dendritic flow. Amphibole dendrites branch down for up to 10 cm from an apparent contact (not shown) into a random oriented texture (Figure 2-5). The texture is interpreted to represent a rapid cooling event. Arrow points to the northeast, which is approximately perpendicular to the strike of the assemblage.

Figure 2-4: Photomicrograph of branching actinolite needles in the dendritic flow. Photo is taken from the same location as Figure 2-3. Randomly oriented actinolite and plagioclase are interstitial to the actinolite dendrites. Bar length is 0.5 mm.

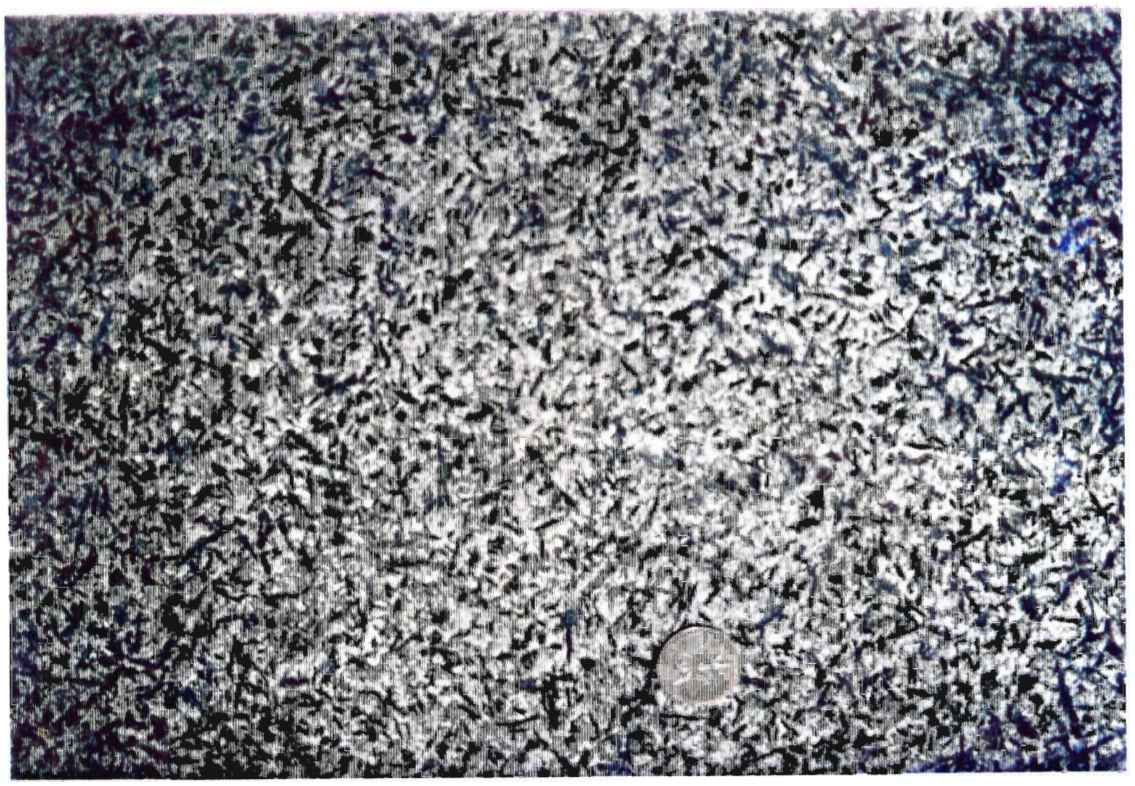

Figure 2-5: Outcrop photograph of randomly oriented actinolite needles with interstitial plagioclase. Photograph taken approximately 25 cm below outcrop for Figure 2-3 indicating that the textures grade into one another.

Figure 2-6: Photomicrograph of random orientation within the dendritic flow. Photograph shows gabbroic texture with lath shaped actinolite and interstitial plagioclase. Black mineral is titanite. Bar length is 0.5mm long.

contact ranging in thickness from 1 cm to 10 cm, upon which the sequence repeats itself. Two apparent contacts of igneous "layering" were observed in the field, (but limited due to poor outcrop exposure). There is no penetrative deformation in the hornblende gabbro, therefore a structural explanation for these "contacts" is unlikely. Also, in regions where the dendrites occur as pods, sharp contacts are not observed. In this situation, dendritic pods approximately 1 m^2 are isolated in a region of randomly oriented amphibole.

Dendritic flows are medium to coarse-grained (2-5 mm) and contain 20-30% groundmass and 70-80% crystalline phases. Primary mineral associations include lath shaped plagioclase (40-60%) and bladed acicular clinopyroxene (30-40%). Typical greenschist facies mineral associations or assemblages in the hornblende gabbro include actinolite, sausseritized plagioclase commonly displaying exsolution features, epidote, anomalous blue chlorite, quartz, sphene, ilmenite and stiplomelane (Figure 2-4, 2-6). Primary clinopyroxene has been replaced by metamorphic actinolite, sphene and chlorite. Actinolite is commonly replaced by chlorite and stilpnomelane. Plagioclase is sausseritized to a mix of epidote, quartz, carbonate and sericite. The exsolution textures may indicate that plagioclase alteration is not complete. Where plagioclase replacement is complete, pseudomorphs of the original grain shape are preserved. The preserved primary gabbroic textures indicates that secondary deformation processes have been minimal.

Dendritic textures have been interpreted to result from rapid cooling (Easton and Johns 1986) typical for volcanic flows, suggesting this unit has an extrusive rather than intrusive origin. Also, the branching of the dendrites is in stratigraphic agreement with other facing indicators. Intrusive contact features such as chill margins or xenoliths were not observed in the field where contacts were identified.

2.1.3 Leucogabbro

Stratigraphically above the dendritic flows is a mineralogically and texturally different unit classified as a leucogabbro. The leucogabbro is approximately 200 metres thick and has limited lateral distribution. It is found only in the southeast portion of the McElroy assemblage. The leucogabbro is light green on both weathered and fresh surfaces and contains approximately 15% mafic minerals.

The rock consists of 60% plagioclase replaced by epidote, sericite and carbonate, 15% relict clinopyroxene cores, 10% chlorite clots replacing clinopyroxene, 10% epidote existing in the groundmass and minor amounts of opaques and titanite. Grain size ranges from 1 to 3 mm. Relict ophitic texture is preserved among the plagioclase and the clinopyroxene and its replacement minerals (Figure 2-7).

2.1.4 Ultramafic flows

As noted by Jensen and Langford (1985), ultramafic flows are distinguished from the majority of the volcanic flows by their colour and texture. The ultramafic flows have a bluish-grey fresh surface and weather a rusty brown. These rocks are soft and can be easily scratched yielding a talc-like powder. Thin beige serpentine veinlets weather up and produce a boxwork texture. Characteristic polygonal jointing interpreted by Jensen and Langford (1985) to represent a cooling feature which reflects high temperature resulting from a high Mg content is present.

The ultramafic flows are fine grained to medium grained (0.5-2 mm) and consist of 10-20% olivine pseudomorphed by serpentine, carbonate and magnetite and 30-40% clinopyroxene pseudomorphed by tremolite, serpentine, chlorite, ilmenite and sphene. Plagioclase is rare to absent. The groundmass phase (20-40%) is very fine grained (<0.1 mm). Relict clinopyroxene cores (up to 10%) are mantled by secondary minerals (Figure 2-

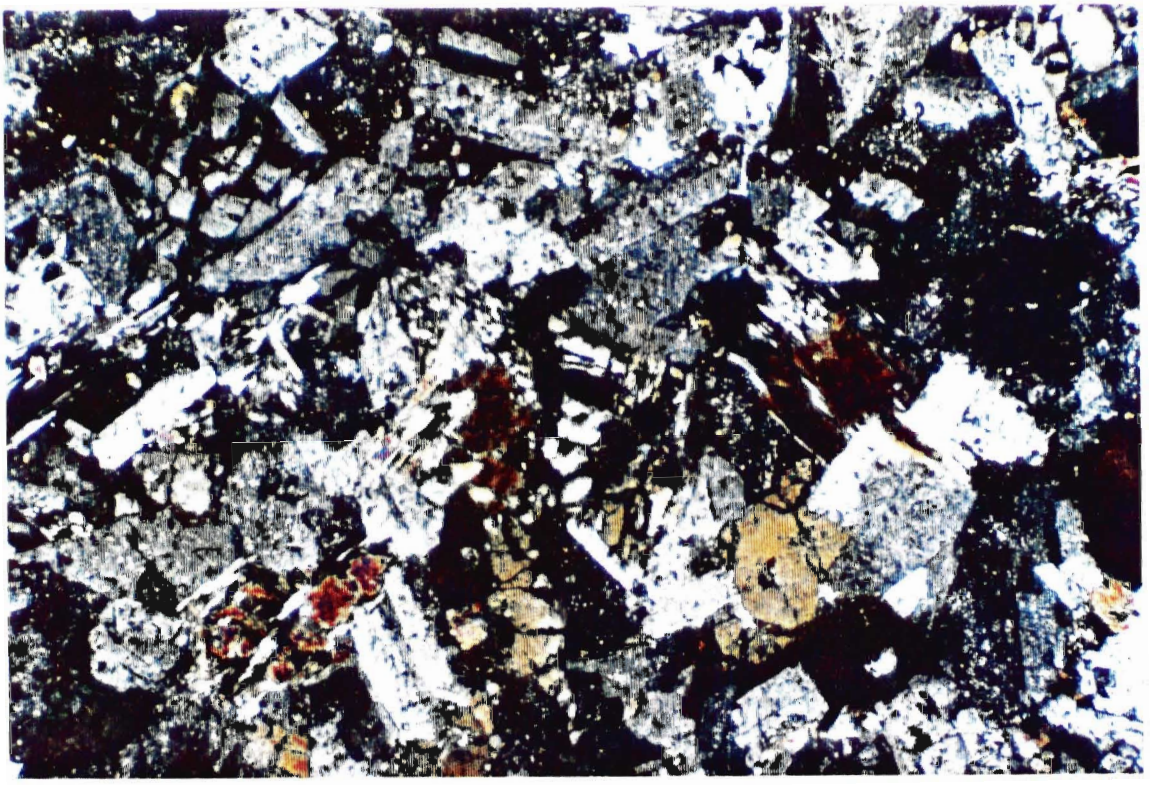

Figure 2-7: Photomicrograph of leucogabbro displaying a hich plagioclase content. Field of view is approximately 8 mm.

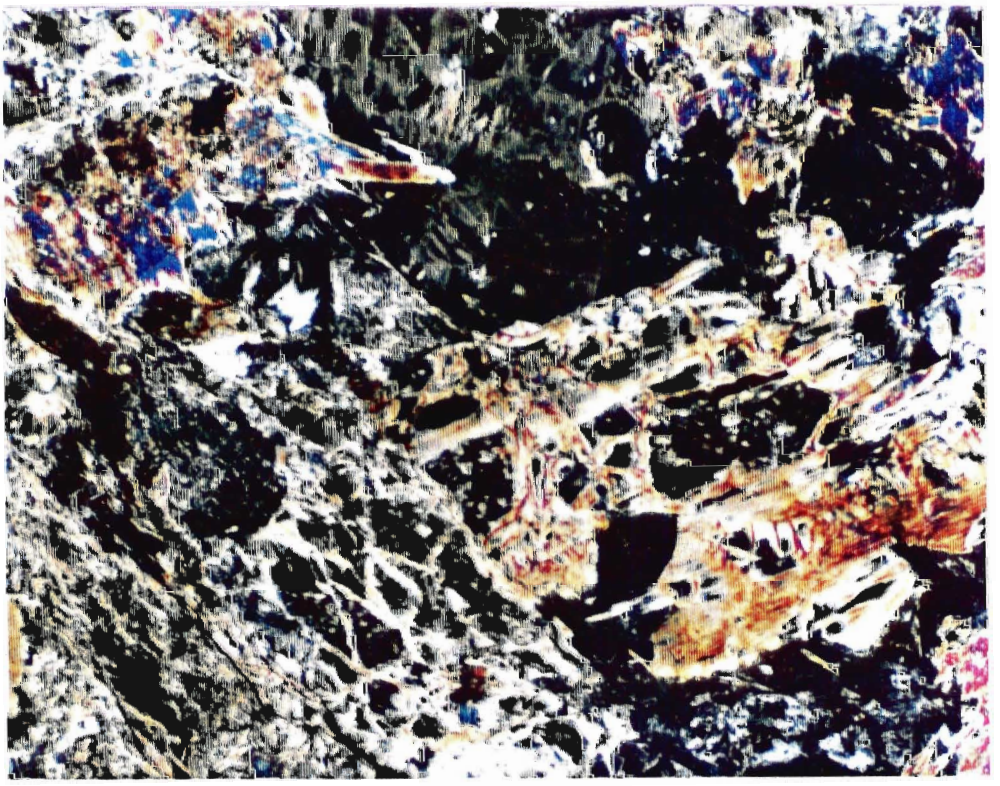

Figure 2-8: Photomicrograph of ultramafic flow with olivine and clinopyroxene being replaced by actinolite, chlorite and serpentine. Field of view is approximately 8 mm.

8). A weak penetrative fabric is expressed by fibrous chlorite and serpentine in the groundmass.

2.1.5 Intermediate to Felsic Volcanic Rocks

Intermediate pyroclastic volcanic rocks are interbedded with but less voluminous than the mafic metavolcanic rocks. Pyroclastic rocks in the McElroy assemblage include tuff, crystal/lithic tuff (Figure 2-9), lapilli tuff and tuff breccia.

Intermediate tuffs are aphanitic (<1 mm) to aphyric, weathering light beige and have a pale green fresh surface. The tuffs consist mainly of sericite with accessory carbonate, chlorite, quartz, plagioclase and sulphide.

Crystal/lithic tuffs range in grain size from 1 to 2 mm. Crystal tuff consists of anhedral to subhedral plagioclase. Clasts in the lithic tuffs are outlined by sharp contrasts in grain size. The lithic tuff are monolithic since both the clasts and the groundmass consist of plagioclase. Some lithic tuffs contain chlorite in the groundmass. Altered samples commonly display a wavy fabric expressed by chlorite and eye-shaped recrystallized quartz.

Lapilli tuffs are poorly sorted, massive and contain clasts that are angular and range in grain size from 1 mm to 5 cm and contain 95% plagioclase and 5% mafic minerals (amphibole). The lapilli tuffs are commonly also monolithic. Chlorite is usually foliated in the groundmass.

Tuff breccias consist of angular clasts and blocks 2 to 10 cm in size. Sorting is poor and most clasts contain an alteration rind (Figure 2-10).

The ash tuff contains >95% groundmass whereas crystal tuffs contain 60-70% crystalline material and 30-40% groundmass. Lithic tuffs are characterized by the presence of fragments which have a sharp contrast in grain size from the groundmass of the host rock.

Figure 2-9: Photomicrograph of intermediate lithic tuff. A weak chloritic fabric is present which is not visible in the mafic volcanic lithologies. Bar length is 0.5 mm.

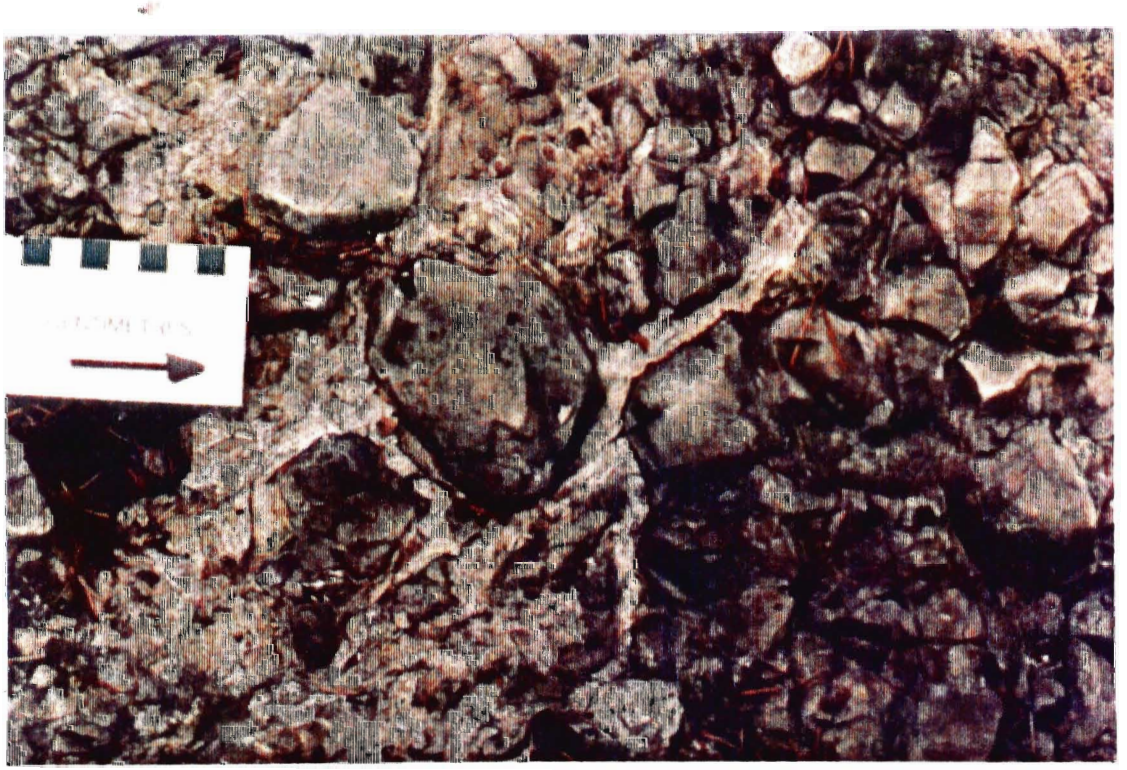

Figure 2-10: Outcrop of monolithic, tuff breccia within an intermediate fine grained matrix. The subangular fragments range in size from < 1 cm to > 5 cm in diameter.

The groundmass in the fragments consists of microlitic plagioclase whereas the host groundmass is granoblastic.

The intermediate rocks display a fabric which is not as obvious in the adjacent mafic rocks. Most likely, the intermediate rocks record the affects of deformation readily than the mafic rocks because of variations in mineralogy and differences in competency.

2.1.6 Medium to coarse grained flows

Medium to coarse grained flows are spatially related to mafic, aphanitic metavolcanic rocks. These two rock types are transitional into one another. "Knobby", glomerophyric and typical gabbroic textures have been recognized in the field (Figure 2-11). Medium to coarse grained rocks weather to a brownish-grey colour with local rusty staining. Fresh surfaces are dark greenish-grey. A visibly distinctive "knobby" texture within the McElroy assemblage consists of 30-35% subhedral, equant pyroxene crystals (pseudomorphed by actinolite) set in a plagioclase-rich groundmass. The rock contains 50-60% medium to coarse grained (2-5 mm) crystals and a 30% fine grained (<1 mm) groundmass. Ophitic texture is common in this unit.

Plagioclase glomerophyric texture in this unit (Figure 2-11) consists of 1 cm^2 to several cm^2 accumulations of plagioclase. The glomerophyres are generally subrounded which may result from either primary igneous resorption processes or secondary metamorphic processes. This gives the rock a porphyritic texture. Contacts with the overlying fine grained to aphanitic flows are gradational (Figure 2-12).

The medium to coarse grained flows are similar to the aphanitic flows in terms of primary and secondary mineralogy. Groundmass minerals represent 20-40% of the rock and crystalline phases represent 60-80% of the rock, giving it a coarser texture. Crystalline

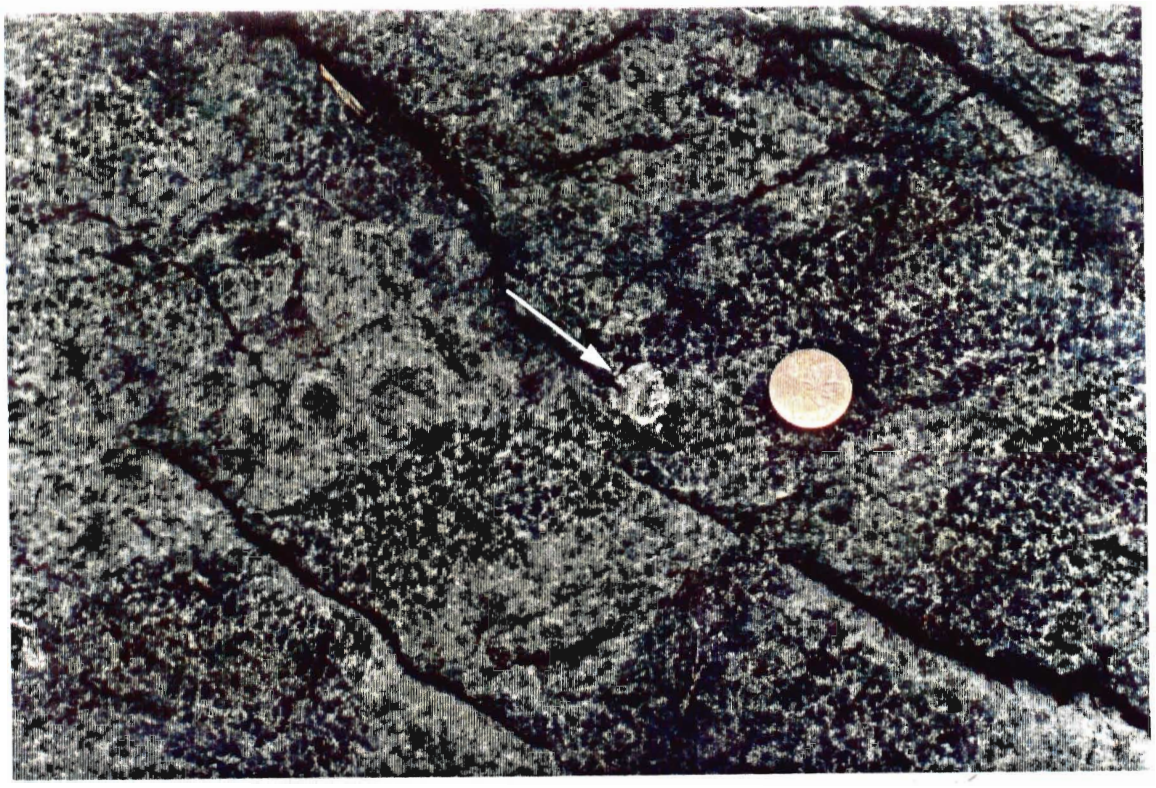

Figure 2-11: Coarse grained massive flow containing plagioclase phenocrysts. Arrow points to plagioclase phenocryst.

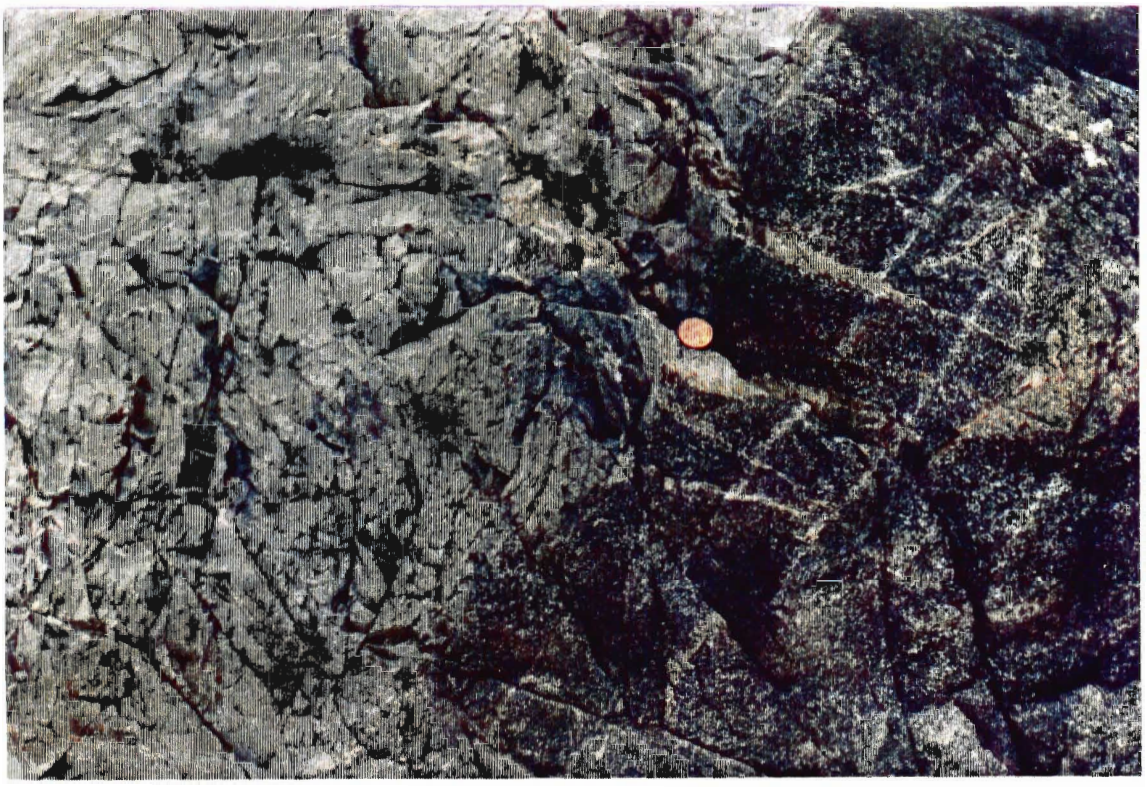

Figure 2-12: A rare example of an exposed contact. The gradual contact is between an aphanitic to fine grained massive flow and a medium to coarse grained flow.

clinopyroxene and plagioclase (1-3 mm) display a blastosubophitic to porphyritic texture. Plagioclase glomerophyres locally range up to 2 cm in diameter. A penetrative fabric is not evident.

2.1.7 Aphanitic to fine grained flows

Mafic metavolcanic rocks in the McElroy assemblage include fine grained to aphanitic massive and pillowed flows, plagioclase glomerophyric, amygdaloidal flows and rare variolitic flows. The pillowed flows are found near the top of the assemblage and can be traced along strike for 10 km in a northwest direction. The pillowed sequence is approximately 250 m thick.

Pillowed flows (Figure 2-13) indicate the younging direction is to the northeast. The facing direction of the pillowed flows is consistent with the regional facing direction of units between the Round Lake Batholith and the Lincoln Nipissing Shear Zone (Figure 1-2).

Pillows have a length:width ratio of 3:1. Selvages are 1 cm thick and tend to weather out more easily than the pillow cores. Uncommon amygdules are found associated with pillowed basalts and are fine grained (<1 mm) and subrounded. Amygdules consist of carbonate, epidote, chlorite and quartz. The rarity and fine grain size of the amygdules may indicate that these lavas erupted at great depths in a deeper, oceanic basin (Easton and Johns 1986) or else that the magma had a low vapour pressure.

Plagioclase glomerophyric flows are present in the southeast portion of the McElroy assemblage. These are similar to the glomerophyric gabbroic units found stratigraphically below the mafic metavolcanic rocks (Figure 2-14). The only difference is that the grain size of the groundmass in this unit is finer than that of the underlying unit.

Rocks in this unit are generally aphyric to fine grained (<1 mm) holocrystalline.

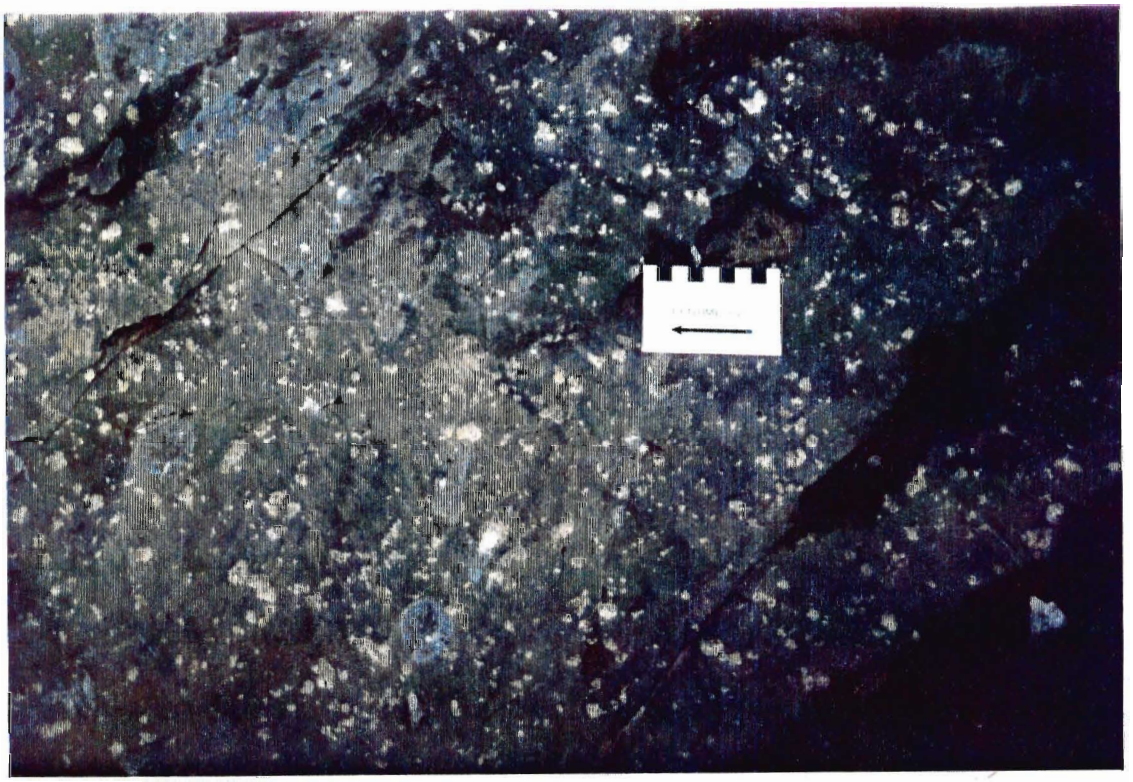

Figure 2-13: Pillowed flows within the McElroy assemblage.

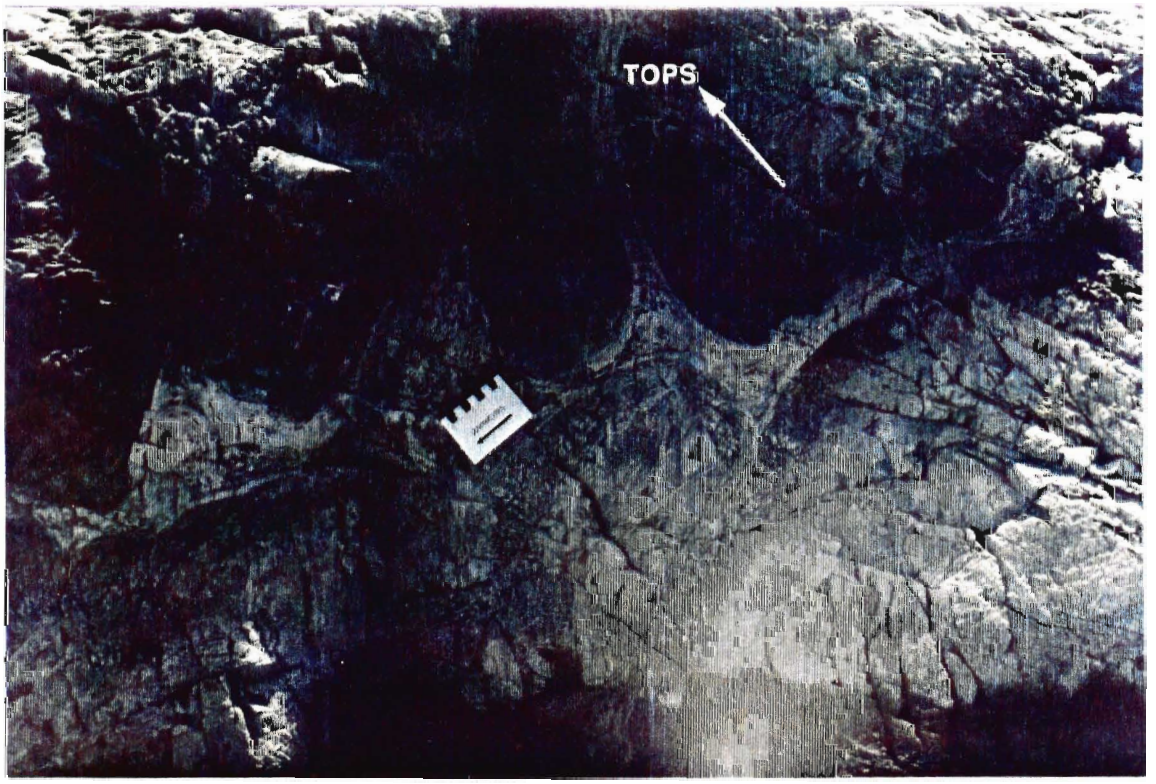

Figure 2-14: Plagioclase glomerophyric texture in aphanitic massive flow. Plagioclase phenocrysts can range in size from less than 1 cm to several cm in diameter.

Blastophenocrysts of plagioclase (glomerophyric) and to a lesser extent actinolite are present. Aphanitic groundmass represents 80-90% while 10-20% of the rock is crystalline. The estimated primary mineralogy based on relict igneous textures and minerals, metamorphic minerals and whole rock chemistry, consisted of 50-70% bladed to stubby clinopyroxene and 30-50% lath shaped plagioclase. Greenschist facies minerals replace the primary minerals, typically containing very fine grained actinolite (40-70%), albitized plagioclase (30-40%), fine grained epidote (5-10%) and chlorite (5-10%) with minor amounts of carbonate, quartz, sphene, ilmenite. Clinopyroxene has been completely replaced by needle-like actinolite, chlorite, carbonate and ilmenite. Primary plagioclase laths are sericitized and sausseritized and contain very fine grained accumulations of carbonate, quartz, epidote often creating a dusty appearance. The groundmass is very fine grained, massive and contains fibrous amphibole, chlorite and granoblastic epidote, quartz and feldspar. The overprinting of plagioclase and clinopyroxene by secondary minerals create undeformed pseudomorphs which preserve primary textures.

2.2 Assemblage Boundaries

The McElroy assemblages has several boundary types with the other assemblages. These boundaries include faults (Lincoln Nipissing Shear Zone and the Boston Creek Fault), an intrusion (Lincoln Nipissing Peridotite) and an unconformity (Proterozoic Huronian sedimentary rocks). The following section is a brief description of the boundaries.

2.2.1 Lincoln Nipissing Peridotite

Partially bounding the McElroy assemblage to the north is a 100 to 200 m thick peridotite (Figure 2-1). Along with the Lincoln Nipissing Shear Zone, this represents the northern boundary of the McElroy assemblage.

The moderately magnetic serpentinite is steel blue to black on fresh surfaces and weathers to a orange/brown colour. Weathered surfaces are typically soft and scratching yields a talc-like powder. Polygonal jointing, characterisitic to Mg-rich rocks, is common in the field (Figure 2-15). In hand sample, olivine pseudomorphs are visible and are fine grained.

The protolith for this unit was a fine grained dunite consisting of 90-95% subhedral olivine. The olivine has been replaced by serpentine (80-85%), opaques (magnetite) (10%) and carbonate (15%). Fibrous serpentine is very fine grained and forms a mesh-like texture which in association with the carbonate and magnetite outlines olivine pseudomorphs. The olivine pseudomorphs are 1-2 mm in diameter and define a cumulate texture. Locally, fine grained (<0.25 mm) relict olivine (<2% of the rock) and rarer clinopyroxene cores are mantled by the secondary minerals. The groundmass (approx. 5%) consists of a fibrous mat of serpentine showing no particular texture (Figure 2-16).

Although, this unit is adjacent to the LNSZ there is no apparent fabric present. Also, the presence of relict mineralogy (olivine and clinopyroxene) suggest that the serpeninite is post LNSZ and therefore post McElroy and Larder Lake volcanism. This indicates that the LNSZ may have acted as a low pressure path along which the peridotite intruded between the two assemblages.

2.2.2 Lincoln Nipissing Shear Zone

The Lincoln Nipissing Shear Zone (LNSZ) extends from the Huronian sediments in the southeast to the Boston Creek Fault in the northwest (Figure 1-2). It separates the homoclinal McElroy assemblage from the structurally complex Larder Lake assemblage. South of the shear zone, the McElroy assemblage is nearly vertically dipping and faces to the northeast. North of the shear zone, the metavolcanic and metasedimentary rocks (Hearst

Figure 2-15: Outcrop exposure of Lincoln Nipissing Peridotite displaying polygonal jointing and a northwest trending fabric.

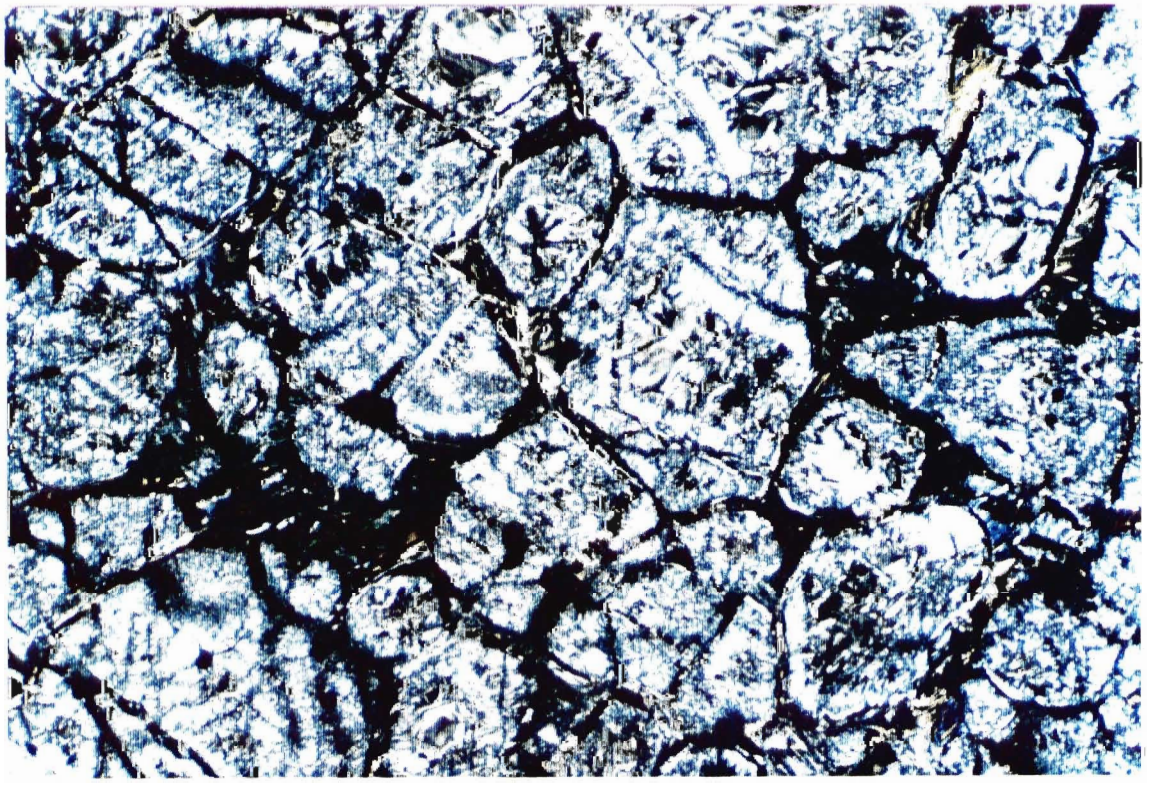

Figure 2-16: Photomicrograph of Lincoln Nipissing Peridotite displaying olivine pseudomorphs replaced by serpentine, chlorite and magnetite.

assemblage) rocks deformed about northeast and northwest striking folds and faults. In places, the shear zone is intensely carbonatized with ferro-dolomitization alteration (Figure 1-3). It has also been offset by northeast trending faults (e.g. Bensen Creek, Boston Creek and Manor Faults) and syenitic intrusions. South side up displacement along the shear zone is suggested, resulting in the present configuration (Hewitt 1951).

2.2.3 Boston Creek Fault

The Boston Creek Fault is a northeast trending, post-2700 Ma structure which separates the McElroy assemblage from the Boston assemblage (Jackson and Fyon 1991).

2.2.4 Skead assemblage

The amount of intermediate volcanoclastic material in the McElroy assemblage increases as the contact between the McElroy and Larder Lake assemblage is approached (Figure 2-17). In addition, the degree of deformation in both the intermediate and mafic rocks also increases (Figure 2-17). This is in contrast to the majority of the rocks in the McElroy assemblage which lack a penetrative fabric. Also, contacts between mafic and intermediate units away from the McElroy-Skead boundary do not appear deformed (Figure 2-18). Therefore, the contact between the McElroy and the Larder Lake assemblage is interpreted to be a fault.

2.2.5 Huronian Sedimentary Rocks

The McElroy assemblage is unconformaby overlain by the Cobalt Group.

2.3 Larder Lake assemblage

The Larder Lake assemblage is a discontinuous package of metavolcanic rocks

Figure 2-17: Deformed contact between mafic and intermediate volcanics near the Skead-McElroy boundary.

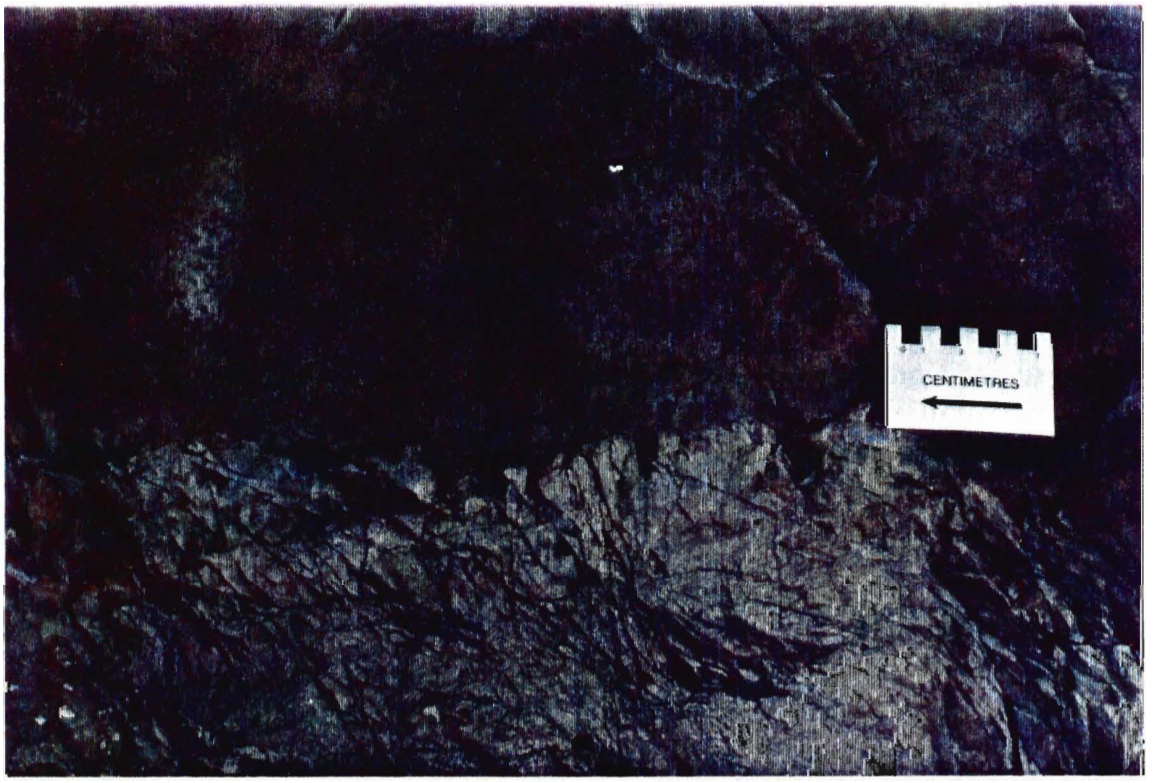

Figure 2-18: Undeformed contact between mafic and intermediate volcanics in the central part of the McElroy assemblage.

structurally disrupted by folds and faults (Figure 2-19). The Larder Lake assemblage is bounded to the north by the Cadillac Larder Shear Zone, to the west by the Boston Creek Fault, to the south by the Lincoln Nipissing Shear Zone and to the east by the Huronian Supergroup. The Larder Lake assemblage is also unconformably overlain by Hearst assemblage sediments.

Pillowed flows are abundant throughout the assemblage yielding abundant younging directions. The variation of the younging directions indicates that the Larder Lake assemblage is multiply folded (Thomson 1949). Folds strike west to northwest and may be offset by northeast to northwest trending faults (Figure 2-19). Shear zones 1-10 m wide are found throughout the assemblage. Rocks adjacent to areas of deformation tend to be stretched out and display a penetrative fabric. This type of deformation was not observed in the McElroy assemblage.

Rock types present in the Larder Lake assemblage are similar to the McElroy assemblage, however they occur in different proportions. The Larder Lake assemblage consists of variolitic, pillowed basalts (Figure 2-20) with minor associated coarse flows. Pillowed units are typically Mg or Fe-rich tholeiitic basalt and can be distinguished in the field based on their colour (Jensen and Langford 1985). Mg-rich tholeiites are light green to grey whereas Fe-rich tholeiites are dark green to black on weathered surfaces. Pillowed flows commonly contain spherules which coalesce to the centre of the pillow (Figure 2-20). The pillowed flows grade into fine grained to aphanitic massive flows and eventually coarse grained flows. Komatiite is common and displays both olivine spinifex and massive textures. The presence of olivine spinifex indicates a proximal eruptive pipe (Jensen 1985b). Peridotite intrusions cut the komatiite but not the underlying rocks (Jensen 1985b). This suggests that the komatiite volcanics were restricted to areas where the volcanic pile was not yet developed

Figure 2-19: Distribution of Larder Lake assemblage (modified after Jensen 1985b)

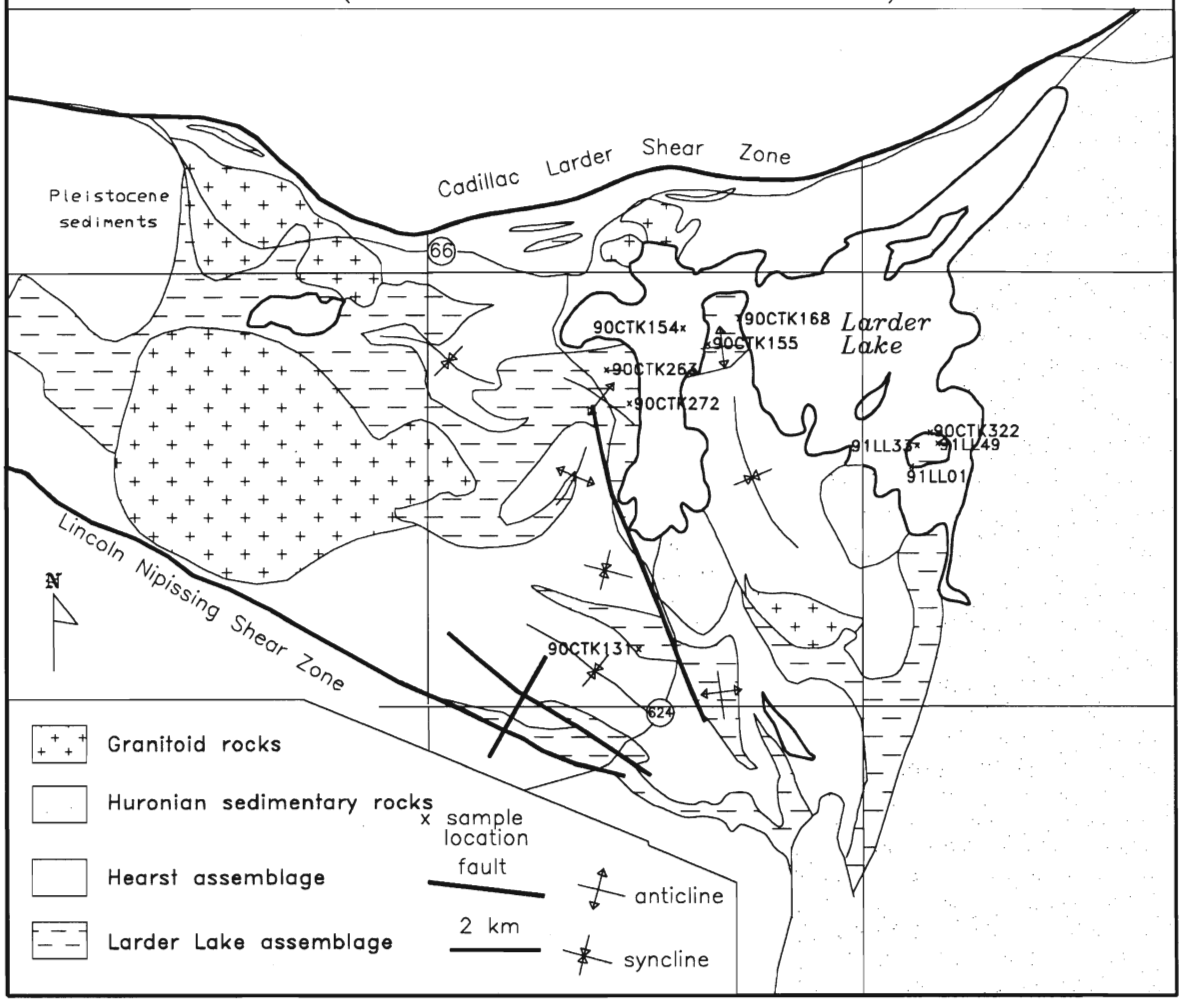

Figure 2-20: Spheriolitic pillowed basalt from the Larder Lake assemblage.

Figure 2-21: Spinifex texture in komatiite from the Larder Lake assemblage. Width of canoe paddle in top left of the photo is approximately 20 cm.

(Jensen 1985b) prior to tholeiitic magmatism.

In thin section the pillowed and fine grained massive flows are generally aphanitic and aphyric. Grain sizes are less than 0.1 mm. Typical greenschist facies minerals include actinolite (after clinopyroxene), epidotized plagioclase, carbonate, quartz, chlorite and opaques. Rare blastophenocrysts of actinolite are up to 1 mm. Grain sizes increase (up to 1 mm) in veins and fracture fillings. Grain boundaries are serrated in most samples. Coarser flows contain serrated actinolite crystals up to 2 mm in diameter with an aphanitic, plagioclase rich groundmass.

Intermediate volcaniclastic rocks are most abundant in the southern portion of the assemblage. These rocks yield ages of 2701 Ma (Corfu et al. 1989).

2.4 Summary

The major differences between the McElroy and Larder Lake assemblages is their lithologic abundance and structural style. The McElroy assemblage is characterized by abundant coarse grained, gabbroic textured rocks with minor aphanitic, pillowed flows. The Larder Lake assemblage contains more aphanitic pillowed flows and less coarser, grained massive flows. The McElroy assemblage also has a distinctive dendritic flow, plagioclase glomerophyric units and leucogabbro. The Larder Lake assemblage contains more komatiitic flows and fewer dendritic textured flows and no leucogabbroic units. The McElroy assemblage is homoclinal (Figure 2-2) whereas the Larder Lake assemblage is multiply folded and faulted.

Table 2 presents estimated primary igneous minerals and proportions of the major lithologic units in the assemblages. Table 3 compares the major rock types of the McElroy and Larder Lake assemblages.

The metamorphic grade in this area is lower greenschist (Jolly 1978,1980). Typical mineral associations include actinolite, epidote, chlorite, albite, quartz, opaques, sphene, carbonate and stilpnomelane. Relict pyroxene and olivine cores are rarely observed. Pseudomorphs of primary igneous minerals (olivine, pyroxene, plagioclase) have preserved igneous textures for most of both assemblages. Also, the absence of a penetrative fabric for most rocks indicates that deformation has been limited or it has been partitioned into discrete high strain zones. Both assemblages have been disrupted by syenitic intrusions towards the west (Figure 2-22). Although smaller stocks related to these intrusive bodies did not produce contact aureoles, but they did increase the amount of veining (epidote and carbonate) present in the adjacent rocks (Figure 2-23).

The similar metamorphic facies on either side of the LNSZ suggests that vertical displacement along the shear zone may have been limited and transcurrent movement may also have also been involved.

Figure 2-22: Syenite intruding fine grained massive flow in the northwest part of the McElroy assemblage.

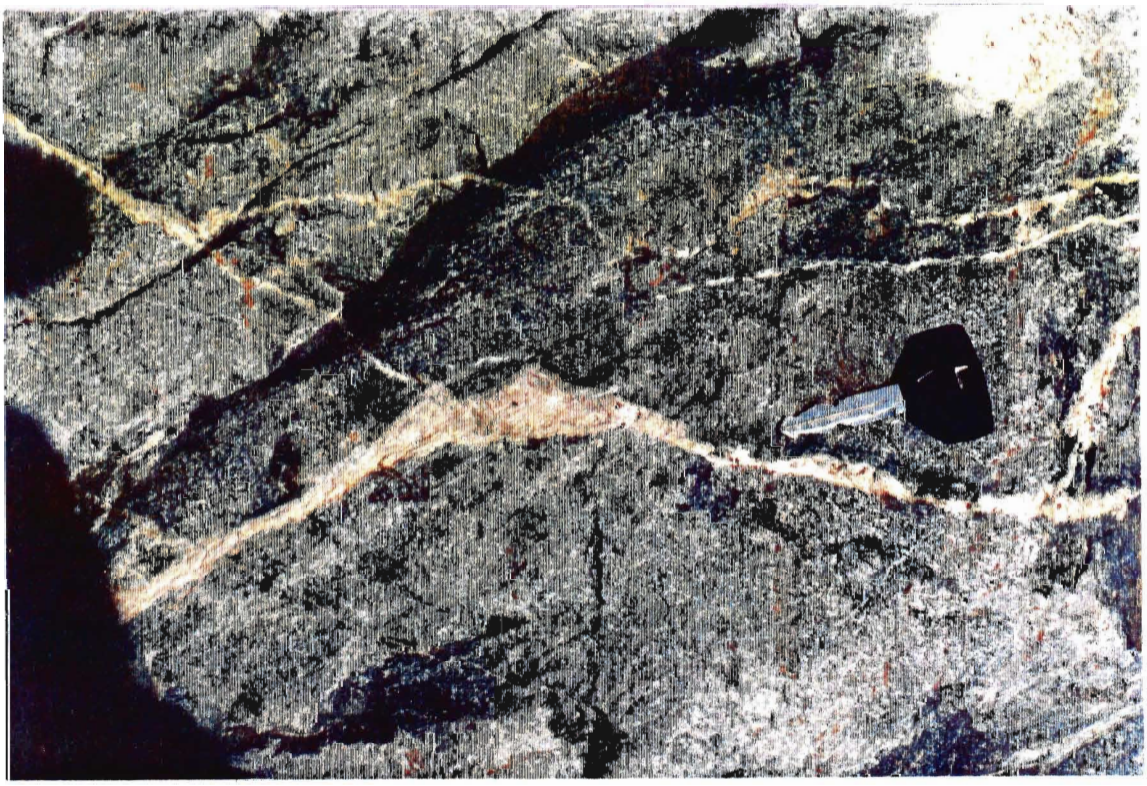

Figure 2-23: Epidote veining in medium grained massive flow in the northwest part of the McElroy assemblage. The epidote veining is thought to be the result of the syenite intrusions, since epidote veining is not extensive in the southeast part of the assemblage where there is no syenite.

Table 2: Visual petrographical estimates of the igneous mineral proportions (typical alteration assemblages are bracketed)

McElroy assemblage (% of assemb.)	GROUNDMASS <1mm	PYROXENE >1mm (act-chl-cb)	OLIVINE >1mm (serp-mt-cb)	PLAGIOCLASE >1mm (ep-cb-ab)
Serpentinite (not in McElroy)*	0-5%	0-5%	90-95%	0%
Aphanitic flow (10-15%)	80-90%	0-5%	0%	0-5%
Coarse flow (50-60%)	40-60%	20-30%	<5%	30-40%
Inter. flow (5%)	40-90%	<5%	0%	20-60%
Ulramafic flow (5%)	20-40%	20-40%	10-20%	0%
Leucogabbro (5%)	30-40%	15-20%	0%	60-70%
Dendritic flow (10-20%)	20-30%	20-40%	0%	40-60%
Larder Lake assemblage				
Aphanitic flows (80-90%)	80-90%	0-5%	0%	0-5%
Coarse flows (10-20%)	30-50%	20-30%	<5%	10-30%

* Serpentinite does not belong to the McElroy or Larder Lake assemblages, but is included for comparison

Table 3: Comparison of major rocks types found in McElroy and Larder Lake assemblages.

Rock Description	McElroy assemblage	Larder Lake assemblage
Lithologic Distribution	structurally homoclinal series of rocks facing northeast	rocks structurally complicated by folds and faults
Mafic Volcanic Rocks	pillowed basaltic flows grade into massive flows; commonly plagioclase glomerophyric	spherulitic pillowed basalts are common with minor massive flows
Gabbroic Textured Rocks	dendritic flow and leucogabbro located near base; knobby massive flows appear gabbroic	minor dendritic and knobby flows; leucogabbro is absent
Sedimentary Rocks	debris flows interbedded with volcanic flows	conglomerates and turbiditic wackes of Hearst assemblage unconformably overlie volcanic rocks
Intermediate to Felsic Pyroclastic Rocks	ash, crystal, lapilli and breccia tuffs are interbedded with mafic volcanic rocks	fewer flows than in McElroy assemblage; located near LNSZ
Ultramafic Rocks	Lincoln Nipissing Peridotite caps top of assemblage; minor massive flows	komatiitic flows with spinifex textures common; also massive ultramafic flows and peridotitic stocks

Chapter 3

Geochemistry of McElroy and Larder Lake Assemblages

3.1 Introduction

Major, trace and rare earth element (REE) abundances have been determined for four mafic metavolcanic assemblages in the Larder Lake region. The major komatiitic to tholeiitic rocks in this region are represented by 21 samples from the McElroy assemblage, 11 samples from the Larder Lake assemblage, 30 samples from the Catharine assemblage (Jackson in press) and 28 samples from the Kinojevis assemblage. The results are presented in Tables 4 and 5. Brief petrographic descriptions for the McElroy and Larder Lake assemblage samples are given in Appendix I and locations are presented in Figure 2-17 and 3-1 respectively. Locations for the Kinojevis assemblage samples are presented as UTM coordinates in Appendix II.

3.1.1 Purpose of Geochemistry Study

Geochemical analysis of the McElroy and Larder Lake assemblages was carried out to determine any chemical links between the two adjacent assemblages, and to follow up field and petrographic results. Internal relationships between the mafic rocks within the McElroy assemblage were also studied. All four assemblages are then compared with other mafic dominated metavolcanic assemblages in order to determine a possible petrogenetic model for the McElroy assemblage.

3.1.2 Methods

Major and trace elements for the McElroy, Larder Lake and Catharine assemblages were determined at the Ontario Geological Survey (OGS) Geoscience Laboratories. Major

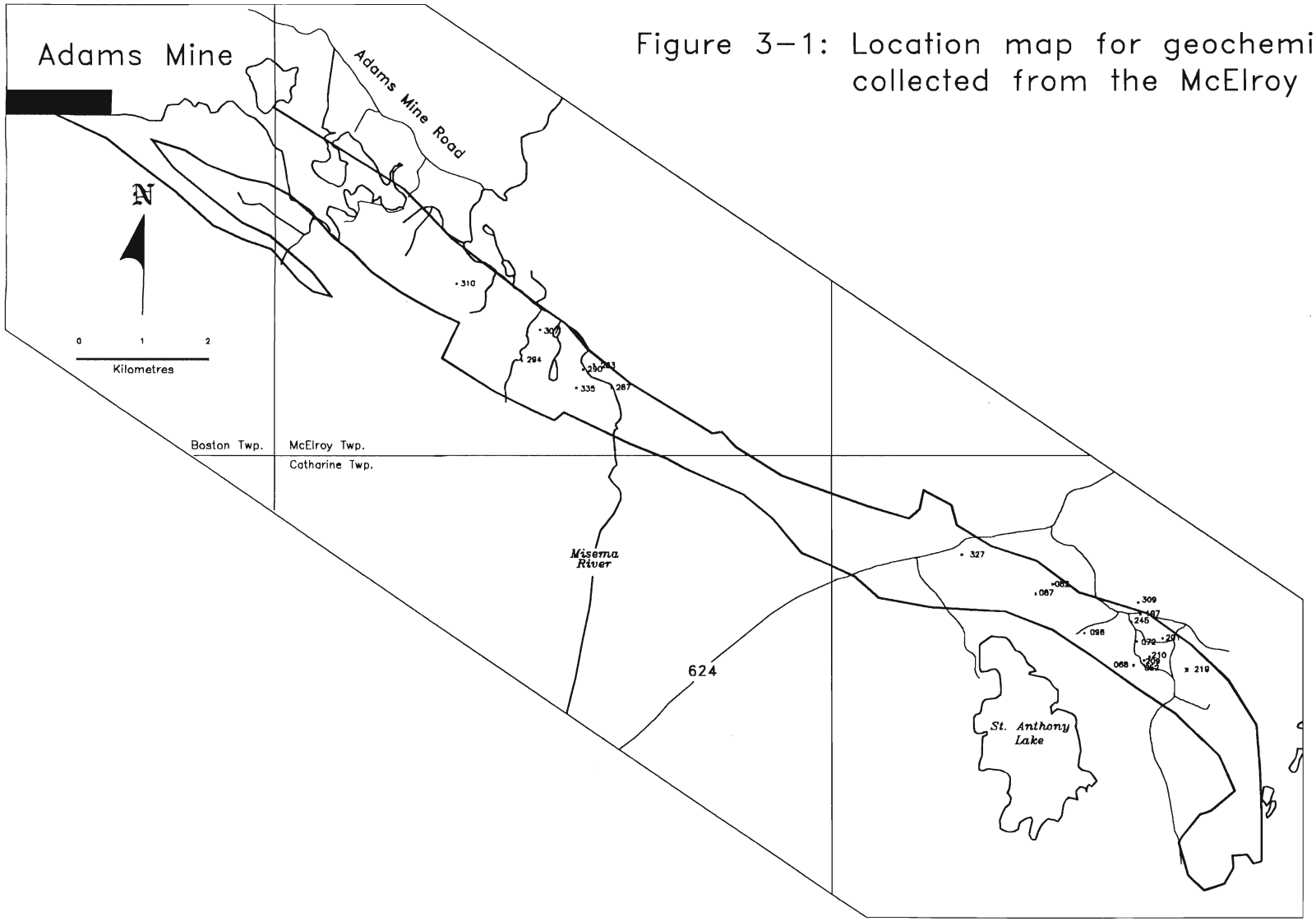

Figure 3–1: Location map for geochemical samples collected from the McElroy assemblage

Table 4: Major and trace element results for McElroy and Larder Lake assemblage

	Larder Lake Basalts												
Major oxides	90CTK045	90CTK131	90CTK154	90CTK155	90CTK263	90CTK272	90CTK322	91LL01	91LL20	91LL20d	91LL33-2	91LL49	AVERAGE
wt%	Fe-tholeiite	Fe-tholeiite	Mg-tholeiite	Mg-tholeiite	Fe-tholeiite	Tholeiitic and.	Mg-tholeiite	Fe-tholeiite	Mg-tholeiite	Mg-tholeiite	Mg-tholeiite	Mg-tholeiite	
SiO2	49.60	50.90	49.10	49.80	53.30	53.70	48.40	54.97	52.99	52.85	51.07	51.12	51.48
Al2O3	14.20	12.70	15.10	14.80	13.40	14.10	14.50	14.03	14.39	14.37	15.32	14.46	14.28
FeOTot	13.60	17.10	10.40	10.60	12.40	11.10	11.50	11.40	11.40	11.30	10.72	11.51	11.92
MgO	6.73	4.61	7.16	7.12	3.84	3.72	8.80	6.67	7.03	6.99	8.07	8.00	6.56
CaO	10.20	6.04	11.50	11.30	6.60	7.81	10.80	7.84	10.28	10.27	11.43	13.14	9.77
Na2O	2.57	3.27	1.32	1.52	3.63	2.61	1.68	3.50	3.12	3.11	2.15	1.00	2.46
K2O	0.36	0.89	1.01	0.30	0.84	0.91	0.09	0.25	0.14	0.14	0.22	0.09	0.44
TiO2	0.80	1.57	0.77	0.72	1.65	1.70	0.88	1.01	0.75	0.76	0.71	0.79	0.99
P2O5	0.05	0.14	0.07	0.07	0.14	0.14	0.06	0.10	0.07	0.08	0.05	0.06	0.09
MnO	0.16	0.21	0.22	0.22	0.27	0.26	0.18	0.17	0.22	0.22	0.18	0.23	0.21
CO2	0.15	0.36	0.23	0.53	0.96	1.39	0.61	NA	NA	NA	NA	NA	0.35
S	0.03	0.02	0.03	0.04	0.20	0.29	0.04	NA	NA	NA	NA	NA	0.05
LOI	1.00	1.80	2.00	2.40	2.40	3.00	2.40	NA	NA	NA	NA	NA	1.25
Mg#	42.70	38.45	54.66	52.58	31.07	30.74	52.35	36.91	38.14	38.22	42.95	41.00	41.65
Total	99.45	99.61	98.91	99.42	99.63	100.73	99.74	99.94	100.39	100.09	99.92	100.4	99.85
Trace element	90CTK045	90CTK131	90CTK154	90CTK155	90CTK263	90CTK272	90CTK322	91LL01	91LL20	91LL20d	91LL33-2	91LL49	AVERAGE
PPM													
Co		27	31	29		32	44						32.60
Cu		66	65	74		106	106	88	111	104	105	125	95.00
Ni		19	76	69		34	103	45	114	114	119	94	78.70
Sc		31	31	28		44	43	48	43	38	52	40	39.80
V		271	182	174		440	244	322	261	260	285	289	272.80
Y		24	11	10		32	15	34	25	25	13	18	20.70
Zn		92	54	54		135	84	72	86	86	79	86	82.80
Rb		28	31	11		33	6	5	3	3	7	1	12.80
Sr		134	117	187		188	157	59	268	269	84	32	149.50
Zr		104	46	48		111	46	113	71	71	36	43	66.90
CIPW Norm													
quartz	1.00	9.76	4.54	6.42	7.52	10.85	1.46	5.61	1.88	1.98	1.52	5.87	
orthoclase	2.13	5.26	5.97	1.77	4.96	5.38	0.53	1.48	0.83	0.83	1.30	0.53	
albite	21.74	27.67	11.17	12.86	30.71	22.08	14.21	29.61	26.40	26.31	18.19	8.46	
anorthite	26.15	17.35	32.30	32.68	17.79	24.07	31.76	21.84	24.85	24.84	31.51	34.70	
diopside	19.78	9.39	19.54	18.52	11.67	11.47	17.38	13.40	21.02	20.93	20.21	24.53	
hypersthene	19.66	10.97	15.33	16.39	14.75	15.12	25.24	21.32	19.64	19.39	21.67	20.43	
olivine	0.00	0.00	0.00	0.00	0.00	0.00	0.00	0.00	0.00	0.00	0.00	0.00	
magnetite	5.19	12.92	5.52	5.03	4.26	2.61	3.78	3.64	3.60	3.28	3.20	3.32	
ilmenite	1.52	2.98	1.46	1.37	3.13	3.23	1.29	1.92	1.42	1.44	1.35	1.50	
apatite	0.12	0.33	0.17	0.17	0.33	0.33	0.14	0.24	0.17	0.19	0.12	0.14	

	McElroy Aphanitic flows						Ultramafic flows			Leucogabbro
Major oxides	90CTK201	90CTK219	90CTK245	90CTK283	90CTK307	AVERAGE	90CTK052	90CTK072	AVERAGE	90CTK209
wt%	Fe-tholeiite	Tholeiitic and.	Fe-tholeiite	Fe-tholeiite	Fe-tholeiite		Basalt komatiit	Basalt komatiite		Mg-tholeiite
SiO2	48.90	44.20	49.20	50.40	49.60	48.46	42.70	44.90	43.80	48.20
Al2O3	13.90	13.40	13.90	13.60	13.50	13.66	9.36	11.00	10.18	17.40
FeOTot	14.10	11.80	13.90	13.60	17.10	14.10	14.80	13.00	13.90	10.30
MgO	6.40	3.35	5.01	7.10	6.02	5.58	19.10	15.70	17.40	6.96
CaO	9.89	12.30	9.15	7.32	6.91	9.11	7.27	8.54	7.91	8.27
Na2O	2.01	2.76	2.26	3.07	2.66	2.55	0.13	1.14	0.64	3.35
K2O	0.10	0.34	0.27	0.84	0.80	0.47	0.01	0.05	0.03	0.32
TiO2	0.90	1.04	1.06	0.77	0.99	0.95	0.56	0.59	0.58	0.70
P2O5	0.08	0.11	0.09	0.08	0.10	0.09	0.07	0.07	0.07	0.06
MnO	0.23	0.28	0.29	0.21	0.24	0.25	0.23	0.19	0.21	0.16
CO2	0.91	7.75	2.87	0.81	0.61	2.59	0.18	0.26	0.22	0.46
S	0.04	0.12	0.03	0.08	0.08	0.07	0.01	0.01	0.01	0.02
LOI	2.40	9.70	4.80	3.00	1.90	4.36	5.20	4.30	4.75	2.80
Mg#	39.02	28.13	33.38	45.60	35.37	36.30	61.41	61.23	61.32	49.15
Total	99.84	107.15	102.83	100.88	100.51	102.24	99.62	99.75	99.69	99.00

	Aphanitic flows						Ultramafic flows			
Trace element	90CTK201	90CTK219	90CTK245	90CTK283	90CTK307	AVERAGE	90CTK052			
PPM										
Co	32	34	34	42	50	38.40	80			
Cu	88	111	105	83	44	86.20	78			
Ni	39	31	31	59	43	40.60	482			
Sc	31	33	31	40	45	36.00	25			
V	179	215	212	224	302	226.40	144			
Y	14	19	17	17	25	18.40	13			
Zn	66	73	90	71	83	76.60	96			
Rb	NA	10	9	16	19	10.80	-5			
Sr	104	124	135	284	277	184.80	6			
Zr	59	81	89	60	76	73.00	39			
CIPW Norm										
quartz	3.84	0	5.29	1.41	3.14		0	0		0
orthoclase	0.59	2.01	1.6	4.96	4.73		0.06	0.3		1.89
albite	17.01	22.12	19.12	25.97	22.51		1.1	9.65		28.34
anorthite	28.61	23.17	26.99	20.85	22.54		24.93	24.75		31.5
diopside	16.65	31.15	14.83	12.18	9.18		8.61	13.82		7.44
hypersthene	22.58	0	19.92	22.94	25.42		31.73	23.27		12.32
olivine	0	3.95	0	0	0		23.11	18.16		8.62
magnetite	4.35	3.33	4.06	6.09	7.09		2.15	2.86		3.35
ilmenite	1.71	1.97	2.01	1.46	1.88		1.06	1.12		1.33
apatite	0.14	0.26	0.21	0.19	0.24		0.17	0.17		0.14

Table 4: Continued

	Medium to coarse flows									
Major oxides	90CTK082	90CTK087	90CTK197	90CTK290	90CTK294	90CTK294D	90CTK309	90CTK310	90CTK335	AVERAGE
wt%	Fe-tholeiite	Mg-tholeiite	Fe-tholeiite	Mg-tholeiite	Mg-tholeiite	Mg-tholeiite	Mg-tholeiite	Mg-tholeiite	Fe-tholeiite	
SiO2	48.60	45.50	48.20	50.50	48.70	49.00	50.80	48.60	48.80	49.18
Al2O3	14.20	15.60	13.90	14.00	14.30	14.30	14.30	14.90	13.60	14.26
FeOTot	14.10	9.92	15.40	11.90	11.70	11.40	8.65	9.85	14.30	11.16
MgO	7.34	10.20	6.27	7.79	7.90	7.52	7.58	8.90	4.51	7.28
CaO	7.97	10.80	7.72	7.88	11.10	11.20	10.70	10.60	9.31	10.58
Na2O	3.07	1.61	3.30	1.84	1.51	1.74	3.11	1.81	1.59	1.95
K2O	0.97	0.57	0.30	0.70	0.28	0.29	0.23	1.38	0.27	0.49
TiO2	0.79	0.60	0.87	0.93	0.78	0.79	0.65	0.67	1.21	0.82
P2O5	0.07	0.06	0.06	0.11	0.07	0.08	0.08	0.06	0.10	0.08
MnO	0.26	0.16	0.24	0.16	0.16	0.16	0.17	0.14	0.30	0.19
CO2	0.24	0.27	0.57	0.11	0.56	0.57	1.22	0.50	3.44	1.26
S	0.02	0.01	0.01	0.01	0.10	0.10	0.01	0.09	0.20	0.10
LOI	1.80	3.50	2.30	3.10	2.20	2.10	2.70	1.90	4.80	2.74
Mg#	42.77	60.00	36.73	48.45	52.01	51.44	48.04	59.97	30.45	48.38
Total	99.43	98.80	99.14	99.03	99.36	99.25	100.20	99.40	102.43	100.13

	Medium to coarse flows									
Trace element	90CTK082	90CTK087	90CTK197	90CTK290	90CTK294	90CTK294D	90CTK309	90CTK310		AVERAGE
PPM										
Co		30		36	38	39	36	38		36.17
Cu		27		29	114	119	36	68		65.50
Ni		114		59	75	78	91	104		86.83
Sc		24		40	37	39	33	36		34.83
V		131		246	213	214	263	186		208.83
Y		12		26	17	17	13	17		17.00
Zn		57		47	57	60	52	69		57.00
Rb		15		18	12	13	7	74		23.17
Sr		176		126	124	124	312	206		178.00
Zr		50		86	56	56	57	57		60.33
CIPW Norm										
quartz	0.00	0.00	0.00	5.84	4.20	3.96	0.00	0.00	8.78	
orthoclase	5.73	3.37	1.77	4.14	1.65	1.71	1.36	8.16	1.60	
albite	25.97	13.62	27.92	15.57	12.78	14.72	26.31	15.31	13.45	
anorthite	22.11	33.66	22.32	27.88	31.42	30.36	24.38	28.46	29.18	
diopside	13.94	15.71	12.98	8.55	18.76	19.97	23.10	19.02	13.67	
hypersthene	11.94	11.62	18.45	26.99	20.01	18.18	12.15	15.97	19.49	
olivine	10.30	11.58	4.98	0.00	0.00	0.00	7.09	3.20	0.00	
magnetite	4.64	3.44	4.94	3.91	5.23	5.10	0.00	4.73	4.16	
ilmenite	1.50	1.14	1.65	1.77	1.48	1.50	1.23	1.27	2.30	
apatite	0.17	0.14	0.14	0.26	0.17	0.19	0.19	0.14	0.24	

	Dendritic flows					
Major oxides	90CTK068	90CTK096	90CTK210	90CTK287	90CTK327	AVERAGE
wt%	Fe-tholeiite	Fe-tholeiite	Fe-tholeiite	Fe-tholeiite	Fe-tholeiite	
SiO2	51.00	50.20	51.40	51.40	51.50	51.10
Al2O3	13.10	13.30	13.40	13.50	14.40	13.54
FeOTot	16.20	15.30	14.60	13.70	11.00	14.16
MgO	4.71	5.09	5.01	5.77	6.20	5.36
CaO	7.09	8.59	8.34	8.54	9.45	8.40
Na2O	3.50	2.71	2.81	2.40	2.20	2.72
K2O	0.49	0.17	0.26	0.13	0.09	0.23
TiO2	1.54	1.40	1.30	1.10	0.75	1.22
P2O5	0.19	0.16	0.16	0.14	0.12	0.15
MnO	0.23	0.22	0.19	0.15	0.14	0.19
CO2	0.65	0.24	0.35	0.17	0.66	0.41
S	0.02	0.05	0.01	0.01	0.03	0.02
LOI	2.00	2.00	1.40	2.40	2.90	2.14
Mg#	32.06	34.98	33.92	41.48	49.17	38.32
Total	100.72	99.43	99.23	99.41	99.44	99.65

	Dendritic flows					
Trace element	90CTK068	90CTK096	90CTK210	90CTK287	90CTK327	AVERAGE
PPM						
Co	33	22	21	37	36	29.80
Cu	29	146	20	11	85	58.20
Ni	24	20	22	44	58	33.60
Sc	32	22	22	39	39	30.80
V	276	181	176	284	217	226.80
Y	28	18	19	32	33	26.00
Zn	61	53	25	40	72	50.20
Rb	15	8	8	7	7	9.00
Sr	158	229	141	165	138	166.20
Zr	115	111	114	111	122	114.60
CIPW Norm						
quartz	4.95	6.88	6.95	9.49		
orthoclase	2.9	1	1.54	0.77		
albite	29.61	22.93	23.78	20.31		
anorthite	18.59	23.63	23.19	25.66		
diopside	12.7	14.8	14.21	12.88		
hypersthene	17.41	16.87	18.44	17.64		
olivine	0	0	0	0		
magnetite	7.42	6.96	5.47	6.76		
ilmenite	2.92	2.66	2.47	2.09		
apatite	0.45	0.38	0.38	0.33		

Table 5: Trace element, REE and elemental ratios for metavolcanic units in the Larder Lake area.

	Y	Zr	Nb	Ba	La	Ce	Pr	Nd	Sm	Eu	Gd	Tb	Dy	Ho	Er	Tm	Yb	Lu	Hf	Ta	Th	SUM
Kinojevis South																						
KJ-3D	12.10	62.90	4.50	16.29	4.83	12.23	1.73	8.05	2.09	0.76	2.35	0.36	2.52	0.48	1.36	0.19	1.25	0.19	1.63	0.39	0.46	136.68
KJ-3	11.81	61.48	4.22	15.95	4.58	11.81	1.66	7.65	2.02	0.72	2.25	0.36	2.35	0.46	1.29	0.18	1.20	0.19	1.58	0.40	0.49	132.65
KJ-4	37.86	135.14	8.24	125.70	8.88	23.54	3.38	15.90	4.56	1.43	5.83	0.96	7.07	1.45	4.25	0.64	4.33	0.66	3.50	0.57	0.88	394.77
KJ-10	36.96	115.16	6.23	57.92	6.13	17.27	2.69	13.39	4.29	1.36	5.69	0.94	7.03	1.44	4.33	0.62	4.17	0.66	3.19	0.56	0.58	290.61
KJ-27	38.23	121.49	6.84	97.06	7.94	20.84	3.05	14.63	4.37	1.38	5.64	0.96	7.02	1.45	4.40	0.65	4.25	0.63	3.35	0.64	0.75	345.56
AVERAGE	27.39	99.23	6.01	62.59	6.47	17.14	2.50	11.93	3.47	1.13	4.35	0.72	5.20	1.06	3.13	0.45	3.04	0.47	2.65	0.51	0.63	260.05
Larder Lake																						
91LL49	15.93	44.83	2.35	22.12	1.97	5.79	0.93	4.98	1.70	0.58	2.38	0.41	2.95	0.60	1.83	0.27	1.76	0.26	1.23	0.50	0.15	113.54
90CTK131	32.66	103.32	5.14	123.44	5.33	14.60	2.27	11.36	3.63	1.23	4.77	0.83	6.19	1.26	3.87	0.57	3.83	0.59	3.06	0.27	0.51	328.77
90CTK155	15.19	42.94	2.10	85.48	2.65	6.65	1.01	5.16	1.69	0.64	2.25	0.39	2.90	0.57	1.77	0.26	1.70	0.26	1.28	0.11	0.15	175.14
90CTK322	14.59	42.52	1.87	36.76	2.16	5.86	0.94	4.71	1.58	0.64	2.25	0.37	2.82	0.57	1.69	0.25	1.63	0.26	1.25	0.10	0.14	124.94
AVERAGE	19.60	58.40	2.86	67.45	3.03	8.22	1.29	6.55	2.15	0.77	2.91	0.50	3.72	0.75	2.29	0.34	2.23	0.35	1.71	0.24	0.24	185.60
McElroy																						
90CTK201	19.57	57.49	2.82	26.54	3.24	8.59	1.32	6.42	2.00	0.73	2.76	0.47	3.66	0.76	2.31	0.36	2.33	0.35	1.67	0.14	0.27	143.79
90CTK245	24.19	85.33	3.96	153.84	4.85	12.69	1.85	9.18	2.78	0.96	3.55	0.62	4.65	0.94	2.90	0.43	2.85	0.43	2.38	0.23	0.45	319.04
90CTK283	18.74	53.91	2.46	108.95	2.93	7.84	1.20	6.03	1.94	0.60	2.67	0.45	3.55	0.74	2.25	0.33	2.27	0.35	1.42	0.13	0.27	219.03
90CTK287	31.29	113.64	5.49	37.07	5.39	15.57	2.38	11.90	3.64	1.09	4.83	0.80	6.06	1.19	3.64	0.52	3.55	0.53	2.99	0.33	0.57	252.46
90CTK052	14.25	36.76	2.67	7.17	2.50	6.69	1.01	4.91	1.59	0.53	2.26	0.36	2.66	0.55	1.66	0.23	1.53	0.24	1.02	0.12	0.24	88.96
90CTK098	31.50	107.16	5.54	59.25	7.03	17.49	2.52	12.09	3.73	1.22	4.87	0.82	6.01	1.21	3.62	0.53	3.56	0.53	2.81	0.29	0.54	272.31
AVERAGE	23.26	75.71	3.82	65.47	4.32	11.48	1.71	8.42	2.61	0.86	3.49	0.58	4.43	0.90	2.73	0.40	2.68	0.41	2.05	0.21	0.39	215.93
Blake River (1)																						
86-5		86.00			9.70	20.20		10.30	2.50	0.82		0.49	2.90	0.71	1.70		1.53	0.26		0.67	1.04	138.82
86-6A		96.00			10.00	21.80		11.10	2.70	0.88		0.51	3.40	0.70	1.70		1.90	0.31		0.93	1.14	153.07
86-10A		108.00			14.60	27.00		11.50	2.70	0.88		0.57	3.40	0.83	1.50		2.00	0.30		1.31	1.91	176.50
86-17		104.00			12.10	25.00		13.20	3.20	0.72		0.70	4.00	1.12	2.30		2.60	0.42		0.85	1.80	172.01
86-11A		208.00			20.20	46.00		24.00	6.40	1.32		1.57	8.80	1.92	4.80		5.80	0.91		2.10	3.50	335.32
86-12		215.00			18.90	44.00		23.00	5.90	0.97		1.46	8.80	1.90	5.60		7.00	1.07		2.20	4.30	340.10
CM-21a		218.00			22.00	53.00		28.00	6.90	1.05		1.42	7.70	1.74	5.00		4.70	0.70		3.30	4.30	357.81
AVERAGE		147.86			15.36	33.86		17.30	4.33	0.95		0.96	5.57	1.27	3.23		3.65	0.57		1.62	2.57	239.09
Kinojevis North (1)																						
F-637		33.00			1.69	4.50		5.10	1.44	0.59		4.00	2.60	0.59	1.70		1.81	0.32		1.32	0.07	58.73
F-462		103.00			6.00	15.40		13.40	4.30	1.70		1.21	6.30	1.36	4.30		4.30	0.70		14.74	0.46	177.17
F-377		146.00			7.70	23.00		20.00	6.50	2.05		1.69	9.90	2.10	6.00		6.40	1.06		2.03	0.75	235.20
F-464		290.00			14.80	43.00		35.00	11.00	3.00		2.90	17.10	3.60	10.00		11.20	1.81		3.00	1.50	447.91
F-414		458.00			62.00	130.00		74.00	19.20	4.80		4.60	25.90	5.90	15.50		16.60	2.50		5.90	2.80	827.70
AVERAGE		206.00			18.44	43.18		29.50	8.49	2.43		2.88	12.36	2.71	7.50		8.06	1.28		5.40	1.12	349.34
Catharine (2)																						
5000	21.00	72.00			3.20	8.70	1.30	7.30	2.50	0.93	3.50	0.60	4.10	0.87	2.50	0.38	2.40	0.39				131.67
5005	27.00	110.00			4.20	12.00	1.80	10.00	3.50	1.30	5.00	0.84	5.90	1.20	3.50	0.51	3.20	0.48				190.43
5010	13.00	75.00			2.80	8.20	1.30	6.80	2.60	0.86	3.30	0.60	4.10	0.88	2.60	0.38	2.40	0.35				125.17
5016	17.00	89.00			3.60	11.00	1.70	8.80	3.00	0.83	3.30	0.58	3.80	0.75	2.00	0.27	1.50	0.21				147.34
5020	20.00	93.00			4.10	12.00	1.80	9.90	3.40	1.10	4.30	0.72	4.50	0.92	2.30	0.33	2.00	0.27				160.64
5024	17.00	88.00			2.90	8.80	1.50	8.10	2.80	0.66	3.70	0.63	3.80	0.78	2.00	0.29	1.80	0.23				142.99
5026	22.00	96.00			5.00	13.00	1.80	9.10	2.90	1.10	3.60	0.64	4.30	0.90	2.60	0.38	2.60	0.36				166.28
5029	21.00	102.00			5.30	14.00	2.00	11.00	3.40	1.30	4.30	0.71	4.60	0.92	2.40	0.35	2.20	0.32				175.80
AVERAGE	19.75	90.63			3.89	10.96	1.65	8.86	3.01	1.01	3.88	0.67	4.39	0.90	2.49	0.36	2.26	0.33				155.04
N-MORB (3)	28.00	74.00	2.33	6.30	2.50	7.50	1.32	7.30	2.63	1.02	3.68	0.67	4.55	1.01	2.97	0.46	3.05	0.46	2.05	0.13	0.12	152.04
E-MORB (3)	22.00	73.00	8.30	57.00	6.30	15.00	2.05	9.00	2.60	0.91	2.97	0.53	3.55	0.79	2.31	0.36	2.37	0.35	2.03	0.47	0.60	212.49
OIB (3)	29.00	280.00	48.00	350.00	37.00	80.00	9.70	38.50	10.00	3.00	7.62	1.05	5.60	1.06	2.62	0.35	2.16	0.30	7.80	2.70	4.00	920.46
PRIM MAN (3)	4.55	11.20	0.71	6.99	0.69	1.78	0.28	1.35	0.44	0.17	0.60	0.11	0.74	0.16	0.48	0.07	0.49	0.07	0.31	0.04	0.09	31.32
IAT (4)	12.00	22.00	0.70	110.00	1.30	3.70		3.40	1.20												0.25	154.55
CHOND (3)	2.25	5.54	0.38	3.41	0.37	0.96	0.14	0.71	0.23	0.09	0.31	0.06	0.38	0.09	0.25	0.04	0.25	0.04	0.18	0.03	0.04	15.71

(1) Fowler and Jensen,1989
(2) Jackson in press
(3) Sun and McDonough 1989
(4) Sun 1982

Table 5: Continued

	La/Yb	La/Sm	Ba/Yb	Sm/Yb	La/Nb	Hf/Ta	Ce/La	Ba/Zr	Zr/La	Zr/Ce	Ce/Nb	Th/Nb	Ce/Zr	Ba/Zr
Kinojevis South														
KJ-3D	3.85	2.31	13.00	1.67	1.07	4.20	2.53	0.26	13.03	5.14	2.72	0.10	0.19	0.26
KJ-3	3.82	2.27	13.29	1.68	1.08	3.95	2.58	0.26	13.42	5.21	2.79	0.12	0.19	0.26
KJ-4	2.05	1.95	29.05	1.05	1.08	6.14	2.65	0.93	15.21	5.74	2.86	0.11	0.17	0.93
KJ-10	1.47	1.43	13.90	1.03	0.98	5.68	2.82	0.50	18.79	6.67	2.77	0.09	0.15	0.50
KJ-27	1.87	1.82	22.83	1.03	1.16	5.27	2.63	0.80	15.31	5.83	3.05	0.11	0.17	0.80
AVERAGE	2.61	1.95	18.41	1.29	1.08	5.05	2.64	0.55	15.15	5.72	2.85	0.11	0.17	0.63
Larder Lake														
91LL49	1.12	1.16	12.60	0.97	0.84	2.48	2.94	0.49	22.78	7.74	2.47	0.07	0.13	0.49
90CTK131	1.39	1.47	32.22	0.95	1.04	11.26	2.74	1.19	19.37	7.08	2.84	0.10	0.14	1.19
90CTK155	1.56	1.57	50.25	0.99	1.26	11.78	2.51	1.99	16.19	6.46	3.17	0.07	0.15	1.99
90CTK322	1.33	1.37	23.82	0.97	1.16	12.71	2.71	0.91	19.66	7.26	3.13	0.07	0.14	0.91
AVERAGE	1.35	1.39	29.72	0.97	1.07	9.56	2.72	1.15	19.50	7.13	2.87	0.08	0.14	1.15
McElroy														
90CTK201	1.39	1.62	11.40	0.86	1.15	11.73	2.65	0.46	17.73	6.69	3.05	0.10	0.15	0.46
90CTK245	1.70	1.75	53.95	0.97	1.23	10.46	2.62	1.80	17.60	6.72	3.21	0.11	0.15	1.80
90CTK283	1.29	1.51	48.01	0.85	1.19	10.59	2.68	2.02	18.42	6.88	3.19	0.11	0.15	2.02
90CTK287	1.52	1.48	10.45	1.03	0.98	9.05	2.89	0.33	21.07	7.30	2.84	0.10	0.14	0.33
90CTK052	1.63	1.57	4.68	1.04	0.93	8.45	2.68	0.20	14.71	5.49	2.50	0.09	0.18	0.20
90CTK096	1.97	1.88	16.64	1.05	1.27	9.60	2.49	0.55	15.25	6.13	3.16	0.10	0.16	0.55
AVERAGE	1.58	1.64	24.19	0.97	1.13	9.98	2.67	0.89	17.46	6.54	3.00	0.10	0.15	0.86
Blake River														
86-5	6.34	3.86		1.63			2.08		8.87	4.26			0.23	
86-6A	5.26	3.70		1.42			2.18		9.60	4.40			0.23	
86-10A	7.30	5.41		1.35			1.85		7.40	4.00			0.25	
86-17	4.65	3.78		1.23			2.07		8.60	4.16			0.24	
86-11A	3.48	3.16		1.10			2.28		10.30	4.52			0.22	
86-12	2.70	3.20		0.84			2.33		11.38	4.89			0.20	
CM-21a	4.68	3.19		1.47			2.41		9.91	4.11			0.24	
AVERAGE	4.92	3.76		1.29			2.17		9.43	4.33			0.23	
Kinojevis North														
F-637	0.93	1.17		0.80			2.66		19.53	7.33			0.14	
F-462	1.40	1.40		1.00			2.57		17.17	6.69			0.15	
F-377	1.20	1.18		1.02			2.99		18.96	6.35			0.16	
F-464	1.32	1.35		0.98			2.91		19.59	6.74			0.15	
F-414	3.73	3.23		1.16			2.10		7.39	3.52			0.28	
AVERAGE	1.72	1.67		0.99			2.64		16.53	6.13			0.21	
Catharine														
5000	1.33	1.28		1.04			2.72	0.00	22.50	8.28			0.12	
5005	1.31	1.20		1.09			2.86	0.00	26.19	9.17			0.11	
5010	1.17	1.08		1.08			2.93	0.00	26.79	9.15			0.11	
5016	2.40	1.20		2.00			3.06	0.00	24.72	8.09			0.12	
5020	2.05	1.21		1.70			2.93	0.00	22.68	7.75			0.13	
5024	1.61	1.04		1.56			3.03	0.00	30.34	10.00			0.10	
5026	1.92	1.72		1.12			2.60	0.00	19.20	7.38			0.14	
5029	2.41	1.56		1.55			2.64	0.00	19.25	7.29			0.14	
AVERAGE	1.78	1.29		1.39			2.85	0.00	23.96	8.39			0.12	
N-MORB	0.82	0.95	2.07	0.86	1.07	15.53	3.00	0.09	29.60	9.87	3.22	0.05	0.10	0.09
E-MORB	2.66	2.42	24.05	1.10	0.76	4.32	2.38	0.78	11.59	4.87	1.81	0.07	0.21	0.78
OIB	17.13	3.70	162.04	4.63	0.77	2.89	2.16	1.25	7.57	3.50	1.67	0.08	0.29	1.25
PRIM MAN	1.39	1.55	14.18	0.90	0.96	7.54	2.58	0.62	16.30	6.31	2.49	0.12	0.16	0.62
IAT		1.08			1.86		2.85	5.00	16.92	5.95	5.29	0.36	0.17	5.00
CHOND	1.48	1.59	13.75	0.93	0.98	6.88	2.61	0.62	15.10	5.79	2.55	0.11	0.17	0.62

and trace elements for the Kinojevis assemblage and additional Larder Lake samples were determined at the Memorial University of Newfoundland (MUN). The major oxides were analyzed by X-ray fluorescence on fused discs at both laboratories. Trace elements analyzed at the OGS laboratories were done by inductively coupled plasma-optical emission spectrometry (ICP-OES) while trace elements determined at the MUN laboratories were done by X-ray fluorescence on pressed pellets. Rare earth elements for the Catharine assemblage were determined at the OGS by inductively coupled plasma-mass spectrometry (ICP-MS) while REE for the McElroy, Larder Lake and the Kinojevis assemblages were completed at the MUN, also by ICP-MS. Precision for REE at MUN is generally less than 10% (Longerich et al. 1990). A comparison of the precision and limits of determination for both laboratories for the major and trace elements is presented in Table 6 and for the REE in Table 7.

Table 6: Elemental precision between Ontario Geological Survey Geoscience Laboratories and the Memorial University of Newfoundland.

OGS				MUN			
Oxide (wt%) XRF	Prec.	Trace (ppm) ICP-OES	Limit/ Prec!	Oxide (wt%) XRF	Prec.	Trace (ppm) XRF	Limit ppm/ Prec%
SiO_2	0.8%	Co	5 10	SiO_2	0.3%	Ba	23 0.97
Al_2O_3	0.3%	Cu	5 10	Al_2O_3	0.3%	Cu	3 1.23
Fe_2O_{3T}	0.2%	Ni	5 10	Fe_2O_{3T}	0.2%	Ni	4 1
MgO	0.3%	Sc	2 5	MgO	0.6%	Sc	6 0
Na_2O	0.5%	V	5 10	Na_2O	0.8%	V	6 0
K_2O	0.15%	Y	5 10	K_2O	1.3%	Y	0.7 0.12
CaO	0.15%	Zn	5 10	CaO	0.3%	Zn	3 0.93
P_2O_5	0.05%	Rb		P_2O_5	2.5%	Rb	0.8 0.08
TiO2	0.12%	Sr	5 15	TiO_2	0.9%	Sr	1.2 0.13
MnO	0.015%	Y*	5 10	MnO	2.7%	Nb	0.7 0.37
		Zr	5 10			Zr	1.1 0.21

! Precision is quoted (in ppm) at the 95% confidence limit for a value at 10X the determination limit (OGS Geoscience Laboratories,1989)

* Y analyzed by XRF.

Table 7: Comparison of REE limits and precision between OGS and MUN laboratiories. Rare earth elements were analyzed by ICP-MS at both laboratories.

ELEMENT	OGS		MUN	
	LIMIT (ppm)	PREC. !	LIMIT	PREC. %
La	0.05	0.05	0.002	3.3
Ce	0.05	0.05	0.003	6.2
Pr	0.05	0.05	0.002	8.4
Nd	0.18	0.18	0.001	8.3
Sm	0.15	0.15	0.001	5.7
Eu	0.07	0.07	0.001	12.3
Gd	0.14	0.14	0.002	14.9
Tb	0.03	0.03	0.005	6.7
Dy	0.13	0.13	0.005	11.1
Ho	0.03	0.03	0.002	4.0
Er	0.10	0.10	0.001	9.7
Tm	0.03	0.03	0.003	7.6
Yb	0.11	0.11	0.003	16.6
Lu	0.04	0.04	0.003	3.9

! Precision is quoted (in ppm) at the 95% confidence limit for a value at 10X the determination limit (OGS Geoscience Laboratories,1989)

3.1.3 Sample Selection

Extreme care was employed in sample selection to avoid analysis of altered rocks. Weathered, fracture surfaces or any signs of visible alteration at sample localities were avoided in the field. Sample bags containing 2 to 3 kg of chip samples were collected in the field. Petrographic results in collaboration with major and trace element geochemical results were used in combination prior to selection of samples for REE analysis.

Samples were taken from visibly, fresh, massive to pillowed flows. Amygdaloidal, variolitic or brecciated horizons were avoided. Intermediate volcaniclastic rocks were not sampled since most of these flows were fragmental or reworked and therefore do not represent a true magmatic signature. Ultramafic komatiites, particularly from the Larder Lake assemblage were excluded because visibly unaltered samples were rare.

From the McElroy assemblage, 5 aphanitic flows, 8 medium grained massive flows, 5 dendritic flows, 2 ultramafic flows and 1 leucogabbro were analyzed. In the Larder lake assemblage, 9 aphanitic flows and 2 medium grained flows were analyzed. All Catharine and Kinojevis rocks are fresh, fine grained to aphanitic mafic rocks.

3.2 Alteration

3.2.1 Introduction

Variation in elemental abundances of rocks can be attributed to primary variation in the bulk chemistry of the magma source, variable degrees of partial melting, assimilation or fractionation. Once in place, rocks may be subjected to secondary alteration processes such as weathering and metasomatism which may effect the chemical signature of the rock. Archean rocks (>2.5 Ga) must be tested for secondary alteration prior to any studies of their primary chemistry.

In modern settings, the alteration of subaqueous basalts with seawater occurs instantaneously upon eruption. Seawater reacts with basalts between 10-28°C. This can create a chlorite-rich assemblage containing >15% chlorite and <15% epidote and/or an epidote-rich assemblage containing >15% epidote and <15% chlorite. Factors influencing alteration assemblage formation include the rock porosity, water/rock ratio, temperature, pressure and the composition of the circulating fluid (Humphris and Thompson 1978a).

Major oxide changes in the chlorite-rich assemblage includes an increase in FeO_T, MgO and TiO_2 (slight increase) and a decrease in SiO_2 and CaO. Al_2O_3 and Na_2O remain unchanged. In the epidote assemblage, major oxide changes include increases in SiO_2 and Na_2O, and decreases in FeO_T, MgO, CaO and TiO_2 (slight decrease) and no change in Al_2O_3 (Humphris and Thompson 1978a). Trace element variations during seafloor hydrothermal alteration include the mobilisation of Sr, Cu, B, Li, Ba, Mn, Ni and Co although some precipitation into secondary mineral assemblages may occur. Vanadium, Y, Zr and Cr do not appear to show mobility due to hydrothermal alteration (Humphris and Thompson 1978b). However, high field strength elements (Ti, P, Zr, Nb, Y) have been shown to be mobile during greenschist facies metamorphism with variable CO_2 activities (Murphy and Hynes 1986). Rare earth element concentrations do not appear to be affected by typical hydrothermal or metamorphic fluid/rock interactions (Bau 1991). Rare earth elements generally considered immobile at greenschist facies metamorphism (Menzies et al. 1979) have been shown to be mobile in amygdaloidal flows (Nystrom 1984).

Abitibi supracrustal rocks have been metamorphosed to regional sub-greenschist to greenschist facies assemblages characterized by prehnite and pumpellyite. Upper greenschist to amphibolite facies contact metamorphic aureoles overprint the regional metamorphic pattern (Jolly 1978a, 1980). Based on the metamorphic history of the region the possibility of element mobility exists.

Gelinas et al. (1982) show that mafic metavolcanic rocks in the Abitibi are characterized by three types of alteration 1) chlorite-epidote-actinolite; 2) chlorite-epidote; and 3) chlorite +/- sericite. However, even though rocks are altered, 40% of the rocks retain pristine FeO/MgO ratios. The chemical changes that do affect the mafic metavolcanic rocks do not cause the rocks to lose their tholeiitic or calc-alkaline affinity.

Ludden et al. (1982) have shown that for Archean metavolcanic rocks at greenschist facies the alkaline elements K, Rb and Ba show large degrees of mobility while high field strength elements and REE remain relatively unchanged.

3.2.2 Major Element Alteration

Awareness of element mobility is important when considering primary geochemical variations. Thus, changes due to alteration must be distinguished from primary diversity. The following section attempts to document the possibility of element mobility within the McElroy and Larder Lake assemblages. Beswick and Soucie (1978) used a graphical procedure to detect metasomatic modification of analytical data in Precambrian metavolcanic suites. They plotted unaltered Mesozoic felsic to ultramafic rocks as oxide molecular proportion ratios in the form log X/Z vs. log Y/Z where X, Y and Z are major oxides. The data set of unaltered Mesozoic rocks formed specific trends on the diagrams. It was suggested by Beswick and Soucie (1978), that Precambrian rocks could also be plotted on the same diagrams and that any deviation from the Meszoic range was the result of metasomatism if oxide X was an immobile element, Y was the element of interest and Z was an immobile normalizing element to reduce scatter due to fractionation. The method assumed that the altered rocks of interest originally had compositions which when plotted on diagrams would conform with trends from the unaltered Mesozoic rock suites. They also assumed that the high field strength elements (HFS) and Al_2O_3 were immobile during metasomatic conditions. Any scatter on the diagrams would be the result of Y mobility since X and Z are immobile elements (Figure 3-2 c). Beswick and Soucie (1978) suggested that these diagrams can be used to detect and eventually correct for metasomatic alteration. This study employed a sligthly modified technique from that of Beswick and Soucie (1978) to identify mobile elements. Instead of plotting hundreds of unaltered Mesozoic rocks, correlation coefficients

a)

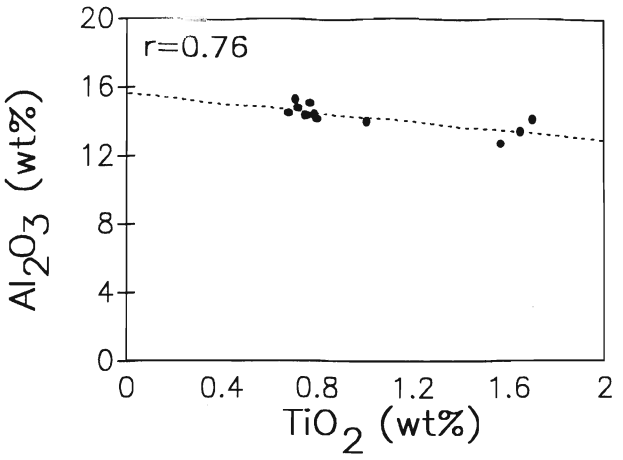

b)

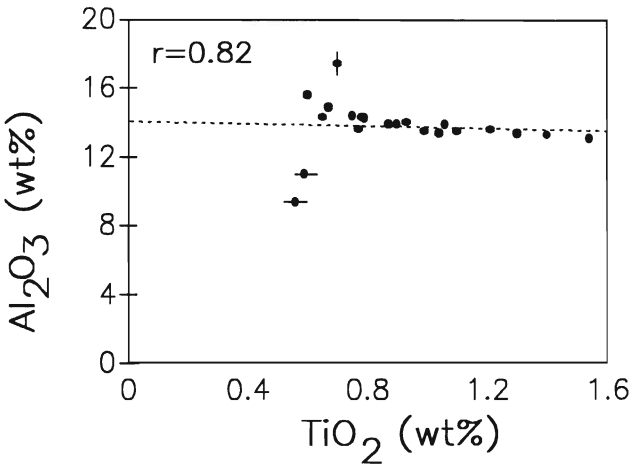

c)

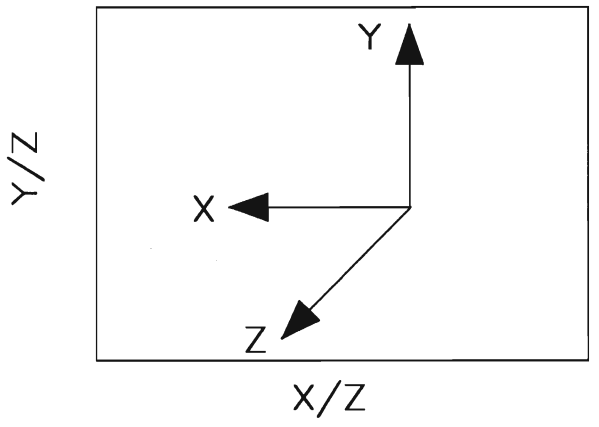

Figure 3-2: Variation plot between Al_2O_3 and TiO_2 for a) Larder Lake and b) McElroy assemblage. The good linear trends imply that Al_2O_3 and TiO_2 have remained relatively immobile since formation. The exception to this case are the ultramafic flows in the McElroy assemblage (b), shown as a dot with a horizontal line which fall below the regression line. These samples lack plagioclase and therefore have low aluminum values. They also have low titanium values which will be reflected in the following figures. c) Vertical scatter is due to element Y, horizontal scatter is due to element X and scatter in the 45 degree angle is due to element Z.

were calculated by the least squares method to identify possible element mobility. This method is preferred since it is dependent only on the data of the specific study. Correlation coefficients document the degree agreement between data points on a graph. High correlation coefficients (approaching 1.0) have the greatest agreement whereas low correlation coefficients (approaching 0) have the least agreement. Therefore the degree of mobility is based on the correlation coefficient (r) where limited mobility (r=0.70-1.00), moderate mobility (r=0.30-0.70) and extreme mobility (r=0-0.30) is arbitrarily defined since the literature lacks a definite scale of mobility.

This method required the identification of two relatively immobile oxides to be used as the X and Z components in the oxides ratios. The immobility of TiO_2 and Al_2O_3 in the Larder Lake and McElroy assemblages is illustrated in Figures 3-2 a and b, respectively. When plotted against each other, TiO_2 and Al_2O_3 show a good linear relationship indicating limited mobility (r=0.76 for Larder Lake and r=0.82 for McElroy assemblage rocks, excluding leucogabbro and ultramafic rocks). A high correlation coefficient on a binary X vs.Y variation diagram will result if the rock retains a prisitne element concentration or if the two elements were fractionating out with the same proportions. The latter case is unlikely, since this would require that an Al_2O_3 phase (plagioclase) and a TiO_2 phase (magnetite) fractionate out with the same proportions. The two McElroy samples (dot with horizontal line) with low Al_2O_3 contents are ultramafic flows which have low plagioclase contents. The leucogabbro sample (dot with vertical line) plots above the trend, which is a function of its anomalously high plagioclase content. Therefore, major and trace elements can be compared to these elements to document the degree of alteration which may have affected the rocks.

The possibility of element mobility is investigated in Figure 3-3. On Figure 3-3 linear trends illustrate immobility while scattered trends suggest some degree of secondary mobility

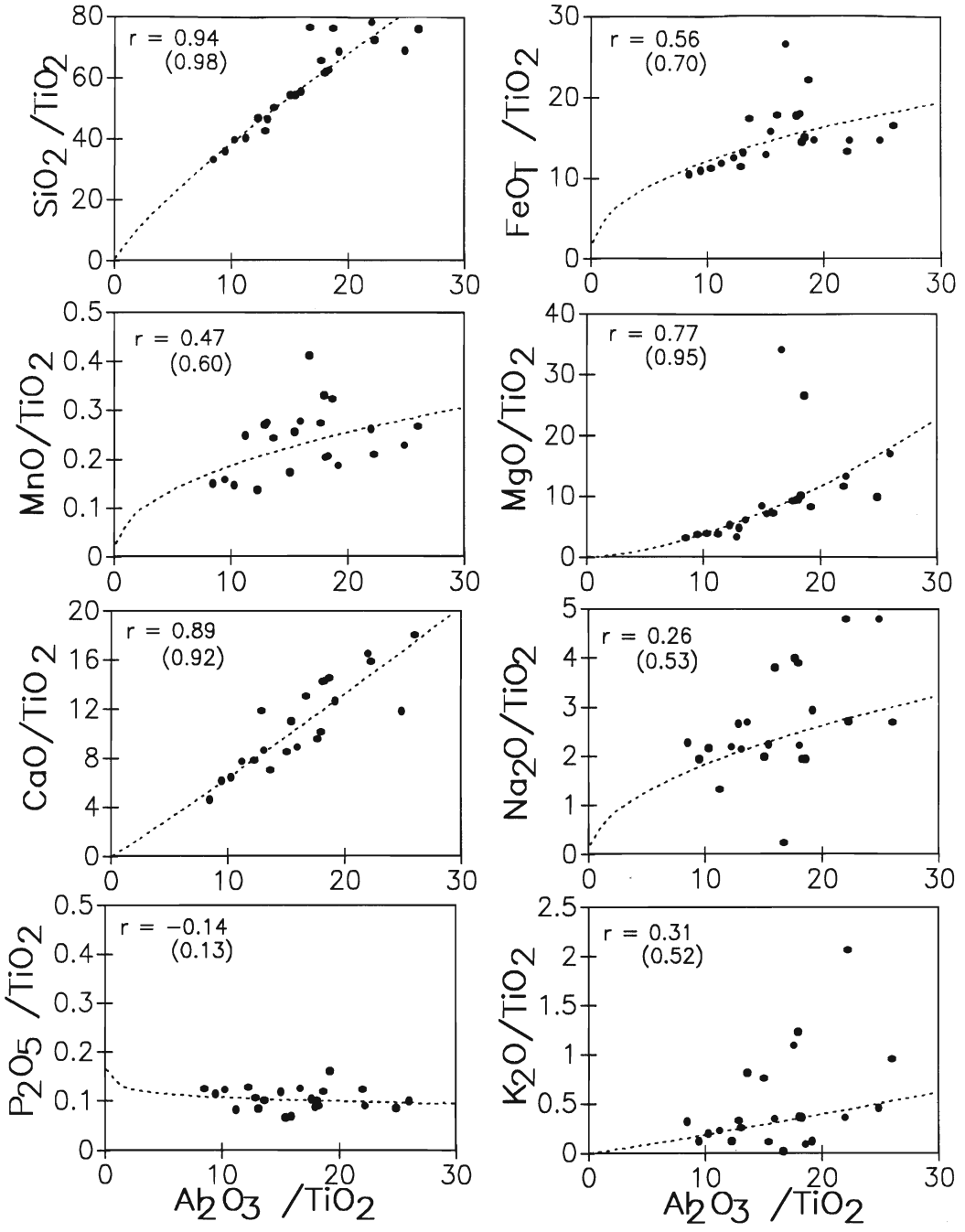

Figure 3-3a: Molecular ratio plots for major oxides of the McElroy assemblage. Linear data indicates limited mobility, whereas scattered data indicates element mobility. Logarithmic regression lines are plotted instead of linear regression lines because of the variation in sample chemistry (Beswick and Soucie1978). The degree of mobility is based on the correlation coefficient (r) where limited mobility (r=0.70-1.00), moderate mobility (r=0.30-0.70) and extreme mobility (r=0-0.30). Bracketed correlation coefficients are plots without ultramafic, leucogabbro and sample 90CTK219.

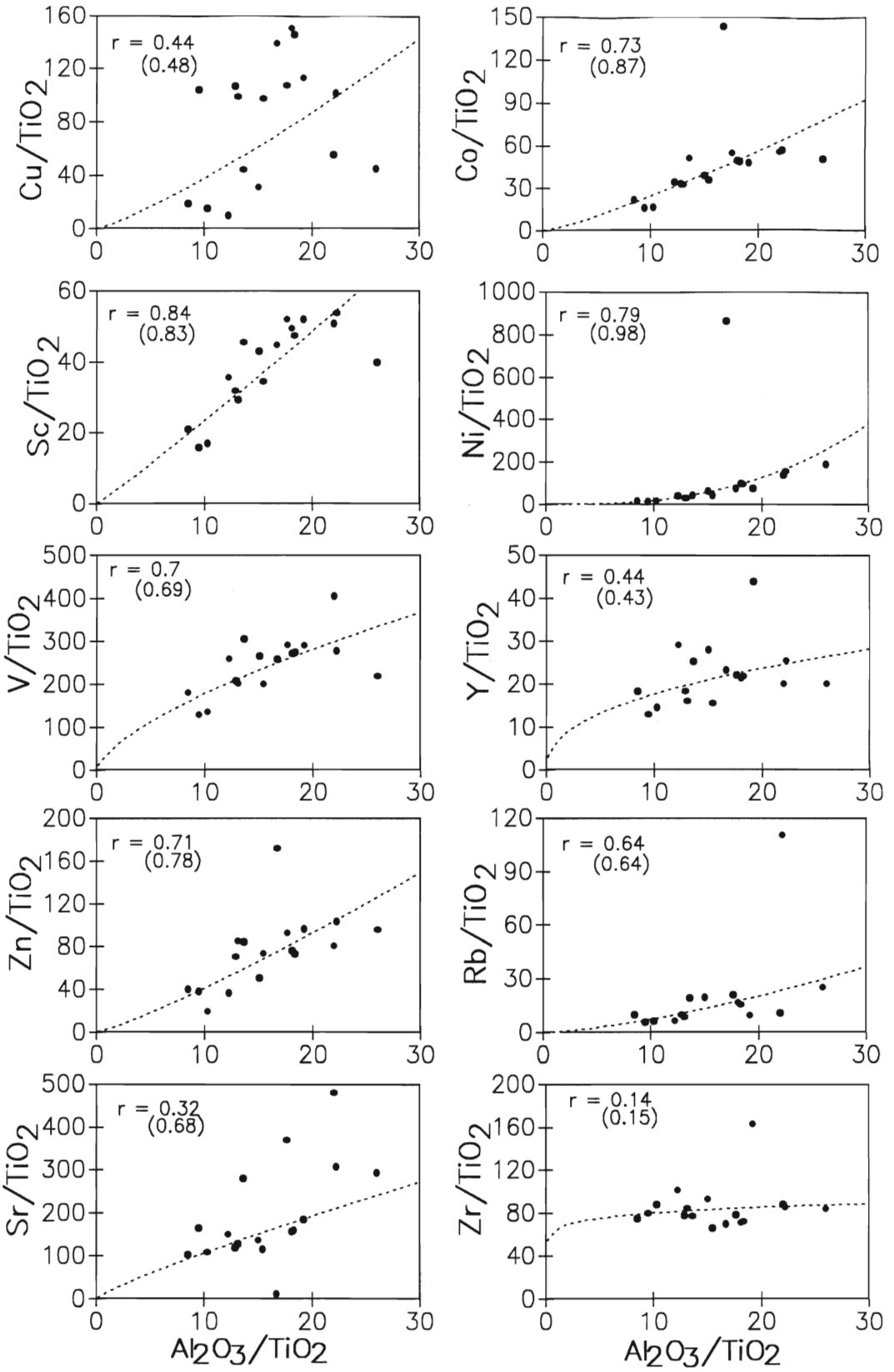

Figure 3-3b: Molecular ratio plots for trace elements of the McElroy assemblage. Limited mobility (r=0.70-1.0), moderate mobility (r=0.30-0.70), extreme mobility (r=0-0.30).

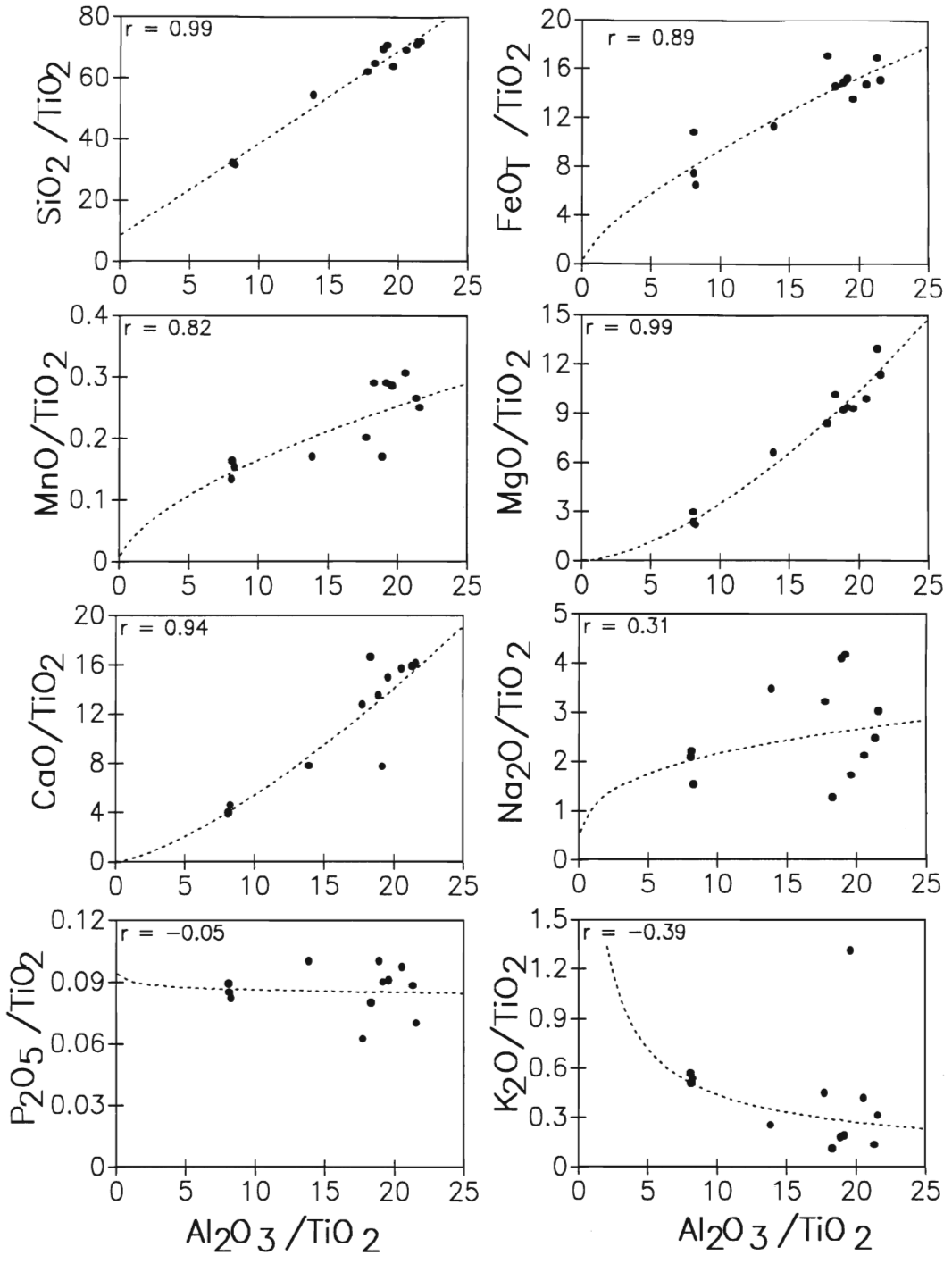

Figure 3-3c: Molecular ratio plots of major oxides for Larder Lake assemblage. Limited mobilty (r=0.70-1.0),moderate mobility (r=0.30-.070), extreme mobility (r=0-0.30).

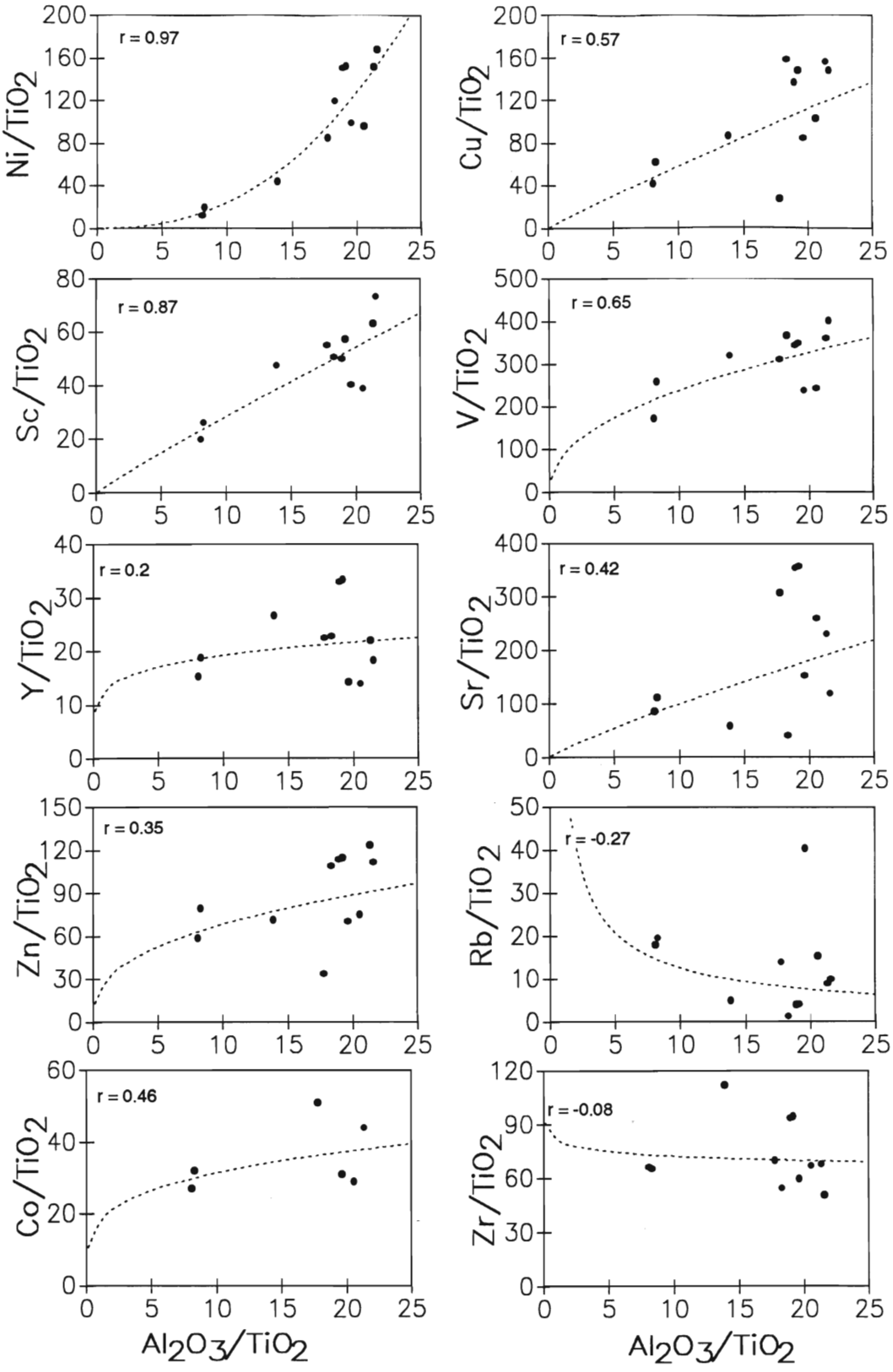

Figure 3-3d: Molecular ratio plots for trace elements of the Larder Lake assemblage. Limited mobility (r=0.70-1.0), moderate mobility (r=0.30-0.70), extreme mobility (r=0-0.30).

of the compared element. Since Al_2O_3 and TiO_2 are immobile, there should be no scatter in the X (Al_2O_3) or Z (45°) (TiO_2) direction of the graphs. The scatter represented by displacement parallel to the ordinate is due to mobility of the element of interest. With the exception of Beswick and Soucie (1978) there are few quantitative guidelines which report when an element is mobile and when an element is not. Logarithmic scales can be used when there is some compositional variability between rocks (Beswick and Soucie 1978).

The degree of scatter is presented in Figure 3-3 and in Table 8. Note that the data is unscreened and correlation coefficients are dependent on the magnitude of the data. The correlation coefficients are increased by removing visibly altered data (eg. 90CTK219) and data greatly affected (or not) by plagioclase control (i.e. leucogabbro and ultramafic units). In the McElroy assemblage, immobile oxides include Al_2O_3, TiO_2, SiO_2, MgO and CaO. Oxides with moderate degrees of mobility include FeO_T, K_2O and MnO. Na_2O and P_2O_5 are quite mobile (Figure 3-3a). Ultramafic flows plot away from the majority of the data. This is interpreted to be a reflection of its primitive geochemical characteristics (see Section 3.3). In the Larder Lake assemblage, immobile oxides include SiO_2, FeO_T, MnO, MgO and CaO. Na_2O and K_2O display moderate mobility while P_2O_5 is extremely mobile (Figure 3-3c) (Table 8).

3.2.3 Trace Element Alteration

Figure 3-3 b,d and Table 8 demonstrate the degree of mobility of the trace elements for the McElroy and Larder Lake assemblages. In the McElroy assemblage, Ni, Sc, Co, Zn and V are immobile trace elements. Cu, Y, Rb and Sr show moderate mobility while Zr is highly mobile (Figure 3-3b). Trace elements displaying limited mobility in the Larder Lake assemblage include Sc and Ni, elements displaying moderate mobility are Cu, V, Sr, Zn and

Table 8: Degree of elemental mobility within the McElroy and Larder Lake assemblages. Determined by observing correlation coefficients in Figure 3-3.

Oxide	McElroy assemblage	Larder Lake assemblage
SiO_2	limited	limited
FeO_T	moderate	limited
MnO	moderate	limited
MgO	limited	limited
CaO	limited	limited
Na_2O	extreme	moderate
P_2O_5	extreme	extreme
K_2O	extreme	moderate
Trace Element		
Co	limited	moderate
Cu	moderate	moderate
Sc	limited	limited
Ni	limited	limited
V	limited	moderate
Y	moderate	extreme
Zn	limited	moderate
Zr	extreme	extreme
Sr	moderate	moderate
Rb	moderate	extreme

Co while elements displaying extreme mobility include Y, Zr and Rb.

Disturbingly, the high field strength (HFS) elements (P, Zr, Y) which are normally considered to be immobile at greenschist grade metamorphism, appear to be scattered on the diagrams. Murphy and Hynes (1986) demonstrated that the HFS elements can undergo variable degrees of mobility depending on the amount of CO_2 present in the rock. However, in thin section the amount of secondary calcite was minor and remained constant throughout both assemblages. The exception to this was sample 90CTK219 which is an aphanitic flow which contained greater than 20% calcite suggesting that the composition of this sample is unreliable. It is not the intention of this section to eliminate elements from further discussions, but to realize that any following outstanding anomalies may be the result of secondary alteration processes. Therefore element mobility is considered in further discussions involving primary chemical variations.

3.3 Classification of McElroy and Larder Lake Rocks

3.3.1 Major Elements

Within the McElroy assemblage, the average SiO_2 content for the aphanitic flows is 49.5 wt% for the medium to coarse grained flows 48.7 wt%, for the leucogabbro 48.2 wt%, for the ultramafic flows 43.8 wt% and for the dendritic flows 51.1 wt%. The averages for the Mg# are as follows: aphanitic flows 38.3, medium to coarse flows 49.2, ultramafic flows 61.3 and for the dendritic flows 38.3. In comparison, the Larder Lake rocks range in SiO_2 from 48.4 to 53.7 wt%, averaging 51.5 wt%. The Mg# range is 30 to 55, averaging 41.6 (Table 4). The Catharine and Kinojevis South assemblages are plotted for comparison on the classification diagrams (Figure 3-4 to 3-6). The rocks fall in the tholeiitic range when plotted on the SiO_2-FeO*/MgO, FeO*-FeO*/MgO and TiO_2-FeO*/MgO diagrams of Miyashiro

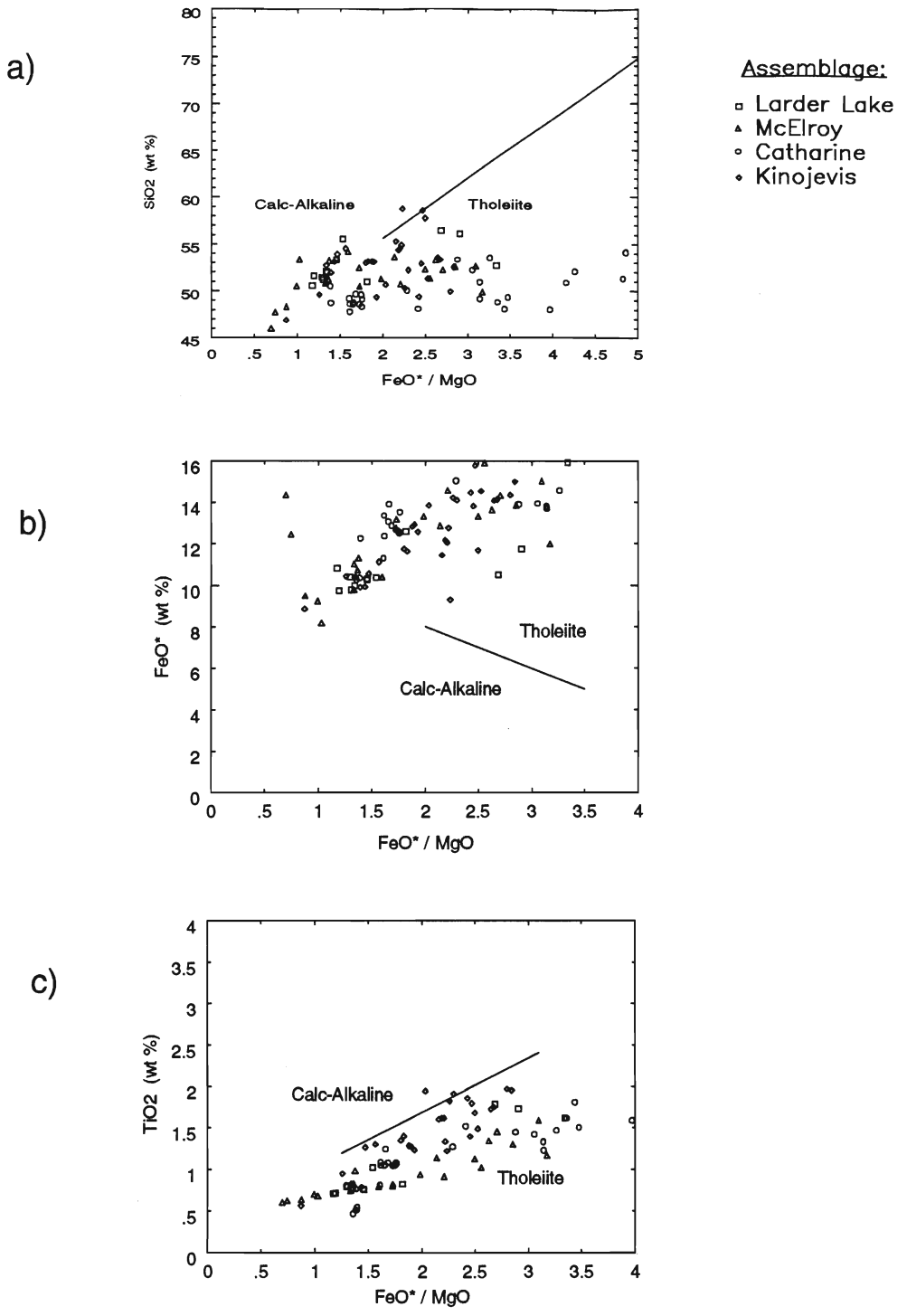

Figure 3-4: Tholeiitic/calc-alkaline discrimination plots for Catharine assemblage (circle), McElroy assemblage (triangle), Larder Lake assemblage (box) and Kinojevis South assemblage (diamond). Tholeiitic and calc-alkaline fields from Miyashiro (1974).

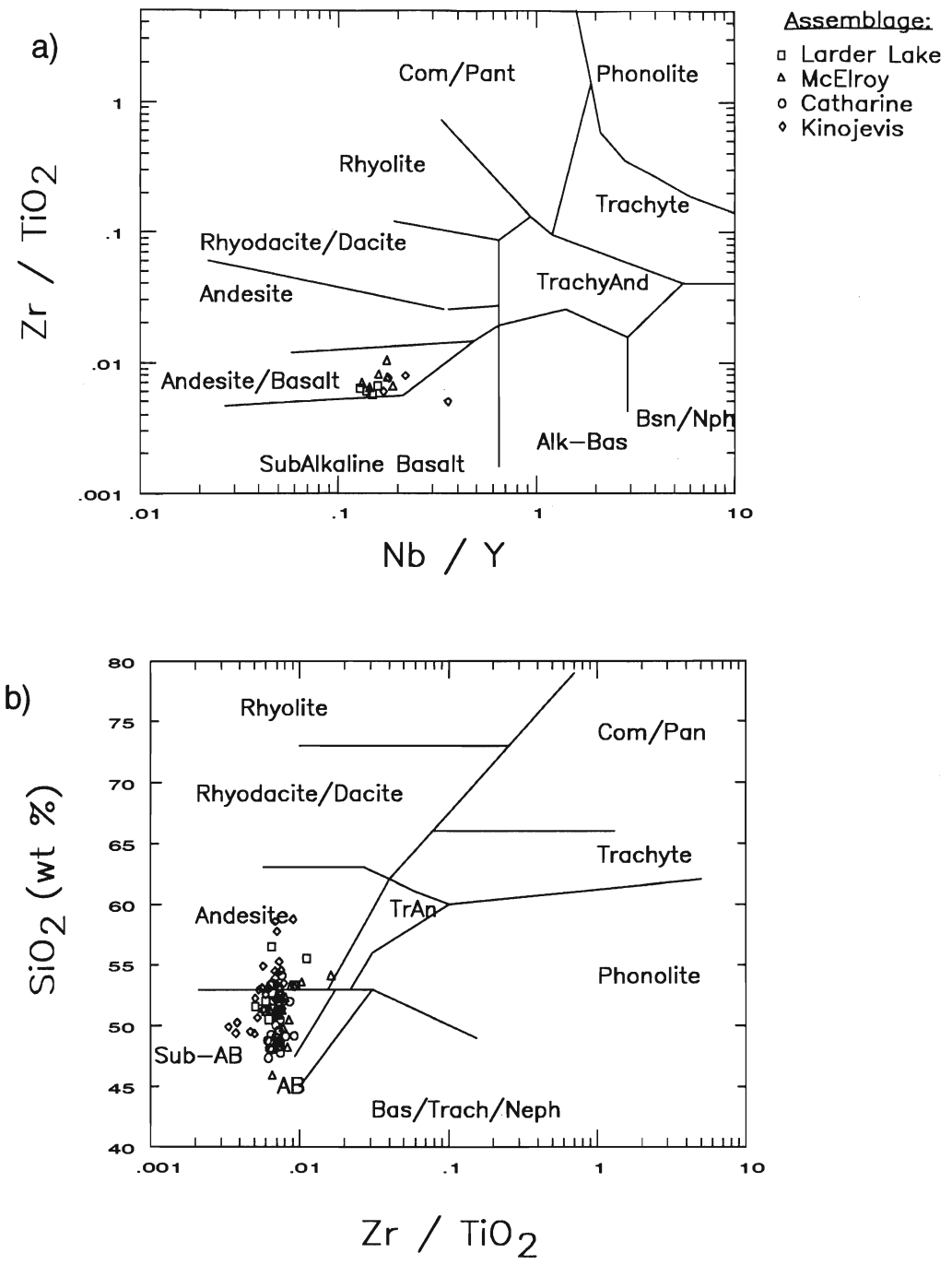

Figure 3-5: Lithologic discrimination plots for Catharine assemblage (circle), McElroy assemblage (triangle), Larder Lake assemblage (box) and Kinojevis South assemblage (diamond). Fields are from Winchester and Floyd (1977).

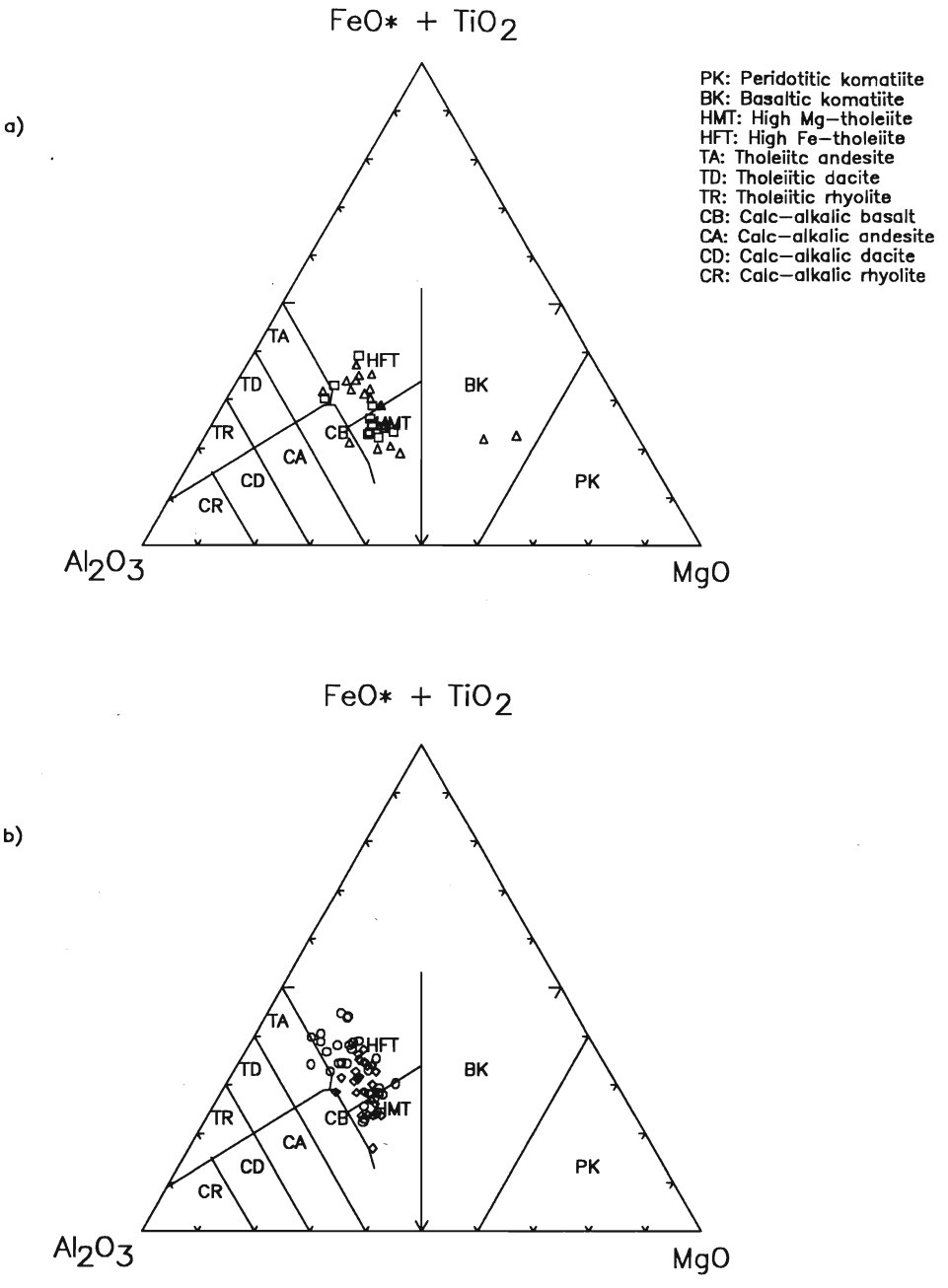

Figure 3-6: Jensen Cation Plots for a) McElroy (triangle) and Larder Lake assemblages (square) and b) Catharine (circle) and Kinojevis South (diamond) assemblages. Fields from Jensen (1976).

(1974) (Figure 3-4 a-c). They range from andesite-basalt on the Zr/TiO_2-Nb/Y and sub-andesite on the SiO_2-Zr/TiO_2 plots of Winchester and Floyd (1977) (Figure 3-5 a,b). On the Jensen Cation plot (Figure 3-6a,b) the McElroy aphanitic flows are Fe-tholeiites, the coarse flows are Mg-tholeiites, the ultramafic flows are basaltic komatiites and the dendritic flows are Fe-tholeiites. Larder Lake aphanitic flows range from Fe-tholeiite to Mg-tholeiite to komatiitic (Jensen and Langford 1985) (Figure 3-6a). Larder Lake tholeiites were collected for this study.

3.3.2 Trace Elements

Chondrite normalized extended trace element plots (normalized values from Taylor and McLennan 1985) are presented in Figure 3-7 and 3-8. In general, the McElroy and Larder Lake samples have a flat pattern in which the pattern decreases with increasing compatibility (Figure 3-7 a and b, respectively). The large ion lithophile elements (LILE) (Th, Rb, Ba, Sr,) show variable ranges from 1-40X chondrite illustrating their highly mobile nature. The compatible trace elements (Sc, V, Zn, Cu, Ni) range from 2X chondrite to less than 0.01X chondrite indicating their role in residual and fractionated phases. The high field strength elements (HFS) (Nb, Ta, Hf, Zr, Ti, Y) elements are relatively flat suggesting that they behave similarly and they are relatively immobile. Slight negative Th and Nb anomalies are more pronounced in the Larder Lake samples. Positive Hf anomalies, similar to ocean floor basalts are present in both McElroy and Larder Lake assemblages.

The Catharine and Kinojevis South assemblages (Figure 3-7 c,d) have similar patterns to the McElroy and Larder Lake assemblages. Compared to patterns of rocks from various tectonic settings, the tholeiitic volcanics in the Larder Lake area resemble normal mid-ocean ridge basalts (N-MORB) (Figure 3-7 e).

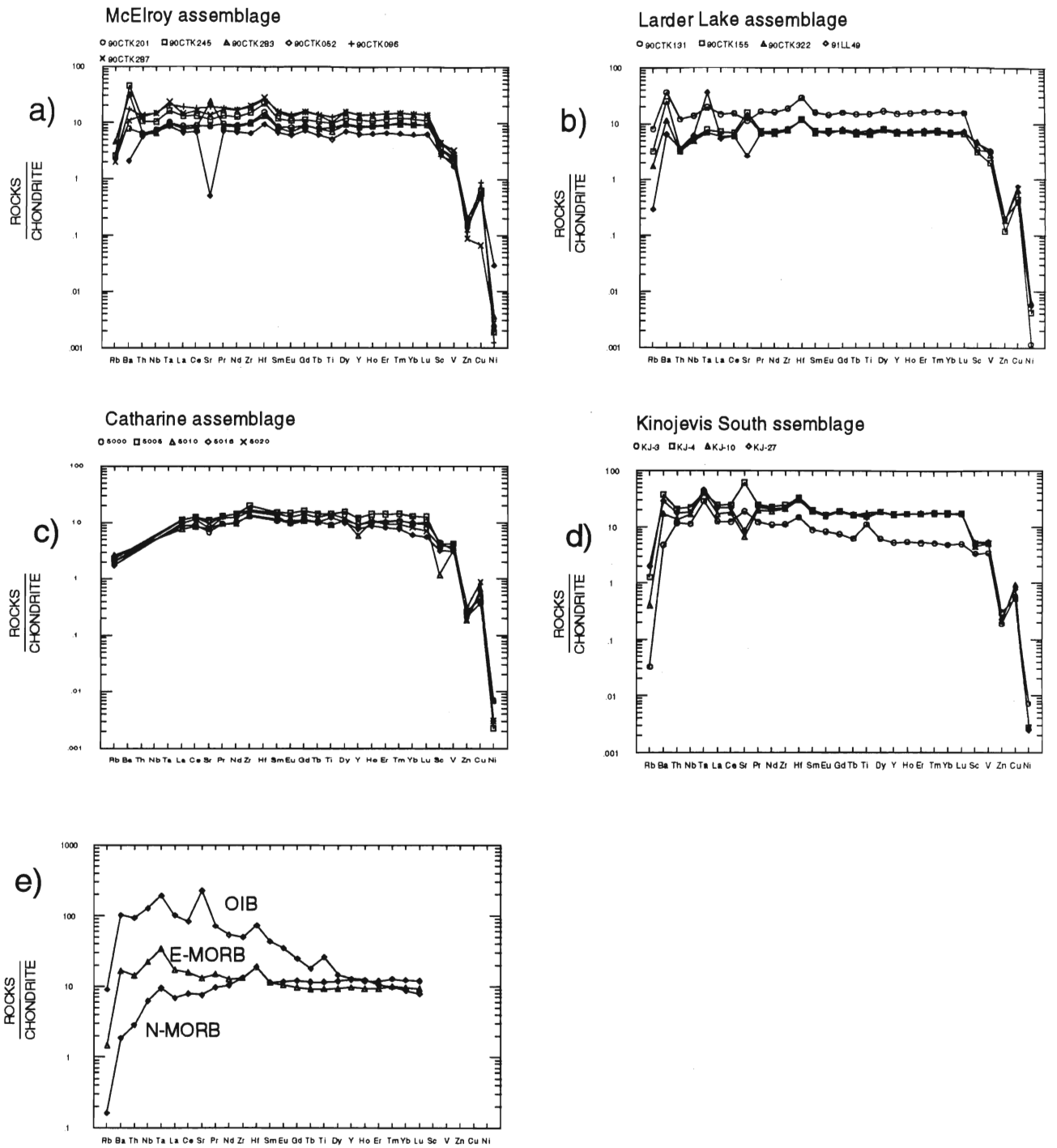

Figure 3-7: Chondrite normalized extended trace element plots for a) McElroy assemblage, b) Larder Lake assemblage, c) Catharine assemblage, d) Kinojevis South assemblage and e) various tectonic settings. Normalizing values are from Taylor and McLennan, 1985.

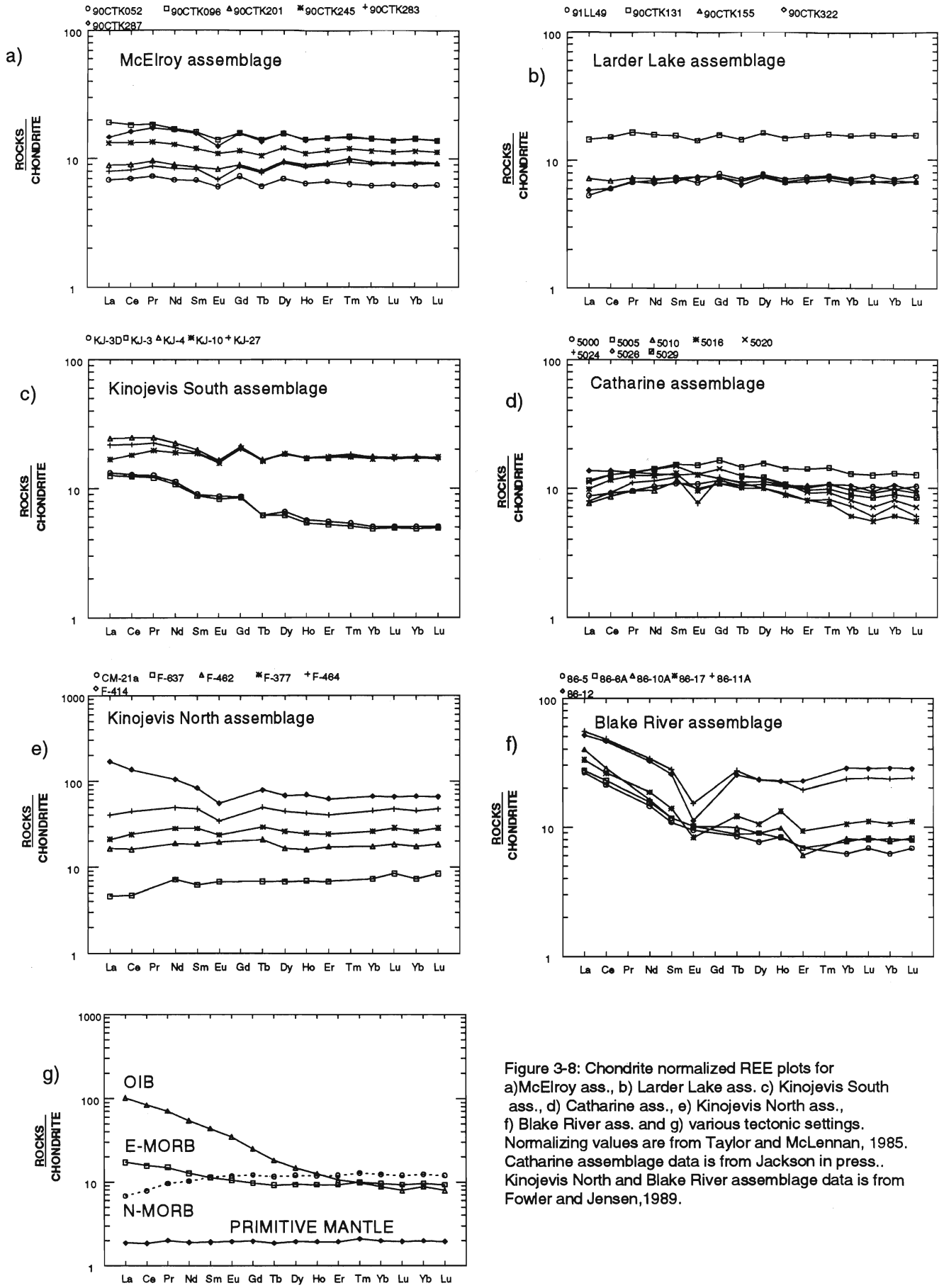

Figure 3-8: Chondrite normalized REE plots for a)McElroy ass., b) Larder Lake ass. c) Kinojevis South ass., d) Catharine ass., e) Kinojevis North ass., f) Blake River ass. and g) various tectonic settings. Normalizing values are from Taylor and McLennan, 1985. Catharine assemblage data is from Jackson in press.. Kinojevis North and Blake River assemblage data is from Fowler and Jensen,1989.

3.3.3 Rare Earth Elements (REE)

Chondrite normalized rare earth patterns are presented for the tholeiitic assemblages in the Kirkland Lake area (Figure 3-8). Both McElroy and Larder Lake assemblages show generally flat MORB-like patterns (Figure 3-8 a and b). McElroy rocks range from 7-20X chondrite while Larder Lake rocks range from 5-15X chondrite. Dendritic flows (90CTK096 and 90CTK287) have slight LREE enrichments whereas aphanitic flows (90CTK201, 90CTK245 and 90CTK283) have slightly depleted to slightly enriched LREE patterns. The ultramafic flow (90CTK052) has a flat REE pattern (Figure 3-8a). Larder Lake rocks have very slight LREE depletions (91LL49 and 90CTK322). Larder Lake samples 90CTK131 and 90CTK155 have flat REE patterns.

Negative Eu anomalies, indicative of plagioclase fractionation, are more evident in the McElroy assemblage than the Larder Lake assemblage (Figure 3-8 a and b). This is consistent with the plagioclase glomerophyric rocks in the McElroy assemblage. The patterns of the McElroy and Larder Lake assemblages are similar to the patterns from mid-ocean ridge basalts (Figure 3-8 g).

The REE patterns of the McEroy and Larder Lake samples are slightly different from the other tholeiitic assemblages in the region. The Catharine assemblage shows a concave pattern with LREE and HREE depletions with respect to the MREE (Jackson in press) (Figure 3-8 d). Kinojevis rocks show more fractionation variability. REE patterns from the North assemblage range from high LREE to low LREE (Fowler and Jensen 1989) (Figure 3-8 e). REE patterns from the Kinojevis South assemblage are flat to slightly increased LREE (Figure 3-8 c). Calc-alkaline rocks from the Blake River assemblage show fractionated patterns illustrated by light rare earth element enrichments and negative Eu anomalies (Figure 3-8 f).

Figure 3-9 illustrates that the McElroy and Larder Lake rocks have slightly different patterns with respect to HFS elements and LREE. Larder Lake rocks have greater LREE and Th, Nb depletions than the McElroy samples (Figure 3-9a). In contrast, the McElroy samples contain negative Ti anomalies which are absent in the Larder Lake samples (Figure 3-9b).

Elemental ratios in the Larder Lake assemblage include (La/Yb) 1.35, (La/Sm) 1.39, (Sm/Yb) 0.97 and (La/Nb) 1.07. In comparison, McElroy assemblage elemental ratios include (La/Yb) 1.58, (La/Sm) 1.64, (Sm/Yb) 0.97 and (La/Nb) 1.13 (Table 5).

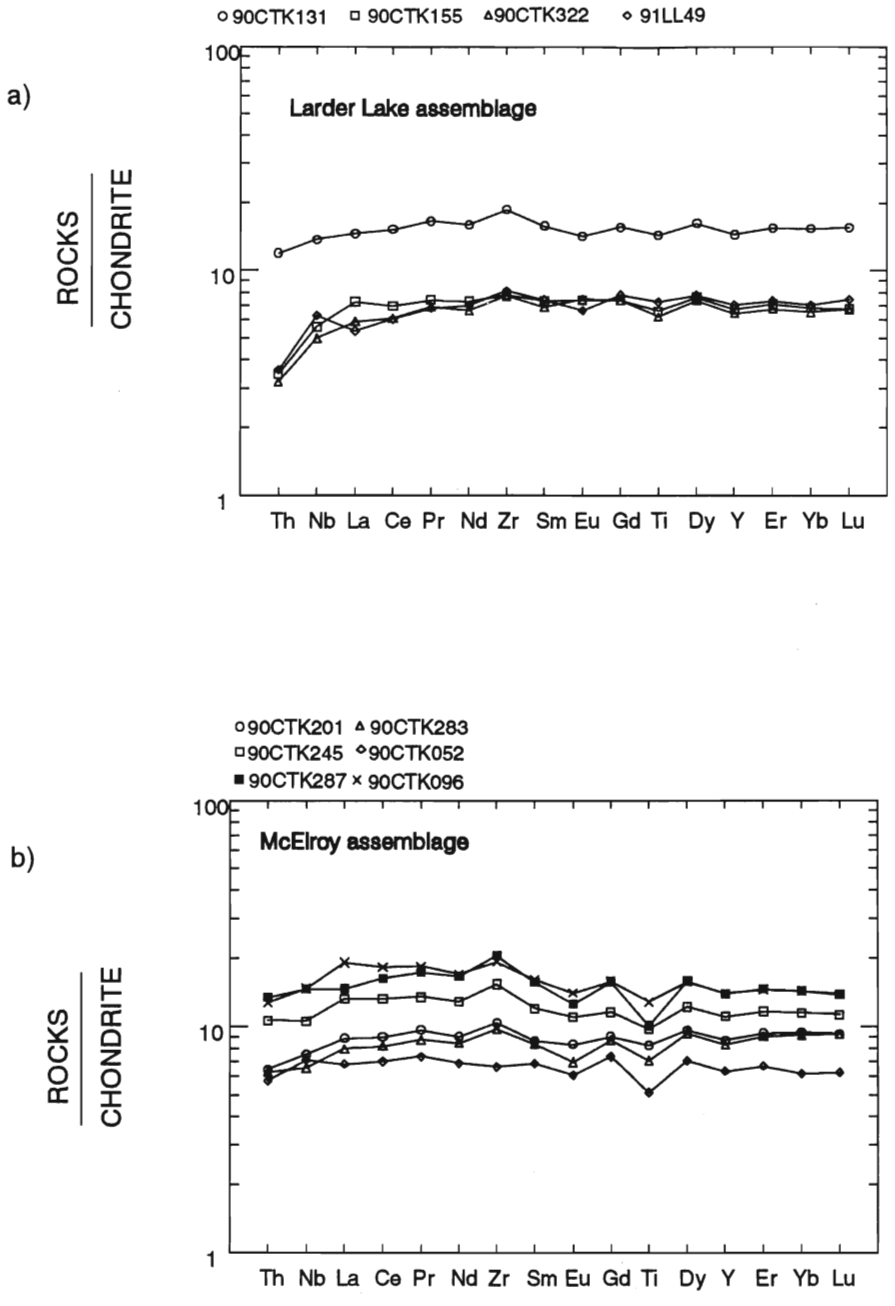

Figure 3-9: HFS and REE patterns for a) Larder Lake and b) McElroy assemblages. The figure illustrates that Th and Nb depletions in Larder Lake rocks are greater than McElroy rocks, whereas the McElroy rocks have greater Ti depletions than Larder Lake rocks.

Chapter 4

Geochemical Variations

4.1 Introduction

Section 3.3 demonstrated that the McElroy assemblage consists of basaltic komatiite to Fe-rich tholeiites. Similarly, the Larder Lake assemblage consists of komatiite to Fe-rich tholeiite. This geochemical variation is often attributed to fractional crystallization of olivine, orthopyroxene, clinopyroxene and plagioclase. Table 2 showed that the units are characterized by various combinations of gabbroic minerals including olivine, pyroxene and plagioclase. Accessory minerals which have the ability to affect the REE (eg. titanite, apatite) were not consistently observed in thin section.

The McElroy assemblage was evaluated to see if the chemical variation between adjacent units is due to gabbroic fractionation processes. This was accomplished by plotting major and trace elements against fractionation indices on bivariant diagrams.

$Mg^{\#}$ and Zr variation diagrams can be used to illustrate relative fractionation trends between adjacent units. Two widely used variation diagrams include oxide versus $Mg^{\#}$ where $Mg^{\#}=\{Mg^{2+}\}*100/\{Mg^{2+} + Fe^{2+}\}$ or oxide versus Zr. $Mg^{\#}$ is a good fractionation index as it decreases as Fe enrichment occurs in tholeiitic rocks. Zr is an incompatible trace element which does not enter the fractionating assemblage until the later stages of differentiation when zircon crystallizes. Therefore Zr continues to increase in concentration in tholeiitic magmas and along with $Mg^{\#}$ illustrates the liquid line of descent. In a relative sense, the most primitive rocks will have high $Mg^{\#}$ and low Zr concentrations. In more evolved rocks the $Mg^{\#}$ will be low and Zr will be higher.

Major oxides are the main components of tholeiitic minerals and show fractionation patterns on variation diagrams. Trace elements also display fractionation patterns by

substituting for major oxides with similar radius and charge. The distribution (partition) coefficient K_D is a measure of how easily a trace element will enter a crystal lattice where;

$$K_D = \text{conc}^n \text{ mineral/conc}^n \text{ liquid} \quad ..(1)$$

The bulk distribution coefficient (D) is a measure of how easily a trace element enters a rock with specific minerals where;

$$D = \Sigma w K_D \quad ..(2)$$

where w is the % of the mineral in the rock and K_D is the distribution coefficient of the element in the mineral (Cox et al. 1979). Elements with D<1 are termed incompatible and prefer to remain in the liquid as long as possible. Therefore as the magma differentiates, the concentration of incompatible elements increases until a mineral which will accept the element is formed. Elements with D>1 are compatible and enter the crystal lattice of a mineral. As a magma differentiates, D for a particular element changes. For example, Zr is incompatible during the early stages of fractionation but becomes compatible during the later stages of differentiation.

4.2 Major Element Variation

On the major oxide fractionation diagrams a relatively flat pattern is expressed as Al_2O_3 is plotted against both $Mg^{\#}$ and Zr (Figure 4-1a and 4-2a). The exception to this are the ultramafic rocks and leucogabbro which have Al_2O_3 contents lower than and higher than the remaining samples respectively. Plagioclase fractionation can explain this pattern. Aluminum is a major component of plagioclase and alkali feldspar. In tholeiitic rocks plagioclase feldspar controls the Al_2O_3 behaviour. The higher Al_2O_3 content in the leucogabbro is a function of its high plagioclase content, whereas the lower content in the ultramafic rocks is due to absence of plagioclase in these rocks (Table 2). The remaining flat

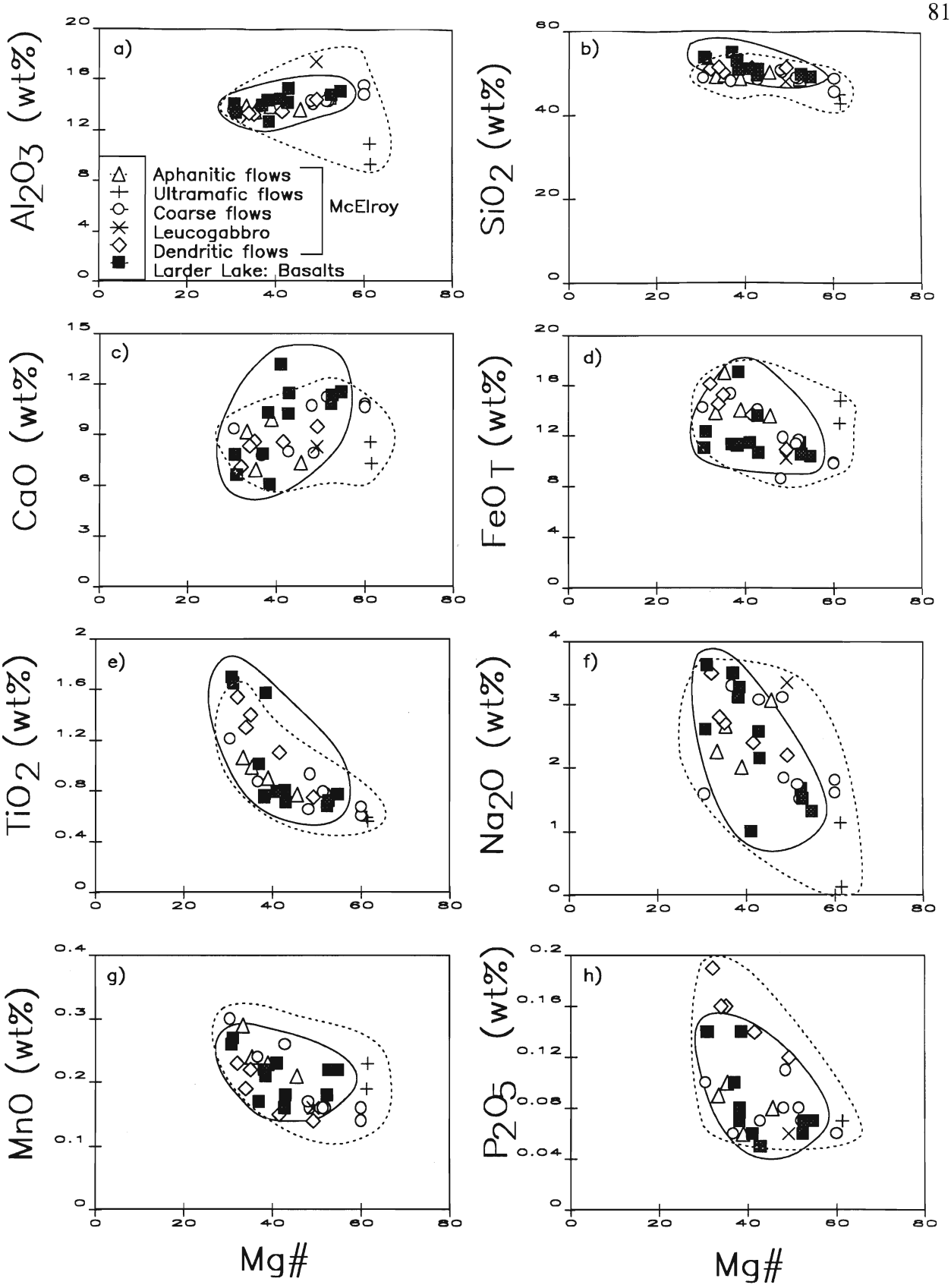

Figure 4-1: Mg#-Oxide variation diagrams for McElroy and Larder Lake assemblage. Dashed line field encircle the McElroy samples. Solid line field encircles the Larder Lake samples.

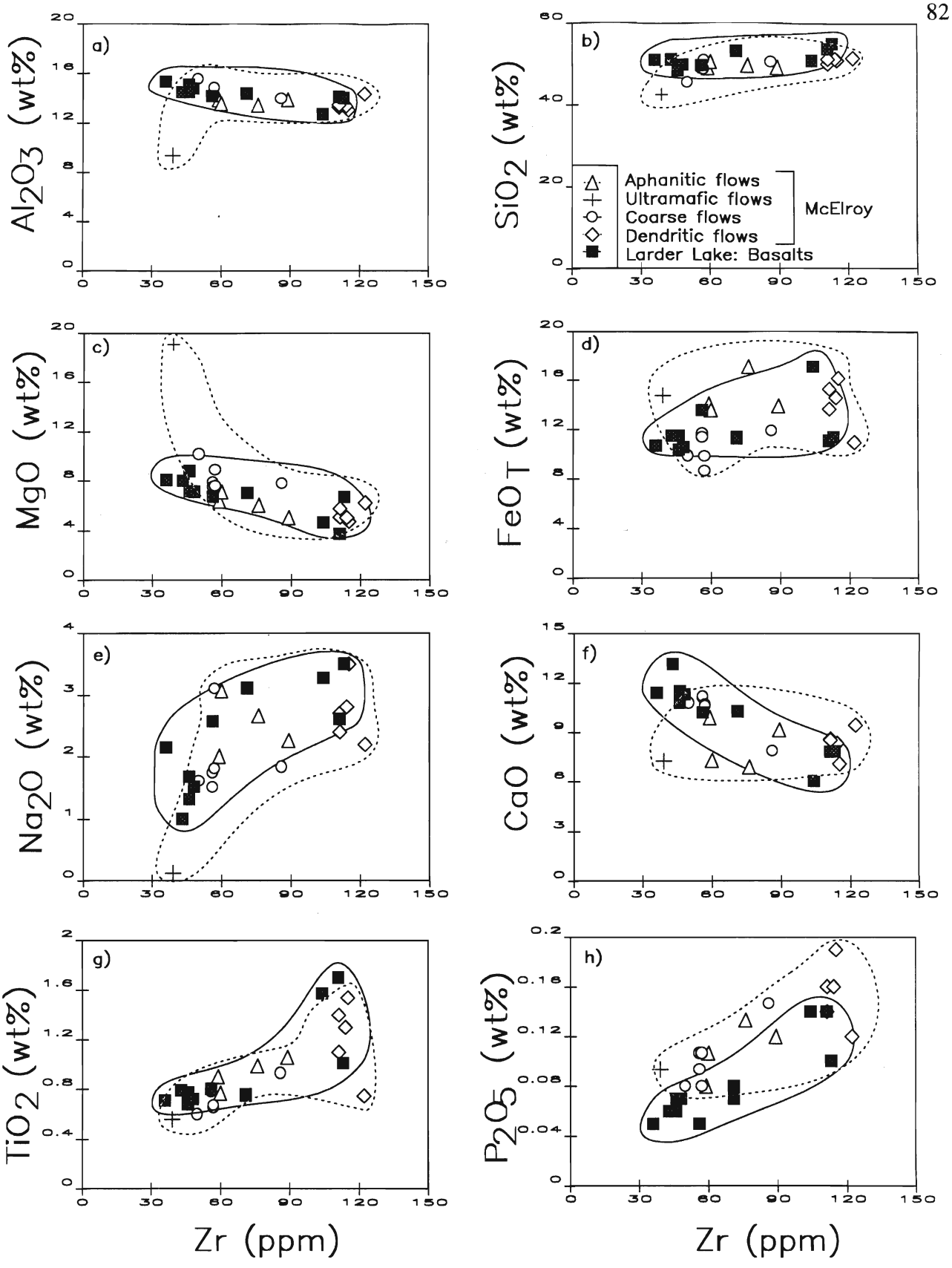

Figure 4-2: Zr-oxide variation diagrams for McElroy and Larder Lake assemblages. The dashed line field encircles McElroy samples whereas the solid line field encircles the Larder Lake samples.

pattern suggests that plagioclase fractionation is a constant factor during the differentiation of these volcanic rocks.

As SiO_2 is plotted on the $Mg^{\#}$ diagram (Figure 4-1b) a slight negative correlation is expressed whereas on the Zr diagram (Figure 4-2 b) a slight positive correlation exists. Silica is the most abundant major oxide in most natural occuring rocks. In tholeiitic rocks, SiO_2 increases in concentration as a magma fractionates as silica-poor minerals crystallize or silica-rich minerals cease to crystallize. Therefore, in addition to $Mg^{\#}$ and Zr, SiO_2 is also a good fractionation index. It is shown on Figures 4-1b and 4-2b that the most fractionated rocks in the McElroy assemblage, are the aphanitic and dendritic flows whereas the ultramafic and coarse grained flows are the least fractionated. Similarly, the Larder Lake rocks show a range in the degree of fractionation from least evolved to more evolved flows.

The CaO patterns show a weak positive correlation on the $Mg^{\#}$ diagram (Figure 4-1c) and a negative correlation on the Zr diagram (Figure 4-2f). Calcium is an element which may enter the mafic minerals (e.g. pyroxene) in addition to An-rich plagioclase during the early stages of fractionation. The patterns are in agreement with Ca-rich clinopyroxene crystallizing early followed by Fe-rich clinopyroxene fractionating as the magma differentiates. The CaO trend is also consistent with albite fractionation being favoured over anorthite fractionation in more evolved rocks.

The Na_2O trend on the variation diagrams (Figure 4-1f and 4-2e) show that the least evolved rocks (ultramafic and coarse grained flows) contain less Na_2O than the evolved rocks (aphanitic and dendritic flows) indicating that Na_2O increased with fractionation. Albite-rich plagioclase has the ability to contol the behaviour of Na_2O in a magma during the later stages of fractionation. However, the basaltic nature of the rocks suggests that albite is probably not removed from the melt and albite fractionation is negligible. However, as mentioned in

Section 3.3, Na_2O may have been mobile during secondary processes. Therefore, albitization of plagioclase during alteration may have also affected the behaviour of Na_2O and CaO.

Figure 4-1 d and 4-2 d show iron enrichment trend with fractionation. This is illustrated by a negative correlation on the $Mg^{\#}$ diagram (Figure 4-1d) and a positive correlation on the Zr diagram. This FeO_T enrichment trend is observed in the tholeiitic rocks as Fe-tholeiites become more common than Mg-tholeiites as a magma fractionates. This fractionation trend is followed by an iron depletion trend in andesites, dacites and rhyolites. However, the complete Fe trend is not observed in the McElroy and Larder Lake Asemblages.

Figures 4-1 e and 4-2 g show that TiO_2 increases in concentration as the magma differentiates with the dendritic flows containing the highest TiO_2 values. Figure 4-2g also shows that the TiO_2 content in the dendritic flows drops off after reaching a maximum value at 1.54 wt% to 0.75 wt% (Table 4). Titanium behaves as a trace element in most tholeiitic sequences. During the early stages of magma differentiation, titanium tends to enter the lattice of clinopyroxene or magnetite as a trace element. Titanium is also a major component of ilmenite and/or titanite. Therefore TiO_2 should increase in concentration while it acts as a trace element until a mineral such as titanite begins to crystallize and TiO_2 is removed from the magma. This suggests that a TiO_2 rich mineral was probably crystallizing out of the magma responsible for the dendritic flows.

Manganese behaves similarly to iron (Figure 4-1g and 4-1d) showing a negative correlation with $Mg^{\#}$.

The P_2O_5 plots show a negative correlation on the Mg# diagram and the positive correlation on the Zr diagram. Phosphorus, like TiO_2, is incompatible with early tholeiitic fractionating minerals. The oxide P_2O_5 enters apatite in later fractionated phases (Anderson and Greenland 1969). Therefore P_2O_5 will increase in concentration until apatite begins to

crystallize.

4.3 Trace elements

High field strength (HFS) elements Ti, Zr, Y and P (Figures 4-3, 4-4) are incompatible with early tholeiitic fractionating minerals (i.e. olivine, clinopyroxene, orthopyroxene and plagioclase) and therefore they tend to increase in concentration during early to middle stages of fractionation. The minerals which commonly host these trace elements are ilmenite and titanite (Ti), zircon (Zr), garnet (Y) and apatite (P). On Figure 4-3g Y displays a negative correlation indicating that it is increasing in concentration during fractionation. The inverse is shown on the Zr variation diagram (Figure 4-4f). In contrast, transition metals Sc, Ni and Co are compatible with mafic tholeiitic fractionated assemblages during the early stages of fractionation. As a result, they tend to fractionate out in the early to middle stages of differentiation and are concentrated in the ultramafic and coarse flows. These elements show positive correlations on the $Mg^{\#}$ fractionation graphs (Figure 4-3 e,d,b) and negative correlations on the Zr variation graphs (Figure 4-4 d,c,a). However, Sc does not show a good correlation.

Copper and Zn show considerable scatter on these graphs. This could be a reflection of either alteration or sulphide control or both.

The previous variation diagrams have illustrated that crystal fractionation has affected the various rocks in both McElroy and Larder Lake assemblages. In the McElroy assemblage, the most primitive litholgies (high $Mg^{\#}$ and low Zr) are the ultramafic and coarse grained flows. The more evolved rocks are the aphanitic and dendritic flows. In the Larder Lake assemblage, the volcanic rocks show a greater range in the degree of fractionation of the basalts.

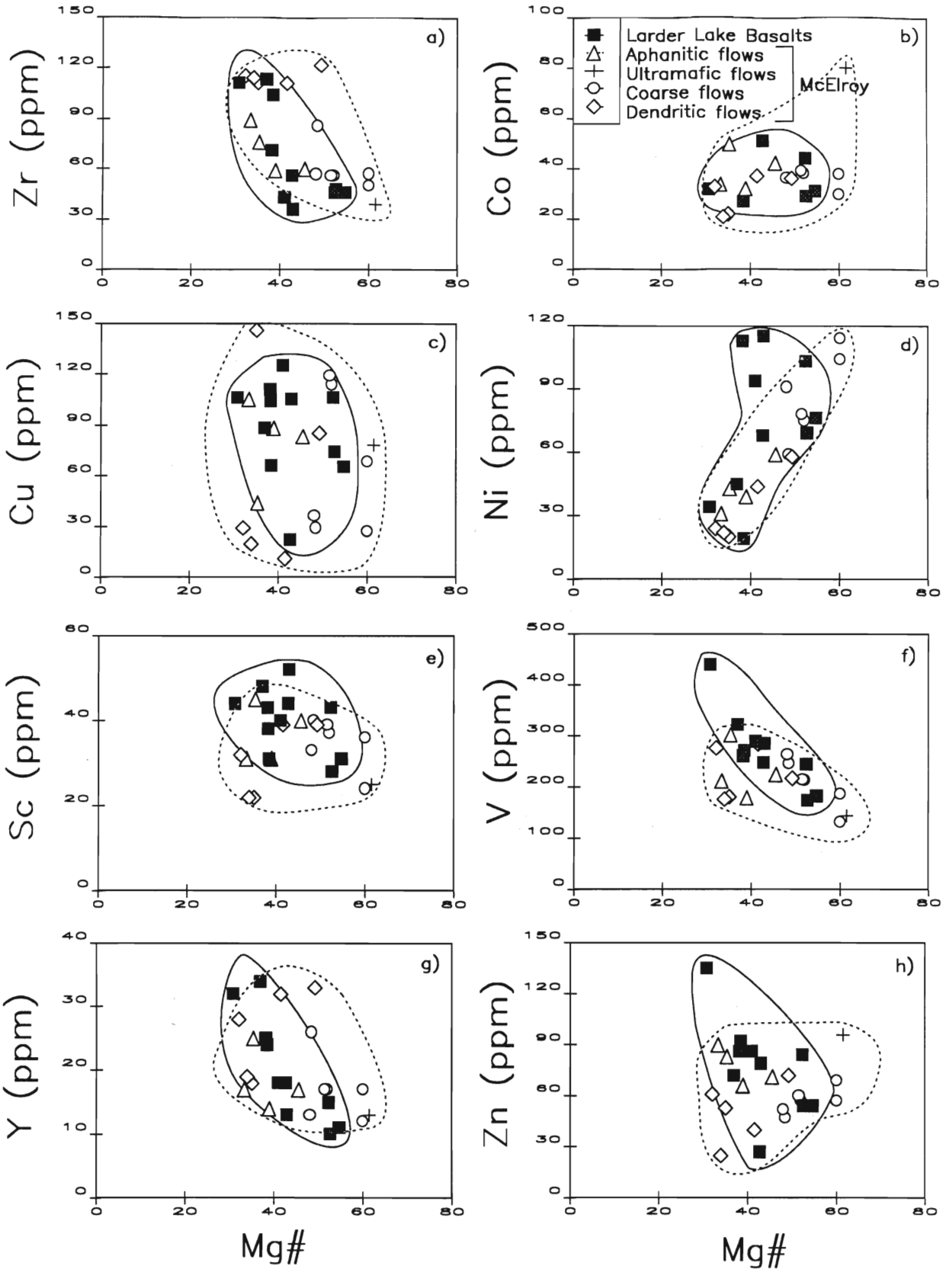

Figure 4-3: Mg#-trace element variation diagrams for McElroy and Larder Lake assemblages. The dashed line field encircles McElroy samples whereas the solid line field encircles the Larder Lake samples.

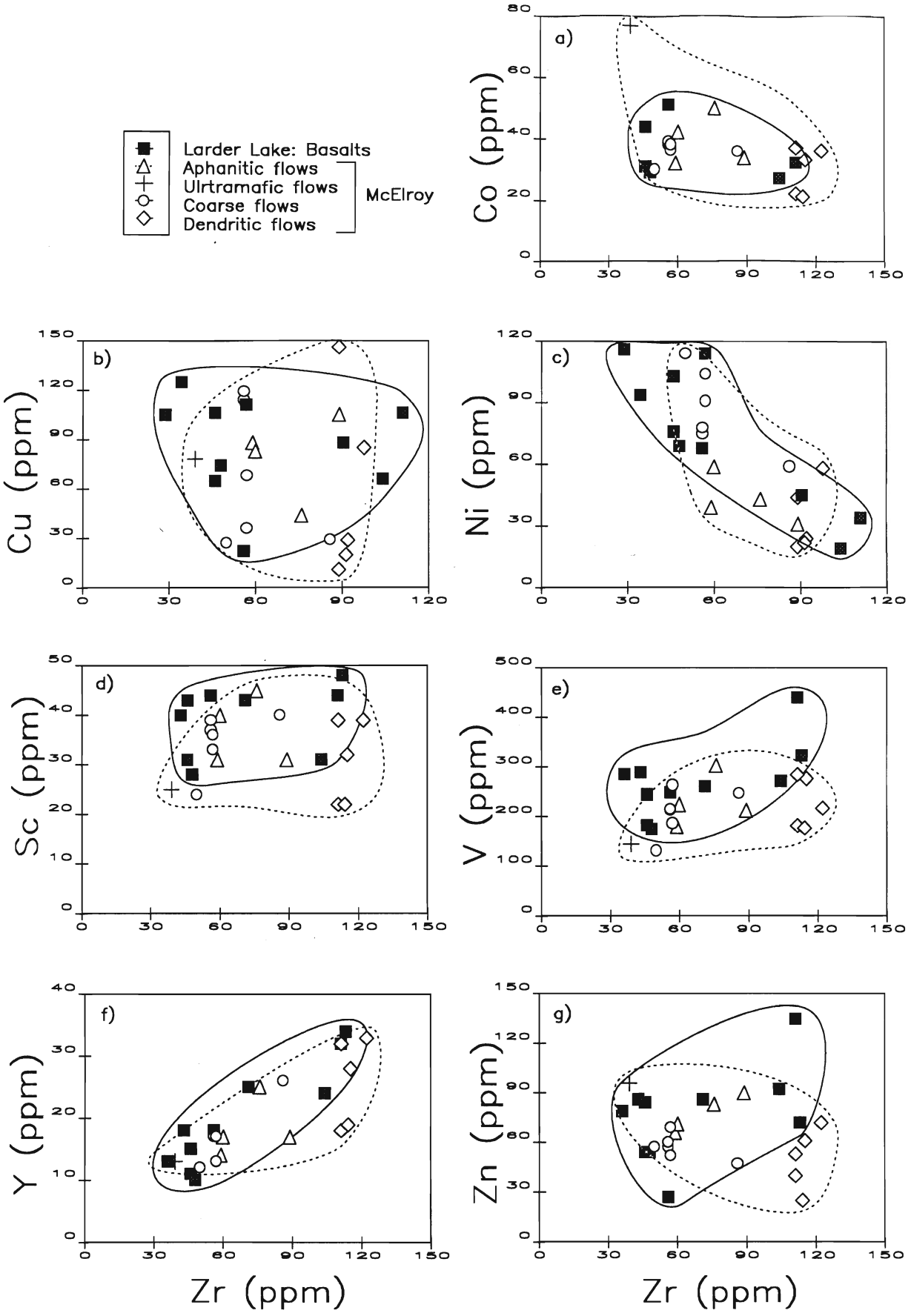

Figure 4-4: Zr-trace element variation diagrams for McElroy and Larder Lake assemblages. The dashed line field encircles McElroy samples whereas the solid line field encircles the Larder Lake samples.

4.4 Molecular Proportion Ratios

Molecular proportion ratio plots (Figure 4-5) were used to distinguish primary magmatic processes from secondary alteration or metamorphic trends. Ratios between SiO_2 and FM (FeO_T + MgO) display igneous trends when normalized to a component that does not fractionate into olivine, clinopyroxene, orthopyroxene or plagioclase. The fractionation plots are valid for any part on the graph. The elements used were considered to be relatively immobile from the previous discussions. The ratios displayed on the diagrams are indicated as follows:

clinopyroxene $Ca(Mg,Fe)(SiO_2)_2$; SiO_2:FM = 2:1

olivine $(Mg,Fe)_2SiO_4$; SiO_2:FM = 1:2

orthopyroxene $(Mg,Fe)SiO_3$; SiO_2:FM = 1:1

An-plagioclase $CaAl_2Si_2O_8$; SiO_2:FM = 1:0

Figure 4-5 shows that for various normalizing factors, most of the data falls in between the clinopyroxene and plagioclase fractionation trend. Two samples (ultramafic flows; 90CTK052 and 90CTK072) are displaced between the orthopyroxene and the clinopyroxene fractionation trend. These fractionation trends are in agreement with petrographic observations that clinopyroxene and plagioclase were involved during crystal fractionation. The majority of the rocks contained primary pyroxene and plagioclase while the ultramafic rocks contained some olivine relicts and pseudomorphs. In general, the fractionation trends are in agreement with the CIPW norm calculation.

The graphs illustrate that the compositional variation within the McElroy and Larder Lake assemblages are due to primary processes such as fractionation and/or melting of clinopyroxene and/or orthopyroxene. Secondary processes appear to have minor affects on the major oxides used in this discussion (Table 8).

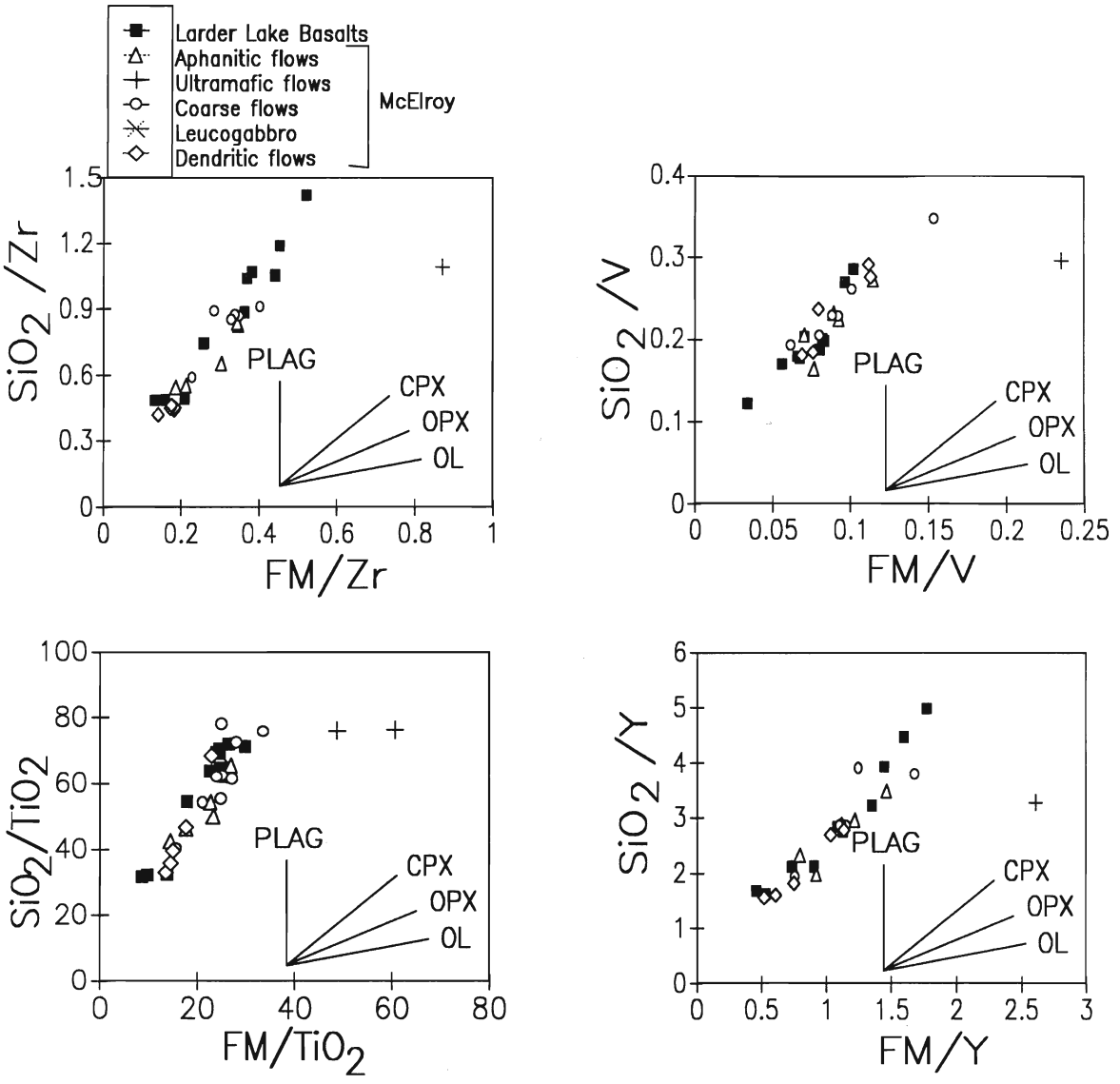

Figure 4-5: Molecular proportion ratios illustrating possible plagioclase (PLAG), clinopyroxene (CPX), olivine (OL) and orthopyroxene (OPX) control during fractionation of the McElroy and Larder Lake assemblages. FM represents FeOt + MgO.

4.5 Discussion

A chemostratigraphic relationship may exist in the Catharine assemblage whereby the komatiitic Wawbewawa Formation is overlain by Formation A-A' which is overlain by the tholeiitic Catharine Formation (Jackson and Harrap 1989). However, this pile of increasingly more evolved rocks could also result from tectonic stacking as a fault of unknown displacement is present in the Catharine Formation (Jackson in press).

Within the McElroy assemblage, a general fractionating sequence from most primitive to most evolved consists of ultramafic flows, coarse grained flows, aphanitic flows and dendritic flows (Figure 4-1 to 4-4). This roughly parallels the homoclinal nature of the stratigraphy (Figure 2-2) in which the ultramafic flows are overlain by the coarse flows which are overlain by the aphanitic flows. The exception is the dendritic flows which are located at the base of the sequence, but are the most evolved rocks. If these rocks were generated from one homogeneous magma chamber, the ultramafic flows would be the first to erupt, and represent the most primitive magmas, as there was little time for the magma to fractionate. The coarse flows, overlay these rocks and are slightly more evolved than the underlying ultramafic flows. The upper portion of the assemblage is capped by the evolved, aphanitic flows (Figure 2-2). Overlap exists between units suggesting that this was a gradual process without significant temporal breaks.

A problem with this proposed fractionation model exists with the highly evolved dendritic flows and their apparent stratigraphic position. The fractionation model suggests that the rocks at the base of the volcanic pile should be the most primitive, yet the dendritic flows do not agree with this suggestion. Five possible explanations may explain why the dendritic flows do not follow this trend: i) these rocks may be intrusive and had a separate magma responsible for the evolution; ii) they may be an exotic unit which were juxstaposed

against the ultramafic flows; iii) they may be related to the McElroy supracrustal rocks, but were formed from a separate magma or the top of a holding chamber; iv) the dendritic flows are an example of reverse fractionation stratigraphy or v) the dendritic flows represent early, less dense fractionated lavas which fractionated first.

Field evidence does not support the possibility that the dendritic rocks are intrusive. A contact between dendritic flows and massive mafic flows was found. This contact did not show any evidence (i.e. xenoliths, chill margins) of an intrusive relationship (Figure 4-6). Also, the dendritic flows exhibit a variety textures and grain size variations at the outcrop scale suggesting that a variable cooling rate was active, which is common for effusive rocks but not for intrusive rocks.

If the rocks are an exotic or allocthonous unit or if the assemblage was folded, field evidence should support this idea. Again, in the field, there were no indications to suggest that this unit is in fault contact with the adjacent units (Figure 4-6). Facing directions indicate that the McElroy assemblage has a homoclinal structure and structural placement of the dendritic flow at the base of the assemblage is unlikely.

The lack of good field evidence for a mechanical explanation of the dendritic flows suggests that a geochemical explanation is more probable. Archean volcanism has been shown to be affected by various processes such as normal and reverse fractional crystallization (Sutcliffe et al.1991), magma mixing, liquid immiscibility and compositionally zoned magma chambers (Thurston and Fryer 1983).

4.6 Summary

The McElroy and Larder Lake assemblages have similar geochemical characteristics and follow comparable fractionation trends. Both assemblages show fractionated major and

Figure 4-6: Outcrop exposure of a contact between a dendritic flow and a massive flow. The contact is sharp and lacks evidence of either an intrusive relationship or a fault relationship.

trace element patterns. In the McElroy assemblage, fractionated rocks are the aphanitic and dendritic flows, whereas less fractionated rocks are the ultramafic and medium grained flows. In the Larder Lake assemblage, aphanitic flows are both primitive and fractionated. Although there are geochemical similarities, various textures differentiate the two assemblages. Since the Larder Lake rocks generally lack textural variations (i.e. all aphanitic to fine grained), a constant cooling rate at relatively shallow levels is probable. In contrast, the McElroy assemblage shows variable textures indicating variable cooling rates and possible variable depths of cooling.

Chapter 5

Generation of McElroy Melts

5.1 Introduction

Processes governing magma composition include partial melting, fractional crystallization, assimilation-fractional crystallization and/or liquid immiscibility models.

Partial melting models can be used if the rocks are thought to have a direct linkage to a source material. Partial melting occurs when a source is heated to produce a liquid and a residual phase. The amount of liquid generated and the composition of the magma and remaining residue is a function of the degree of partial melting that has occurred. The degree of partial melting is a function of pressure and temperature. This initial melt may erupt soon after generation undergoing limited modification and erupt as a primitive magma (e.g. komatiite). Magmas may also "pond" for a period of time during which the melt differentiates by crystal fractionation. Melts modified by limited fractionation appear to be the most "primitive" while later liquids are more evolved, having had more time to differentiate. During ascent the magma is in constant contact with the wall rock, causing some of the wall rock to become incorporated into the magma and possibly melt, thus changing the composition of the magma. Modifications are greatest if the wallrock has a different composition than the magma whereas the changes are limited if the magma and wallrock are similar. Wallrock assimilation, in conjunction with differentiation during fractional crystallization is called assimilation-fractional crystallization (AFC) or contamination (DePaolo 1981).

5.2 Magma Genesis in the Kirkland Lake Area

In the Kirkland Lake area, previous workers Smith (1980), Thurston (1980), Ludden

et al. (1986), Ujike and Goodwin (1987) and Fowler and Jensen (1989) have modelled the Blake River and Kinojevis assemblages based on trace elements. Processes cited in the generation of these metavolcanic dominated assemblages include fractional crystallization, partial melting or assimilation-fractional crystallization.

Smith (1980) suggested that sequential batch melting may have generated the Blake River assemblage metavolcanic rocks. Contrasting REE patterns for mafic members of the Blake River assemblage result from different residual mineral assemblages formed during partial melting of a mantle lherzolite. Flat REE trends of tholeiitic rocks were produced by 10% melting of the previous residue. A residual assemblage of olivine and orthopyroxene remained. The calc-alkaline source contained clinopyroxene, and garnet or amphibole. Thurston (1980) compared the rhyolites of the two groups and suggested that the Blake River rhyolites and dacites formed from 10-20% partial melting of a garnetiferous amphibolite/eclogite or by 30-60% partial melting of granulite. Ludden et al. (1986) in examining the Blake River assemblage in Quebec, conclude that the rocks differentiated by assimilation-fractional crystallization. Ujike and Goodwin (1987) suggest the variability of the Blake River rocks was due to differing degrees of partial melting followed by fractional crystallization. Fowler and Jensen (1989) suggest that the Blake River assemblage was formed from fractional crystallization of plagioclase and clinopyroxene or by assimilation of tonalite in conjunction with fractional crystallization.

The Kinojevis assemblage may have been formed by fractional crystallization of olivine, pyroxene, plagioclase and Ti-oxides (Fowler and Jensen 1989). Jackson (1980) suggested that the flat REE patterns in the Kinojevis assemblage evolved from a parent magma with 6X chondritic source REE abundances. The enrichment was due to fractionation of clinopyroxene, plagioclase and olivine. Rhyolites, with 100X chondritic values resulted

from continued fractionation of clinopyroxene and plagioclase. The parent magma was not indicated.

In the Larder Lake assemblage, Blum and Crocket (1992) recognized three suites of extrusive rocks which range from: i) a high Mg-suite of komatiitic to Mg-basalt; ii) a tholeiitic series of Mg and Fe-rich basalt: and: iii) a low-magnesian series of basalt through rhyolite. Within these various suites, fourteen subcycles of repetitive volcanism was observed. Blum and Crockett (1992) suggest that the Larder Lake magma series was generated by partial melting of a chondritic mantle and subsequent fractional crystallization. Tholeiitic magmas were generated first by low degrees of partial melting of a chondritic mantle. Fractional crystallization differentiated the magmas into Mg-rich and Fe-rich tholeiites. Magnesian suites were later derived by partial melting of the residual peridotitic mantle from which the tholeiitic magmas were previously produced.

In general, most models envisage partial melting and/or gabbroic fractional crystallization processes as being dominate during the generation of these tholeiitic to calc alkaline metavolcanic assemblages.

5.3 Magma Genesis in the McElroy and Larder Lake assemblages

5.3.1 Introduction

Models have been developed to quantify the changes that trace elements undergo during partial melting and crystal fractionation. These calculations have been used to determine whether relationships exist between adjacent metavolcanic units within the McElroy assemblage. NEWPET, a computer program developed at the Memorial University of Newfoundland, uses Rayleigh equations to model partial melting and crystal fractionation processes of trace elements and was applied to the McElroy assemblage. Distribution coefficients used in the calculations are presented in Table 9a,b.

Table 9a: Distribution coefficients used in Rayleigh crystal fractionation calculations (from NEWPET).

	ol	opx	cpx	plag	garn
La	0.0089	0.0260	0.2880	0.1800	0.1210
Ce	0.0090	0.0325	0.3030	0.1200	0.1440
Pr	0.0095	0.0417	0.3410	0.0970	0.1880
Nd	0.0100	0.0508	0.3790	0.0810	0.2320
Sm	0.0105	0.0790	0.4760	0.0670	0.5410
Eu	0.0110	0.0990	0.3540	0.3400	0.6230
Gd	0.0120	0.1260	0.5610	0.0630	1.1900
Dy	0.0140	0.1970	0.6630	0.0550	2.5600
Er	0.0190	0.3550	0.7060	0.0630	4.2400
Yb	0.0230	0.4700	0.7190	0.0670	5.7300
Lu	0.0270	0.5900	0.7190	0.0600	6.3000
K	0.0060	0.0060	0.0270	0.3600	0.1500
Rb	0.0036	0.0030	0.0300	0.2000	0.2000
Sr	0.0090	0.0500	0.3000	3.6000	0.0900
Ba	0.0020	0.0400	0.0250	0.4600	0.0500
Cr	3.1000	10.0000	20.0000	0.0400	0.1000
Ni	19.0000	5.0000	4.4000	0.0400	0.8000
Ti	0.0100	0.1000	0.5000	0.04500	0.6900
Sc	0.2200	1.2000	3.2000	0.0400	6.5000
Y	0.0200	0.4000	0.8000	0.0250	5.0000
Nb	0.0080	0.0150	0.2160	0.0100	0.1000
Zr	0.0100	0.0200	0.4200	0.0100	0.6000
Mn	1.8000	1.4000	1.3000	0.0500	5.0000
V	0.0300	0.5000	1.0000	0.0800	0.2700
U	0.0070	0.0070	0.2530	0.0100	0.1000
Th	0.0070	0.0070	0.1584	0.0100	0.1000
Ga	0.0400	0.7000	0.5800	1.0000	12.0000

Table 9b: Distribution coefficients used in batch melting calculations (from NEWPET).

	ol	opx	cpx	plag	garn
La	0.0005	0.0005	0.0200	0.1800	0.0010
Ce	0.0008	0.0009	0.0400	0.1200	0.0033
Pr	0.0010	0.0013	0.0620	0.0970	0.0075
Nd	0.0013	0.0019	0.0900	0.0810	0.0184
Sm	0.0019	0.0028	0.1400	0.0670	0.0823
Eu	0.0019	0.0036	0.1600	0.3400	0.1333
Gd	0.0019	0.0045	0.1800	0.0630	0.1800
Dy	0.0019	0.0074	0.1930	0.0550	0.5100
Er	0.0022	0.0130	0.2000	0.0630	1.6000
Yb	0.0040	0.0286	0.2000	0.0670	4.0000
Lu	0.0048	0.0380	0.1900	0.0600	7.0000
K	0.0002	0.0010	0.0020	0.1700	0.0010
Rb	0.0002	0.0006	0.0011	0.1000	0.0007
Sr	0.0002	0.0070	0.0670	1.8000	0.0011
Ba	0.0001	0.0010	0.0011	0.2300	0.0015
Cr	2.1000	10.0000	8.4000	0.0400	0.1000
Ni	14.0000	4.0000	3.0000	0.0400	0.8000
Ti	0.0020	0.0040	0.2000	0.0450	0.2000
Sc	0.2500	1.1000	3.1000	0.0400	6.5000
Y	0.0050	0.0300	0.2000	0.0250	2.0000
Nb	0.0004	0.0004	0.0150	0.0100	0.0150
Zr	0.0020	0.0030	0.1200	0.0100	0.0450
Mn	1.2000	1.4000	0.9000	0.0500	5.0000
V	0.0300	0.5000	1.5000	0.0800	0.2700
U	0.0015	0.0015	0.0220	0.0100	0.0100
Th	0.0015	0.0015	0.0110	0.0100	0.0100
Ga	0.0200	0.3500	0.2000	1.0000	1.0000

5.3.2 Partial Melting Modelling

During batch partial melting the liquid remains at the site of melting and is in chemical equilibrium with the solid residue until it is allowed to escape as a single batch of primary magma. The Rayleigh equation for batch partial melting is as follows:

$$C_L/C_O = 1/F+D-FD \quad ...(3)$$

where C_L is the element concentration in the liquid, C_O is the element concentration in the unmelted source, F is the weight proportion of the melt formed and D is the bulk distribution coefficient for the residue solid.

It has been suggested that chondritic ratios of REE and HFS elements existed in the earth's primitive mantle (Sun 1982). It has also been suggested that late Archean komatiites had elemental ratios similar to chondritic ratios suggesting that komatiites may represent melts derived by partial melting of a primitive mantle source (i.e. chondrite).

Relationships between HFS incompatible elements Y-Zr, Y-Ti, Zr-Ti, TiO_2-P_2O_5 and TiO_2-Al_2O_3 are plotted in Figure 5-1. Close coherence to chondritic ratios implies that little fractionation of the elements has occurred after partial melting. Deviation away from the chondrite ratio implies that one element has been either enriched or depleted with respect to the other element. Element enrichment and depletion can be caused by fractional crystallization or retention in the residual phase during partial melting since the assemblage probably does not represent the full, closed system magma chamber.

In Figure 5-1 the ultramafic rocks, some coarser grained flows and some Larder Lake basalts plot on or near the chondritic ratio. This may indicate that these rocks are the most primitive and possibly derived by a high degree of partial melting of a chondritic source in which limited fractionation has occurred. Aphanitic flows and the dendritic flows in the McElroy assemblage and some Larder Lake assemblage basalts lie off the chondritic ratio line

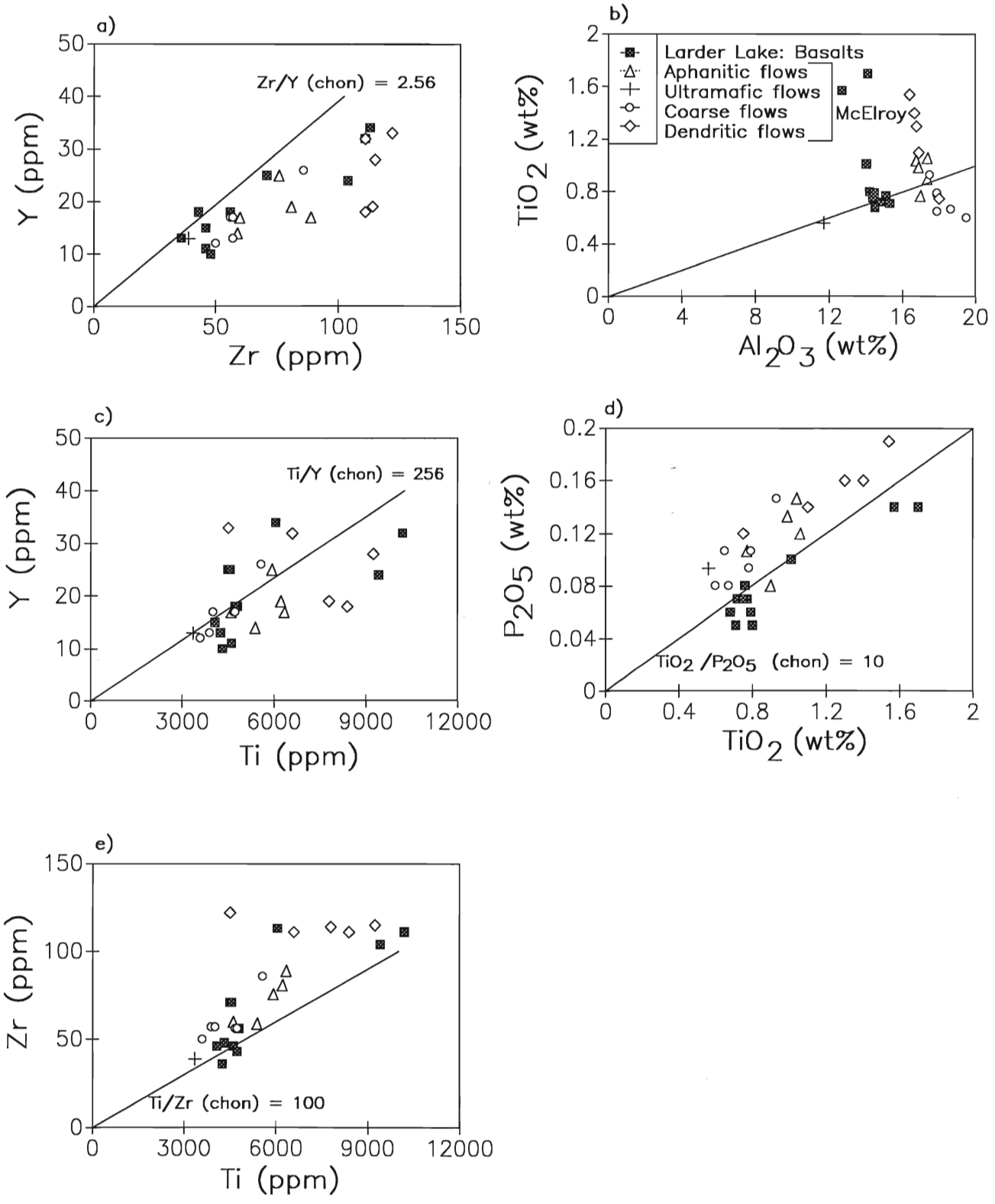

Figure 5-1:Elemental variation in the Larder Lake and McElroy assemblages with respect to chondrite data. Chondrite data from Sun and McDonough (1989).

indicating that either processes other than partial melting have affected these rocks or that they were produced by lower degrees of partial melting.

Data in Figure 5-1c,d straddle the chondrite line which indicates that Ti, Y, and P retain their chondritic ratios. In Figure 5-1a the data are below the chondritic ratio while in Figure 5-1b,e the data plot above the chondrite ratio. The trend in Figure 5-1a is due to either retention of Y into residual clinopyroxene or enrichment of Zr during fractionation. Since Y has been shown to retain its chondritic ratio with Ti (Figure 5-1c), the Zr/Y trend cannot be explained by Y retention in a residual phase such as garnet. This is confirmed by Blum and Crocket (1992) who indicate that garnet was not a residual phase in the source for the Larder Lake assemblage magmas. The Zr/Y pattern is due to Zr enrichment during fractional crystallization. A similar argument exists for the Ti-Zr trend (Figure 5-1e). The deviation away from the chondrite ratio is due to either the retention of Ti or the enrichment of Zr. Ti was shown to retain its chondritic ratio with Y and P. Thus, the Ti-Zr ratio must be the result of Zr enrichment. Enrichment of Zr with fractionation is illustrated in Figure 4-2 and 4-4.

In general, partition coefficients indicate that there are no common mantle minerals which are compatible with most of the HFS elements (Table 9). This indicates that observed deviation cannot be accounted for by retention of an element in a residual phase (typically olivine and/or orthopyroxene) and must be due to fractionation processes. Exceptions would be Y which can enter garnet, clinopyroxene and/or hornblende and Ti which is compatible with hornblende and ilmenite.

The chondrite normalized HFS element abundances are greater than chondrite indicating that these elements were concentrated into the melt portion (Figure 3-7). The chondrite normalized compatible trace elements approach the chondrite value which indicates

that these elements tend to remain in the residual phase (Figure 3-7). These two features , the HFS ratios and chondrite normalized trace element patterns, indicate that the McElroy assemblage rocks may have been derived from a chondritic source.

Partial melting calculations were used to further test this concept. In the model, the source was a primitive mantle lherzolite with element abundances from McDonough and Sun (1989). Variable mineral combinations were used. Figure 5-2 is based on a mineral assemblage of 65% olivine, 20% orthopyroxene, 10% clinopyroxene and 5% plagioclase. Garnet was not considered to be part of the partial melting process (Blum and Crocket 1992) therefore plagioclase was used as the aluminum-bearing phase. However, the starting mineral assemblage is arbitrary since during batch partial melting the minerals remain in equilibrium with the liquid (Cox et al. 1979). The original trace element concentration of the chosen source is what changes during partial melting.

Figure 5-2 shows that in the McElroy assemblage, the units can be reproduced by partial melting of a primitive mantle lherzolite source. The aphanitic flows (Figure 5-2a) can be derived by 15-20%, the ultramafic flows can be derived from 25-30% partial melting of a primitive mantle (Figure 5-2b) and the dendritic flows by 10% melting of a primitive mantle source. There is good agreement between the calculated results and the actual trace element and REE patterns. However, partial melting of a primitive mantle can not reproduce the Th, Nb and Ti abundances.

Larder Lake flows can be derived from 25-30% partial melting of a mantle lherzolite (Figure 5-3). Partial melting of primitive mantle to produce the Larder Lake samples is consistent for MREE and HREE. However, there is very little agreement between calculated results and actual LREE abundances.

In general, both assemblages may be derived from 10-35% partial melting of a

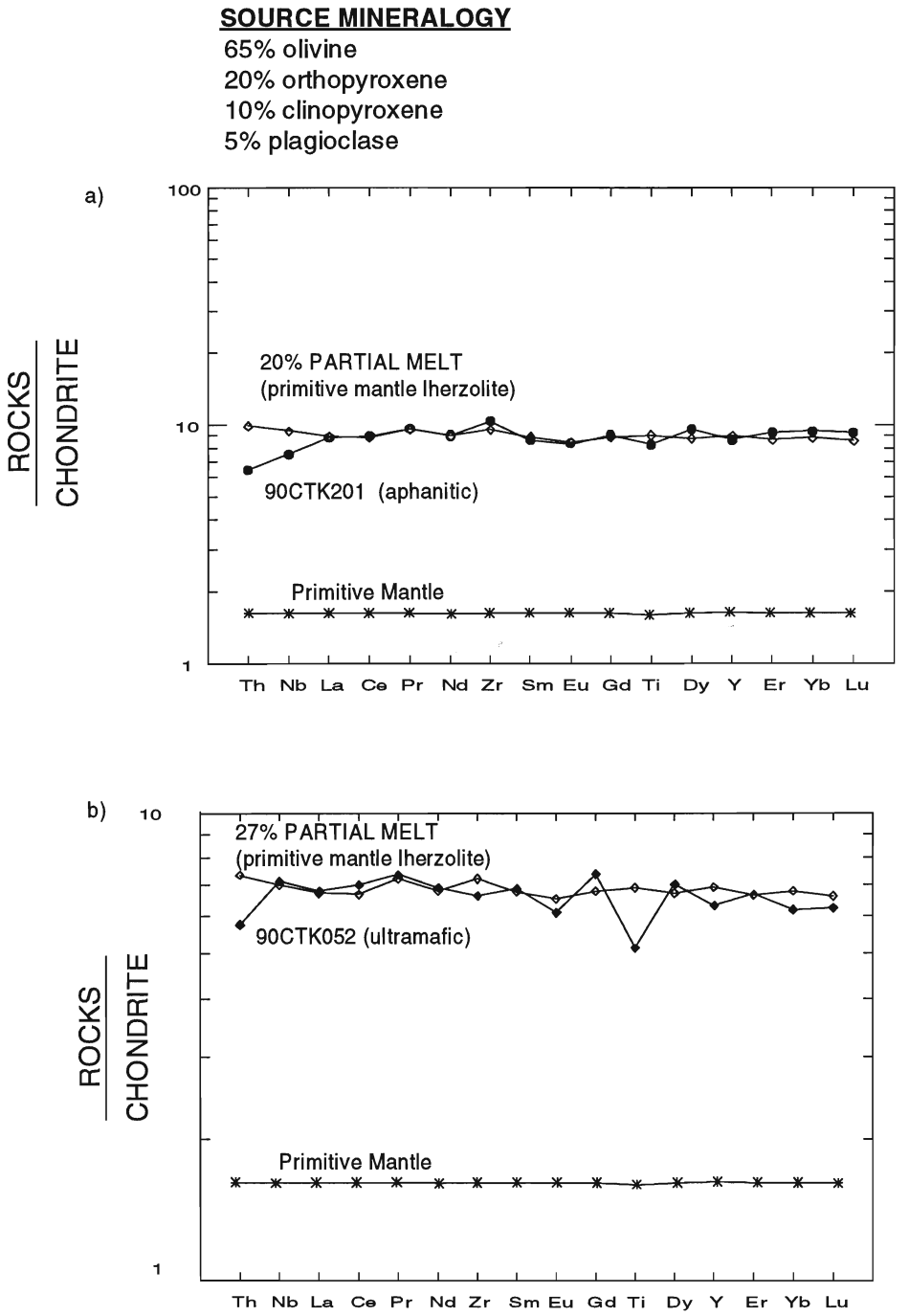

Figure 5-2: Figure presents the results of partial melting calculations for McElroy assemblage. Source material is a primitive mantle lherzolite where a) compares sample 90CTK201 (aphanitic flow) to a 20% partial melt of the lherzolite.
In b) sample 90CTK052 (ultramafic flow) is compared to a 27% partial melt of the lherzolite. Note that the evolved aphanitic flow (90CTK210) requires less partial melting than the ultramafic flow (90CTK052). The elemental patterns between actual patterns of the goal (sample) and the calculated values (partial melt) are similar suggesting that a primitive mantle lherzolite source is possible.

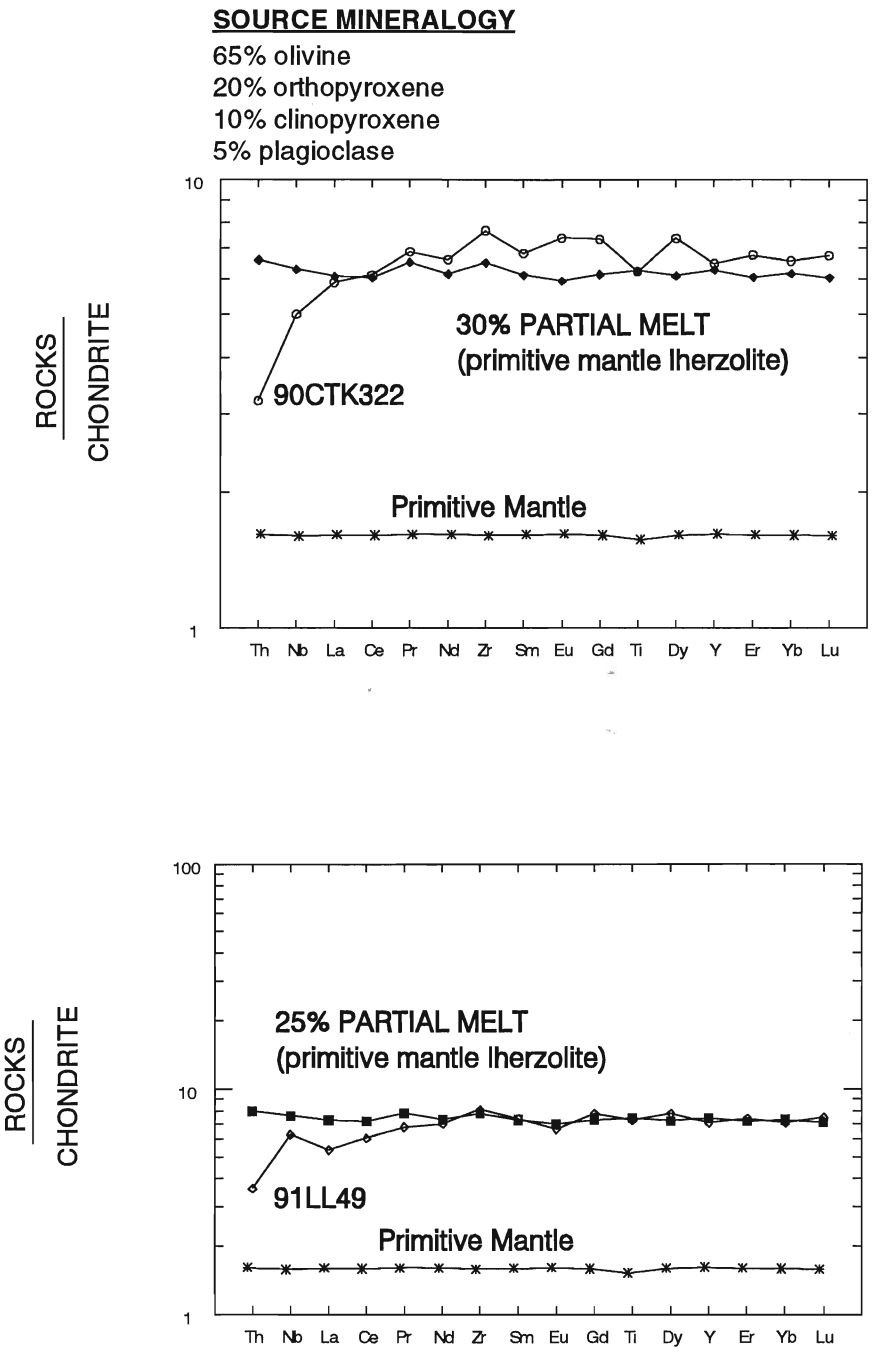

Figure 5-3: Results of partial melting calculations of Larder Lake assemblage from a primitive mantle source. The Th, Nb and LREE patterns of the Larder Lake samples and the lava derived from partial melting of a primitive mantle source do not match. This suggestisthat the Larder Lake samples were not derived from a primitive mantle lherzolite.

primitive mantle lherzolite source. However, the slightly depleted LREE patterns of Larder Lake rocks is not as well constrained with the primitive mantle as the McElroy assemblage.

Partial melting of a komatiitic source may have also generated the rocks in the McElroy and Larder Lake assemblages. A typical komatiite from Munro Township (Jochum et al. 1991) was used as a possible source. Partial melting of komatiite does not reproduce trace and REE patterns for the McElroy assemblage (Figure 5-4a,b). Depleted LREE patterns in the komatiite and values derived from partial melting calculations of a komatiite are less than the slightly depleted to flat patterns of the McElroy assemblage. The HREE patterns of the calculated and actual values show better agreement. In comparison, the Larder Lake rocks show better agreement between the calculated and the actual trace element and REE abundances (Figure 5-5). Larder Lake samples can be reproduced by 15-40% partial melting of the komatiitic source (Figure 5-5).

Partial melting calculations indicate that the McElroy assemblage is best produced by partial melting of a primitive mantle whereas the Larder Lake assemblage shows better agreement with a komatiitic source.

Alternatively, other sources may have been involved in generation of the Larder Lake assemblage. A depleted komatiite (e.g. Munro Twp. komatiite) source implies that the original source could be a depleted mantle source. Therefore, the same results may also be derived by lower degrees of melting of the mantle source which gave rise to the komatiite. The remaining evolved Larder Lake lavas could be derived by komatiitic fractionation. However, the komatiite was used as the source for the Larder Lake assemblage since the original source for the komatiite is unknown.

5.3.3 Crystal Fractionation Modelling

Section 4.2 (variation diagrams) demonstrated that the rocks within the McElroy

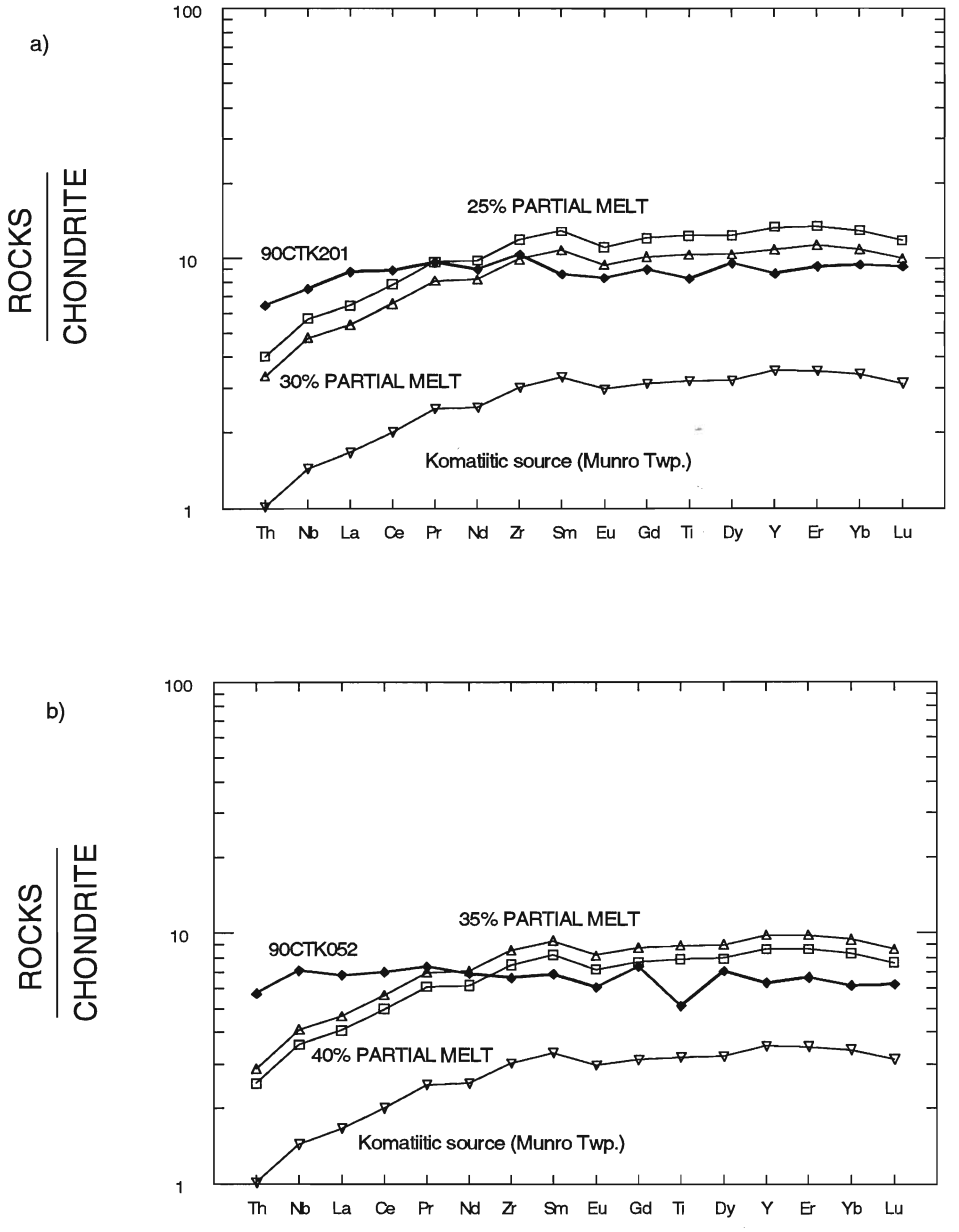

Figure 5-4:Results of partial melting calculations of McElroy rocks (a) aphanitic flow, b) ultramafic flow) from komatiitic source. Figure illustrates that McElroy samples were not derived from partial melting of a komatiitic source. Komatiitic composition from Jochum et al. (1991).

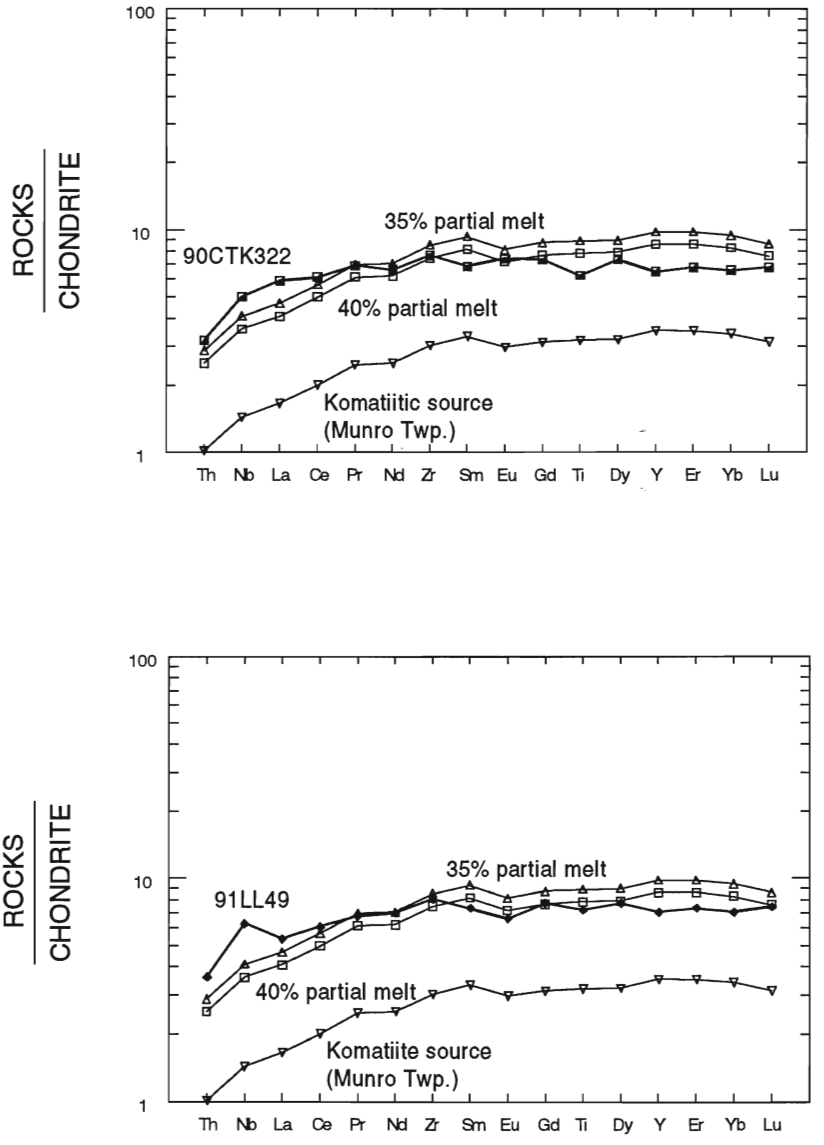

Figure 5-5: Results of partial melting calculations of Larder Lake rocks from a komatiitic source. The depleted LREE, Nb and Th patterns of the Larder Lake samples are similar to the pattern expressed by the partial melt of a komatiitic source suggesting that a komatiitic source is possible.

assemblage ranged from primitive (ultramafic flows) to evolved (dendritic flows). The variation was shown to be, in part, the result of crystal fractionation. This section attempts to quantify the type of fractionation (i.e. which minerals were involved) and the degree of fractionation that affected the various rocks.

Minerals are removed from a magma during crystal fractionation. This causes the composition of the remaining magma to change. These changes can be documented if the source and fractionated rock are known as well as a probable fractionating assemblage. Crystal fractionation models commonly use the Rayleigh equation where:

$$C_L/C_O = F^{(D-1)} \qquad ...(4)$$

where C_L is the concentration of the element in the evolved liquid (represented by an evolved rock); C_O is the concentration of the element in the source rock (represented by a primitive rock); F is the degree of fractionation; and D is the bulk distribution coefficient for the element (determined by the fractionating assemblage). In this model, the calculated trace element concentration of C_L is compared to the actual concentration of the evolved rock.

This application of the Rayleigh equation has been used to examine if the more primitive rocks are related to more evolved rocks by crystal fractionation. In Equation 4, all of the variables are controlled. Sample 90CTK052 (ultramafic flow) was chosen as the primitive, source rock (C_O) and is compared to the more evolved aphanitic, medium to coarse grained rocks and the dendritic flows (C_L) (Table 10). Various mineral combinations (olivine, pyroxene, plagioclase) were used during fractionation modelling. The minerals selected for the modelling were based on petrographic analysis which indicated that plagioclase and clinopyroxene were the major fractionated minerals. Olivine was observed in some thin sections and was included in some of the trials. Therefore, the bulk distribution coefficient (D) is a controlled variable in Equation 4 since it is dependent on the selected mineral

Table 10a: Results of Rayleigh calculations for crystal fractionation of 90CTK052

	SOURCE 90CTK052 % fract.	PLAG:CPX 1:1 65-75%	PLAG:CPX 3:1 60-70%	PLAG:CPX 1:3 70-85%	AVERAGE DENDRITIC FLOW
	OBS.	CALC.	CALC.	CALC.	OBS. n=5
Mg#	61.4				38.2
Ti	0.56	1.20-1.54	1.21-1.54	1.18-1.82	1.22
Y	13	24.1-29.4	26.6-33.3	20.9-27.5	26
Zr	39	88.9-115.8	87.9-113.5	88.7-142.4	115

	SOURCE 90CTK052 % fract.	PLAG:CPX 1:1 40-45%	PLAG:CPX 3:1 30-40%	PLAG:CPX 1:3 45-50	AVERAGE M.G.-C.G. FLOW
	OBS.	CALC.	CALC.	CALC.	OBS. n=6
Mg#	61.4				47.8
Ti	0.56	0.81-0.87	0.76-0.86	0.81-0.86	0.81
Y	13	17.5-18.5	17.2-19.4	16.5-17.1	17
Zr	39	58.2-62.4	53.5-61.4	58.7-62.6	60.3

	SOURCE 90CTK052 % fract.	PLAG:CPX 1:1 50-55%	PLAG:CPX 3:1 40-50%	PLAG:CPX 1:3 55-65%	AVERAGE APHANITIC FLOW
	OBS.	CALC.	CALC.	CALC.	OBS. n=5
Mg#	61.4				36.3
Ti	0.56	0.93-1.00	0.86-1.00	0.92-1.08	0.95
Y	13	19.5-20.8	19.4-22.3	17.8-19.7	19.5
Zr	39	67.2-73.0	61.4-72.1	67.3-79.8	76.5

TABLE 10b: Results of Rayleigh calculations for crystal fractionation of 90CTK310.

	SOURCE 90CTK310 % fract.	PLAG:CPX 1:1 50-60%	PLAG:CPX 3:1 40-55%	PLAG:CPX 1:3 60-65%	AVERAGE DENDRITIC FLOW
	OBS.	CALC.	CALC.	CALC.	OBS. n=5
Mg#	60.0				38.2
Ti	0.67	1.11-1.30	1.03-1.31	1.18-1.28	1.22
Y	17	25.5-29.1	25.3-31.7	24.4-25.7	26
Zr	57	98.2-117.0	89.7-115.8	106.5-116.7	115

	SOURCE 90CTK310 % fract.	PLAG:CPX 1:1 5-20%	PLAG:CPX 3:1 5-20%	PLAG:CPX 1:3 2-25%	AVERAGE M.G.-C.G. FLOW
	OBS.	CALC.	CALC.	CALC.	OBS. n=6
Mg#	60.0				47.8
Ti	0.67	0.70-0.79	0.70-0.81	0.69-.080	0.81
Y	17	17.5-19.4	17.7-20.2	17.3-19.0	17
Zr	57	59.3-67.9	59.7-69.5	59.0-69.4	60.3

	SOURCE 90CTK310 % fract.	PLAG:CPX 1:1 20-35%	PLAG:CPX 3:1 15-35%	PLAG:CPX 1:3 30-45%	AVERAGE APHANITIC FLOW
	OBS.	CALC.	CALC.	CALC.	OBS. n=5
Mg#	60.0				36.3
Ti	0.67	0.79-0.92	0.83-0.97	0.77-0.96	0.95
Y	17	19.4-21.9	19.6-21.5	19.3-23.8	19.5
Zr	57	67.9-79.9	72.7-85.7	65.8-83.5	76.5

assemblage. Similarly, the degree of fractionation (F) is also a controlled variable.

In general, the modelling indicated that the primitive and evolved rocks can be related by fractionation. The following is a brief summary of some of the successful results of the crystal fractionation modelling (also see Table 10). If the crystallizing phase is 100% clinopyroxene, then between 50 to 75% fractionation is required to generate the medium to coarse grained flows, whereas upwards of 85% fractionation is required to produce the aphanitic and dendritic flows. If the crystallizing phase is 100% plagioclase, then between 25 and 35% fractionation is required to produce the medium to coarse grained flow and between 50 and 65% fractionation to produce the evolved flows. Pure olivine control was also variable, and was dependent on the fractionated, daughter rock. The primitive rocks require limited olivine fractionation (5-35%) whereas the more evolved rocks required up to 60% fractionation to derive the fractionated daughter products.

Combined fractionating phases had moderating affects on the degree of fractionation. A 1:1 ratio of plagioclase and clinopyroxene required 40-45% fractionation to derive the primitive rocks and 50-65% fractionation to produce the evolved rocks. A plagioclase and clinopyroxene ratio of 3:1 required 30-40% fractionation for the primitive rocks whereas 60-70% fractionation was required to generate the evolved rocks. A 1:3 plagioclase:clinopyroxene ratio required 45-50% fractionation for the medium grained rocks and 70-85% fractionation for the most evolved rocks.

The most primitive medium to coarse grained rock, 90CTK310 ($Mg^{\#}$ 59), was also chosen as possible source during fractionation (Table 10). Olivine control required between 5 and 15% fractionation for the primitive rocks and 35-50% fractionation for the evolved rocks. Clinopyroxene was variable, requiring 5-30% fractionation for the primitive rocks and up to 70% fractionation for the evolved rocks. Plagioclase fractionation required between 5

and 15% fractionation to derive the primitive rocks and 35-50% fractionation to produce the evolved rocks. Combined plagioclase and clinopyroxene at a 1:1 ratio required between 5 and 20% fractionation for the evolved rocks and up to 60% fractionation for the evolved rocks. A plagioclase:clinopyroxene ratio of 3:1 also required 5-20% fractionation for the primitive rocks and 40-55% fractionation for the evolved rocks. A plagioclase ratio of 1:3 required 5-25% and 60-65% fractionation for primitive and evolved rock generation, respectively.

In general, the samples can be reproduced by crystal fractionation with a crystallizing assemblage of olivine, clinopyroxene and plagioclase from a source rock (e.g. 90CTK052, 90CTK310). The degree of fractionation is dependent on the source rock, daughter product and fractionating assemblage.

The role of crystal fractionation was expanded to relate the McElroy and Larder Lake assemblages. If the assemblages are genetically related then the evolved rocks may be fractionated from a common source (e.g. 90CTK052). Rare earth patterns for the most evolved samples from each assemblage were reproduced with a parent composition of sample 90CTK052 and a fractionating assemblage of plagioclase and clinopyroxene in a 3:1 ratio (Figure 5-6). The Larder Lake sample required more fractionation (60%) (Figure 5-6a) than the McElroy sample (50%) (Figure 5-6b) (assuming the same parent) due to its more evolved character.

It is unlikely that individual mineral phases were responsible for the fractionation within the assemblage, since this would produce cumulate phases of the fractionated mineral. Crystal cumulates of olivine and/or clinopyroxene are common in the Abitibi (e.g. Lincoln Nipissing Peridotite, Black-Grenfell Gabbroic Suite) (Jackson and Fyon 1991) however it is unlikely that these intrusive complexes are the result of crystal segregation during assemblage

a)

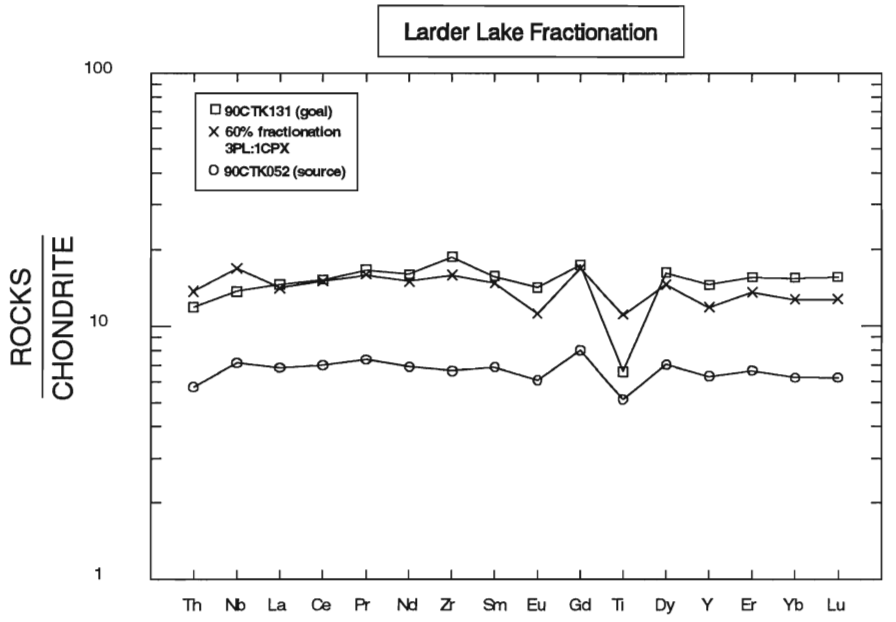

b)

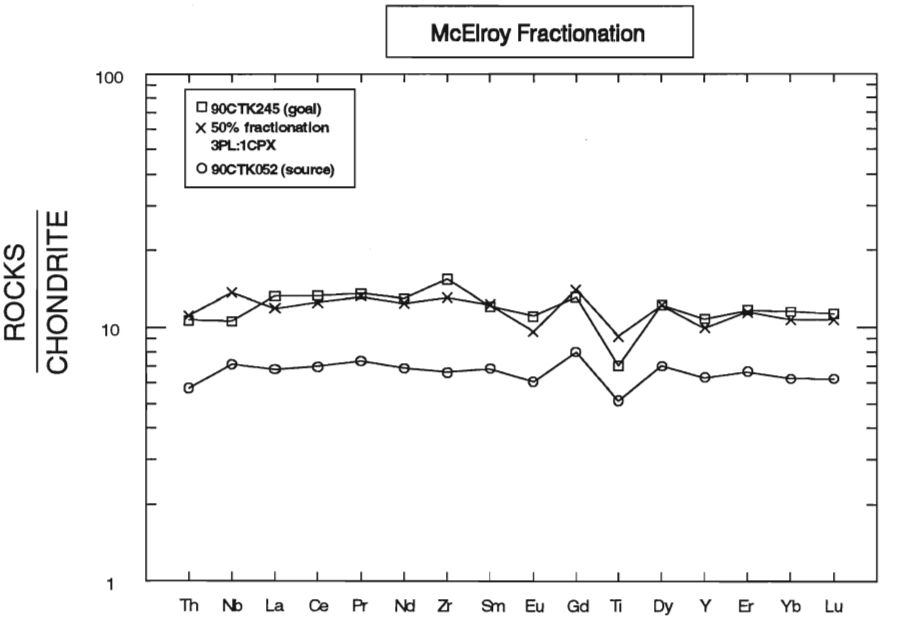

Figure 5-6: Results of trace element (HFS) and REE crystal fractionation calculations for a) Larder Lake assemblage and b) McElroy assemblage. The goal for each assemblage is the most fractionated tholeiite and the source is 90CTK052 (ultramafic flow from the McElroy assemblage). This figure illustrates that the tholeiitic basalts in both assemblages may have been derived by crystal fractionation from a more primitive lava.

formation. Smaller scale cumulate suites were not found in the vicinity of the metavolcanic flows. Also, plagioclase cumulate suites are rare in the southern Abitibi (MacRae 1969). Therefore a combination of olivine, clinopyroxene and plagioclase was a probable fractionating assemblage which affected the variable rock types in the McElroy assemblage.

5.3.4 Crustal Contamination

Contamination from continental crust is possible during magmatic ascent and eruption. Nb/Th ratios are sensitive indicators of crustal contamination and can distinguish contaminated lavas from lavas with primary trace element ratios (Jochum et al. 1991). Contamination will increase the abundance of incompatible elements with crustal affinities (e.g. LREE, Th, U, Ta, Sr) but not affect elements normally depleted in crustal material (Nb, Ti, P, Ni, Sc) (Jolly et al. 1992). The result is a magma enriched in LREE and Th with negative Nb, Ta, Ti anomalies (Jochum et al. 1991).

In Figure 5-7 McElroy and Larder Lake samples are compared to a tholeiite sample from Kambalda contaminated by a crustal component (Jochum et al. 1991). The McElroy assemblage shows slight Nb, Th and Ti depletion (Figure 5-7a) with a Nb/Th ratio of 9.8 (Figure 5-7b). The Larder Lake assemblage shows greater Th depletion, weak Nb depletion and is characterized by a Nb/Th ratio of 12.1 (Figure 5-7b). This is in contrast to the Kambalda basalt which exhibits an enriched LREE pattern and a strong Nb depletion. The Kambalda sample has a Nb/Th ratio of 0.8 (Figure 5-7b). Based on the REE patterns, trace element ratios and comparison with a contaminated sample, there is no evidence of sialic contamination for either McElroy or Larder Lake assemblages.

a)

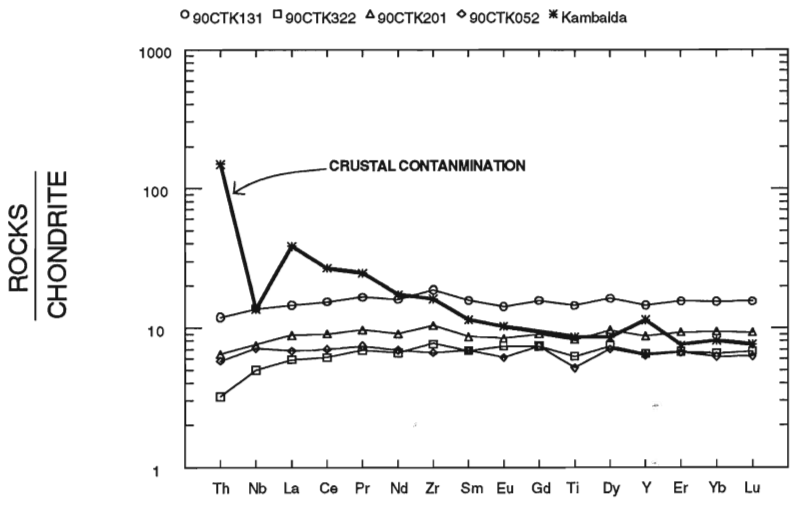

b)

AVERAGE	La/Th	Nb/Th	Nb/La	Th/La
Larder Lake	12.9	12.1	0.946	0.078
McElroy	11.0	9.8	0.88	0.09
Kambalda	2.2	0.80	0.4	0.45

Figure 5-7: a) Comparison of McElroy (diamond & triangle) and Larder Lake assemblages (circle & square) with a crustally contaminated Kambalda tholeiite. Kambalda sample from Jochum et al. (1991).
b) Elemental ratios indicating the difference between contaminated (Kambalda) and non-contaminated (McElroy and Larder Lake) samples.

5.3.5 Summary

Quantitative models provide specific answers to problems which are largely dependent on assumptions. The models represent highly idealized processes and are at best a first approximation to a problem.

The McElroy assemblage is a homoclinal sequence of ultramafic to mafic metavolcanic rocks. Variation diagrams indicate that the rocks can be related by gabbroic fractionation.

Combined partial melting and crystal fractionation may explain the lithologic relationships in the McElroy assemblage. The flows represent the order of eruption in which the dendritic flows were the first to erupt after a low degree of partial melting (10-15%). Continued partial melting (up to 30-35%) produced the ultramafic flows. Ponding allowed for the ultramafic flows to differentiate generating the coarse grained flows and the aphanitic flows (Figure 5-8 b1).

In terms of fractionation, the dendritic flows may represent the upper part of a relict differentiated flow in which the lower sections are no longer present. There is evidence of structural complications at the McElroy/Skead contact and part of the McElroy assemblage may have been removed. The remaining parts of the McElroy assemblage could represent a second pulse of magmatic activity beginning with the partial melting of a primitive mantle lherzolite to generate the ultramafic flows and ending with crystal fractionation to produce the aphanitic flows (Figure 5-8 b2).

The rocks of the Larder Lake assemblage were derived from partial melting of a komatiitic source to produce the primitive samples (i.e. Mg-rich tholeiites and komatiites). This was followed by crystal fractionation which generated the more evolved Fe-rich tholeiitic rocks (Figure 5-8a).

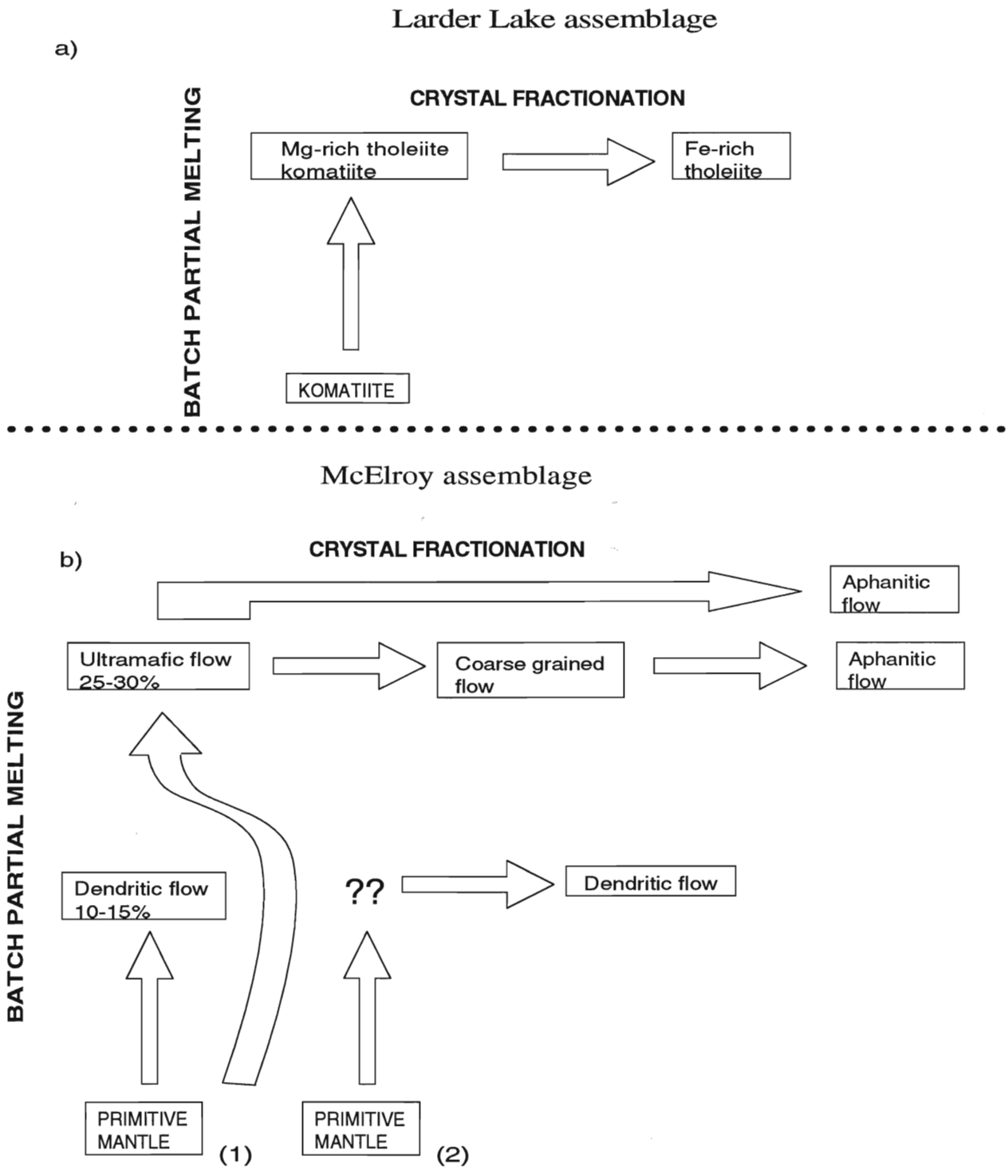

Figure 5-8: Proposed magma generation models for the a) Larder Lake assemblage and b) McElroy assemblage. a) Larder Lake magmas are derived from partial melting of a komatiite source followed by crystal fractionation. b) McElroy magmas can be derived from partial melting of a primitive mantle source followed by crystal fractionation (1). Alternatively, an intermediate step may also be involved in which the dendritic flows are the product of an earlier fractionation process (2).

Chapter 6

Comparison with Phanerozoic Rocks of Known Tectonic Setting

6.1 Introduction

It is difficult to determine the tectonic environment of Archean metavolcanic assemblages because of changes which affected the rocks since formation. Minor elements and immobile trace element discriminant diagrams based on modern volcanic settings are used to document a probable tectonic setting for rocks of unknown origin. The elements that are used have similar chemical characteristics (e.g. ionic radius and charge) and behave similarly during magmatic and alteration processes. Therefore, any changes that affect a rock will affect all elements with similar characteristics to a similar degree such that the element ratios remain unchanged. Elements commonly used are the high field strength (HFS) and rare earth elements (REE) since these elements are relatively immobile (Section 3.2) (e.g. Pearce and Cann 1973, Pearce and Norry 1979).

Modern tholeiitic rocks are found in a wide variety of tectonic settings. Tholeiitic ocean floor basalts can form at divergent plate margins within large ocean basins such as mid-ocean ridge basalts (MORB) (Sun et al. 1978, Flower 1989) or in smaller ocean basins behind island arcs (back-arc basins, e.g. Mariana Trough; Stern et al. 1990). Island arc tholeiites (low K-tholeiites) erupt on oceanic crust at converging plate margins during the early stages of arc development (e.g. Mariana Trough; Stern et al. 1990). Island arc tholeiites are commonly followed by calc-alkalic basalts erupting on continental crust boundaries and/or on oceanic crust as the crust thickens. Within plate basalts can include both ocean island (e.g. Hawaii; Chen et al. 1991) and continental tholeiites (e.g. Columbia River). Ocean island basalts erupt as ocean islands within oceanic basins. Continental tholeiites erupt through continental crust at continental rifts in a within plate setting.

6.2 Discriminant Diagrams

On the Ti/100-Zr-Y*3 (Figure 6-1a) diagram of Pearce and Cann (1973), the majority of the tholeiites in the Larder Lake area fall into field B with some overlap into field D. Field B includes ocean floor basalts, low K-tholeiites and calc-alkali basalts. Field D contains within plate basalts. Similarly, on the Ti-Zr diagram (Figure 6-1b), the majority of the samples fall in fields B and D. On the V-Ti/1000 diagram (Figure 6-1c), the rocks straddle the arc-ocean floor basalt boundary with 75% of the samples falling on the ocean floor basalt field. The TiO_2-MnO*10-P_2O_5*10 diagram of Mullen (1983) (Figure 6-2a) illustrates an island arc tholeiitic affinity for the majority of the samples. There is some overlap into mid-ocean ridge and calc-alkali basalt fields. The Th/Yb-Ta/Yb diagram of Winchester and Floyd (1977) (Figure 6-2b) indicates that the rocks were formed in a within plate setting. Yb was used as a normalizing element as its' abundance in tholeiitic rocks remains the same. Normalizing reduces variability due to fractionation processes so that the chemical signature more clearly reflects that of the tectonic setting. The Ce/Nb-Th/Nb diagram (Figures 6-3) shows a back-arc setting for the McElroy, Larder Lake and Kinojevis assemblages.

6.3 Tectonic Setting of McElroy and Larder Lake assemblages

The four tholeiitic assemblages, Catharine, McElroy, Larder Lake and Kinojevis, within the Kirkland Lake region define fields when plotted on various discriminant diagrams. The samples showed a within plate/ocean floor affinity which can include MORB, ocean island and back-arc basin basalts. However, in many cases there was some overlap into adjacent fields, in particular low K-tholeiites which includes island arc tholeiites.

Basalts from a within plate-setting may erupt through ocean material (e.g. ocean island

a)

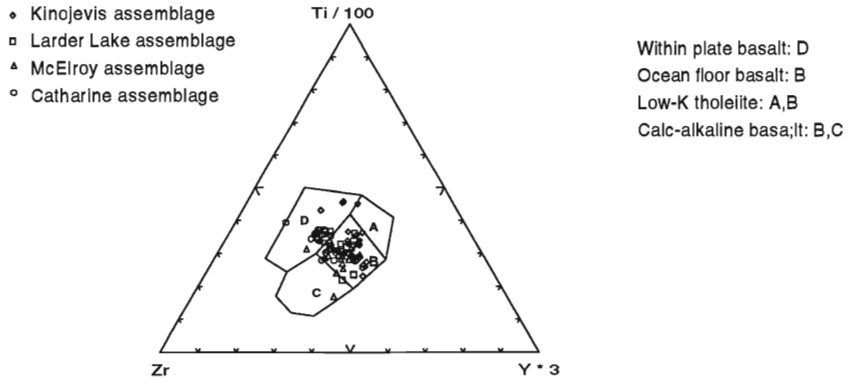

b)

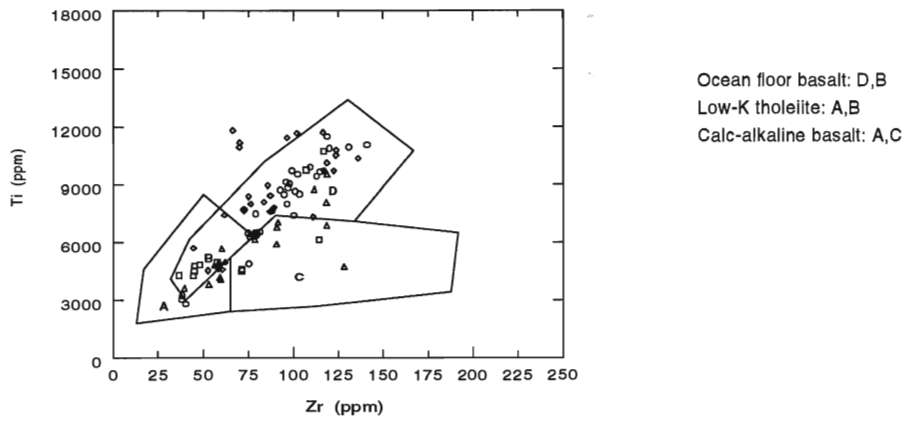

c)

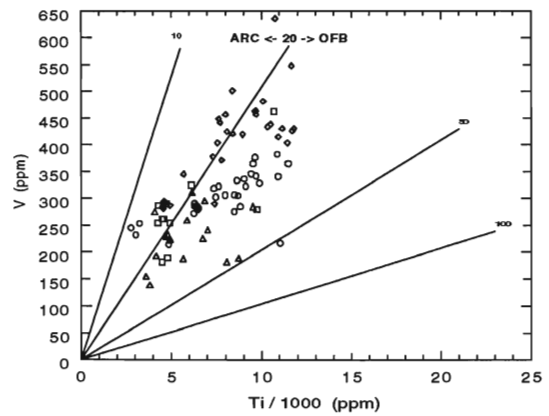

Figure 6-1:Tectonic discriminant diagrams for tholeiitic to komatiitic assemblages in the Larder Lake region. Fields for a) and b) from Pearce and Cann, 1973 fields in c) are from Shervais, 1982.

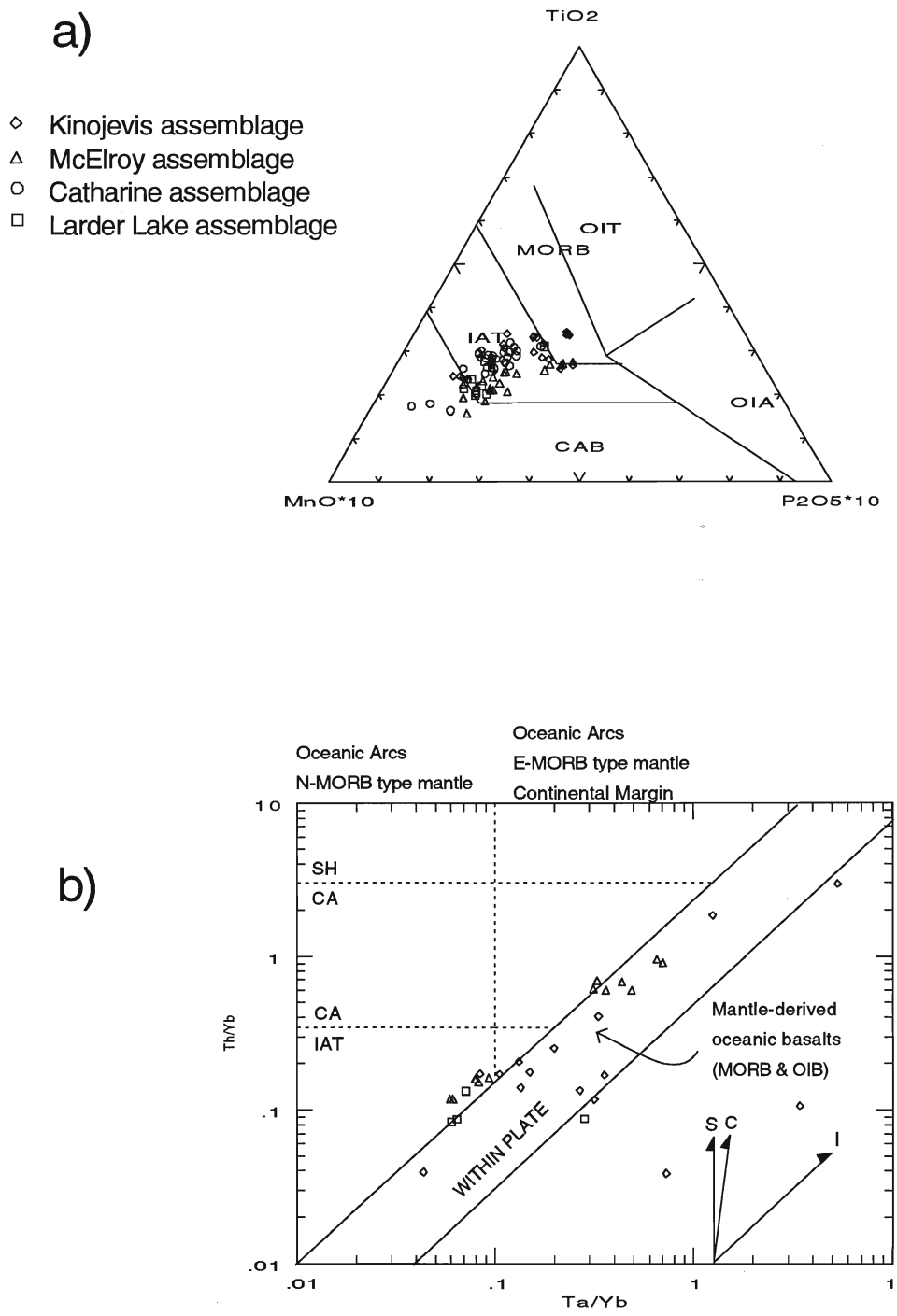

Figure 6-2: Tectonic discriminant diagrams for tholeiitic and komatiitic assemblages in the Larder Lake region. Fields in a) are from Mullen, 1983, fields in b) are from Pearce, 1983. Enrichment vectors in b) are from I: Igneous, C: Contamination and S: Subduction components.

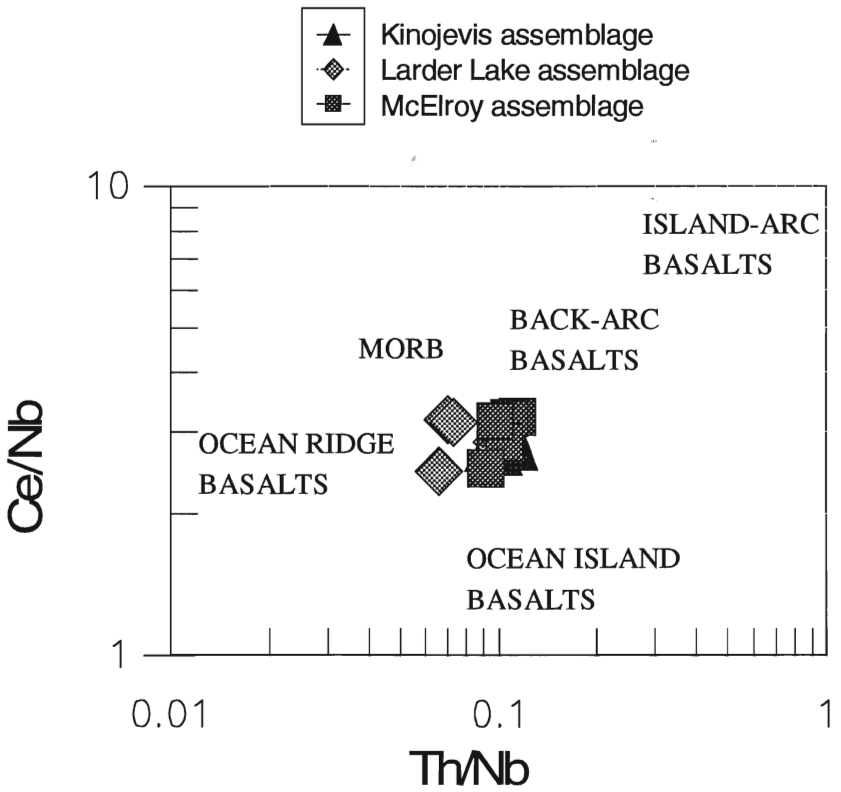

Figure 6-3: Tectonic discriminant diagram for Kinojevis, McElroy and Larder Lake assemblages. Fields from Saunders and Tarney,1989. Graph illustrates that back-arc basalts can be derived by mixtures of MORB-like and arc-like sources.

basalts of Hawaii) or through continental material (e.g. Columbia River flood basalts). Ocean island tholeiites are characterized by having LREE enrichment patterns. Continental tholeiites are characterized by a crustal component of LILE and LREE enrichment patterns and HFS depletions. The tholeiites do not have enriched LREE and LILE patterns (Figure 3-7, 3-8) nor do they contain depleted HFS patterns. In addition, Section 5.3.4 showed that crustal contamination was not likely a process which affected the basalts. Therefore based on the REE and extended trace element patterns, it is unlikely that the basalts erupted in a within plate setting.

Modern N-MORB are characterized by having flat to slightly depleted chondrite normalized REE patterns (Figure 3-7, 3-8). The McElroy and Larder Lake tholeiites are characterized by having slightly depleted to slightly enriched REE patterns (Figure 3-7, 3-8).

Island arc settings exhibit differing characteristics depending on the stage of its development. Early island arc tholeiites erupt through thin oceanic crust and have generally flat REE patterns. As the thickness of the volcanic pile increases, primary melts do not reach the surface as fractionation and contamination can alter the composition of the magma. Also, the sediment input from subduction related settings can alter the composition of the magma (e.g. increasing the U, Pb, Sr, Th contents). As the island arc evolves a back-arc basin can develop. In addition, the chemical signature of the rocks also change. Back-arc basin basalts have been shown to contain both arc and MORB-like characteristics depending on the stage of rifting. Early formed back arc basalts have arc like features (high LREE and low HFS) whereas with continued rifting and basin development, the basalts contain flat MORB-like REE patterns (Stern et al. 1990). Thus, the geochemistry of the McElroy and Larder Lake assemblages are interpreted as the result of processes in an island arc setting.

Chapter 7

7.1 Discussion

Archean greenstone belts from various shield areas have been explained by plate tectonic processes. The Michipicoten Greenstone belt formed at a convergent plate margin that varied laterally from an immature island arc built on oceanic crust to a mature arc underlain by continental crust (Sylvester et al. 1987). Lithologic relationships in the Slave Province led Fyson and Helmstaedt (1988) to conclude that opening and closing of an oceanic basin produced the various lithologic relationships. Komatiitic to tholeiitic rocks from the Norseman area of Australia were formed in a continental back arc basin in which some of the rocks were contaminated (Jolly and Hallberg 1990). Supracrustal rocks of the Ventersdorp Supergroup in South Africa were formed in a continental margin-arc setting (Crow and Condie 1988). The above examples indicate that plate tectonic models can be employed to explain the evolution of Archean supracrustal assemblages.

The Abitibi Greenstone Belt is a complex collage of metavolcanic and metasedimentary assemblages of variable composition and age (Table 1). Tectonic models explaining their evolution include oceanic extension (Hodgson and Hamilton 1989, Barrie 1989, Blum and Crocket 1992), island arc-type settings (Hodgson and Hamilton 1989, Dimroth et al. 1983a) and rifted arc (Ludden et al 1986). In the Larder Lake region there are several komatiitic to tholeiitic assemblages which have similar geochemical signatures (Figure 6-1 and 6-2) and ages (Table 1). This suggests that similar processes and tectonic environments were responsible for their formation. However, these assemblages are often structurally disrupted and fault bounded, preventing inter-assemblage correlations to be established. Intra-assemblage correlations are also commonly problematic as some assemblages are more internally complicated than others (e.g. Larder Lake assemblage

compared to the McElroy assemblage). This suggests that the assemblages were not formed by a single island-arc setting but several arcs may have been operating simultaneously. The time span for assemblage development in the southern Abitibi Greenstone Belt was less than 50 Ma (Corfu and Nobel 1992). Post-eruption movement has stacked similar assemblages against each other.

The McElroy assemblage rocks were generated by partial melting of a primitive mantle, with the resulting magma later modified by crystal fractionation (Figure 5-8). Magma formation occurred during the later stages of arc development as a back-arc basin developed. Pressure release caused by rifting of the basin allowed for upwelling of a primitive mantle and associated partial melting of the mantle lherzolite (Figure 7-1). Low level ponding of the magma allowed it to differentiate into the various units of the assemblage.

In contrast the Larder Lake assemblage can best be explained by partial melting of a komatiitic source with associated crystal fractionation (Figure 5-8). Subduction of komatiitic oceanic crust during the early stages of arc development would provide the komatiitic source for partial melting. Partial melting of subducted komatiitic crust would occur at a shallow depth, as high pressure garnet was not a residual phase. In addition a hotter Archean would also allow for a low angle of subduction. Eruption of partially melted komatiitic material through oceanic crust of similar composition prior to crustal thickening could produce the Larder Lake magmas (Figure 7-1).

Whether the McElroy and Larder Lake assemblages were formed as part of the same island arc system is unknown. Presently, island arc systems have a life span of 40-50 Ma. If the two assemblages were part of the same system, the Larder Lake assemblage should be 10-20 Ma older than the McElroy assemblage. If these assemblages originated from the same island arc system, then the Larder Lake assemblage should be older than the McElroy

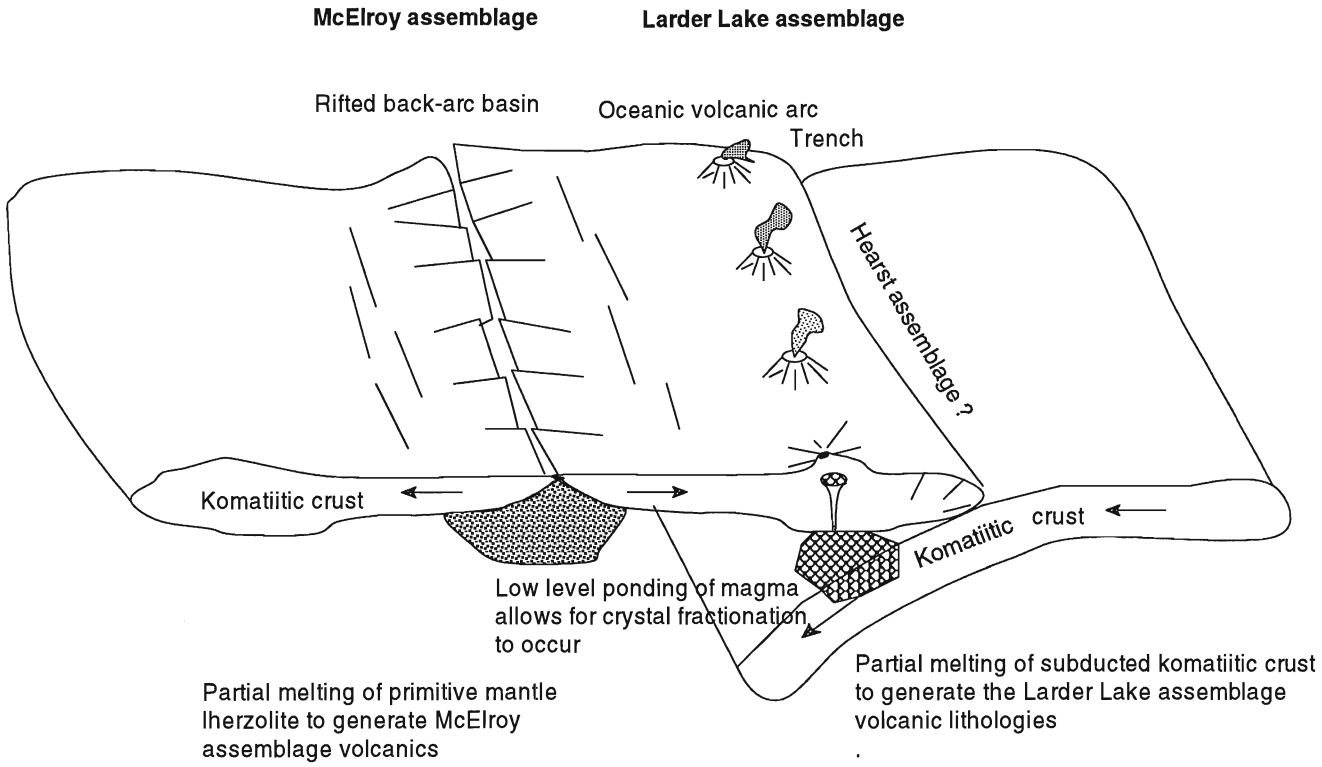

Figure 7-1: Proposed tectonic settings responsible for the generation of the McElroy and Larder Lake assemblages. The McElroy assemblage rocks were derived by partial melting of primitive mantle in a back arc setting. The Larder Lake rocks were formed by partial melting of subducted komatiitic crust during the early stages of arc formation. Both assemblages were modified by crystal fractionation.

assemblage since a volcanic front (Larder Lake assemblage) would develop prior to a back arc basin (McElroy assemblage). At present, only the Larder Lake assemblage has been dated (2701 Ma).

The occurrence of similar metavolcanic assemblages developing over a short period of time and commonly separated by faults suggests that several tectonic environments (e.g. island arc settings) were operating during the late Archean. Post Archean tectonism juxstaposed the assemblages to form the Canadian Shield.

7.2 Archean Heat Flow and Tectonics

Several island arc settings may have been operating during the formation of the Archean Abitibi Greenstone Belt. Windley (1984) suggests that the Archean was a period of increased crustal formation and subduction. Subduction requires negative buoyancy with respect to the mantle which is achieved by cooling of the crust. It has also been suggested that the heat flow in the Archean was 2-3 times greater than at present. Low and medium grade metamorphism, common to Archean greenstone belts, indicates that the Archean heat was not effectively consumed by metamorphic processes (Nisbet and Fowler 1983) and that some other process is responsible for dissipating the heat. Presently, it is estimated that 40-60% of the heat produced in the earth is brought to the surface during the formation and cooling of oceanic crust (Arndt 1983). Archean subduction can be achieved by increasing spreading rate, increasing ridge length (Hargraves 1986) or if the subducting material was komatiitic in composition (Arndt 1983). Increased spreading rates would reduce the cooling time of the oceanic crust preventing the negative buoyancy necessary for subduction. Hargraves (1986) suggests that increased ridge length in the Archean could be accomplished by many small plates moving slowly (Hargraves 1986). This could produce many analogues

to modern tectonic settings (e.g. island arcs) operating over a short time span and satisfy the suggestion of intense Archean crustal generation. The subduction of hotter Archean crust with faster spreading rates may be further explained if the subducting slabs were komatiitic in composition (Arndt 1983). Dense komatiitic crust common to Archean ensimatic settings could provide the negative buoyancy if it was not available due to cooling. This would provide a means of making komatiite a source to be partially melted. In addition, deformed greenstone belt boundaries is an indication that the greenstone belts have moved since their formation (Hoffman 1988). Therefore, adjacent packages of greenstone need not necessarily be generated in the same tectonic setting.

Chapter 8

Conclusions

Variable field, geochemical and geochronological relationships in the Larder Lake area indicate that adjacent fault-bounded packages of metavolcanic rocks have different petrogenetic histories. Two metavolcanic dominated assemblages, the McElroy and Larder Lake are separated by the Lincoln Nipissing Shear Zone. The McElroy assemblage displays a simple homoclinal structure and consists mainly of tholeiitic pillowed, medium to coarse grained massive and dendritic-textured flows. A thin massive flow of basaltic komatiite is present near the base. In the lower portions of the assemblage intermediate to felsic volcaniclastic and debris flows are interbedded with the mafic volcanics. In contrast, the Larder Lake assemblage consists of komatiitic to tholeiitic pillowed and massive flows. Generally, Larder Lake rocks are finer grained than the McElroy metavolcanic rocks. Also the Larder Lake assemblage is more structurally disrupted by folds and faults.

The less complicated structure in the McElroy assemblage allows for the various rocks in the assemblage to be identified and internal relationships to be examined. A genetic link between the units and a source mechanism is postulated. Mafic units include the Fe-tholeiitic dendritic and aphanitic (commonly pillowed) flows and the Mg-rich tholeiitic medium to coarse grained massive flows. Rocks determined in the field to be ultramafic are komatiitic basalt in composition. The geochemical variation among the ultramafic and mafic flows is explained by fractionation of olivine, clinopyroxene, and plagioclase in gabbroic proportions.

Originally, the rocks were produced by various combinations of partial melting of a primitive mantle source with associated crystal fractionation processes. Two possible scenarios for the McElroy assemblage are presented. One model suggests that the dendritic flows were derived by 10-15% partial melting of a primitive mantle lherzolite source. The

dendritic flows erupted prior to undergoing magma modification. This was followed by continued melting (30-35%) to produce the ultamafic flows in which only some of the ultramafic material reached the surface. The remaining liquid underwent crystal fractionation in a shallow magma chamber and generated the evolved rocks of the assemblage. The other model suggests that only part of the original McElroy assemblage is present. In this case, the dendritic flows represent the upper part of a differentiated flow in which the lower portion is no longer present. The remaining McElroy rocks follow a simple fractionated sequence, and were generated by subsequent fractionated magma pulses. Geochemical signatures are consistent with partial melting of a primitive mantle lherzolite.

The Larder Lake tholeiitic (Fe and Mg-rich) rocks are geochemically similar to the McElroy tholeiites and follow similar gabbroic fractionation trends. However, Larder Lake tholeiites show a greater range in the degree of fractionation from primitive to evolved rocks and trace elements show a strong komatiite signature. The Larder Lake tholeiites have greater Th, Nb and LREE depletions, characteristic to komatiitic lavas. These features indicate that komatiitic-like compositions may have had a greater role in magma genesis. Also, the Larder Lake tholeiites are more favourably modelled by partial melting of a komatiitic source as opposed to a primitive mantle source suggested for the McElroy assemblage. A komatiitic source for partial melting can be obtained if the tectonic setting responsible for magma formation was an oceanic volcanic arc. Partial melting of a subducted, komatiitic, oceanic crust could occur if Archean oceanic crust was komatiitic in composition. Eruption of a primitive magma during the early stages arc development would prevent the magma from becoming modified due to contamination. Low level differentiation would produce the various fractionated tholeiites.

References

Abraham,E.M. 1951. Geology of McElroy and part of Boston Township. Ontario Department of Mines, vol.59, pt.vi, 66p.

Anderson,A.T. and Greenland,L.P.1969. Phosphorous fractionation diagram as a qualitative indicator of crystallization differentiation of basaltic liquids. Geochemica et Cosmochimica Acta,**33**:493-505.

Arndt,N,T., 1983. Role of thin, komatiite-rich oceanic crust in the Archean plate-tectonic process. Geology,**11**:372-375.

Barrie,C.T., Naldrett,A.J. and Davis,D. 1990. Geochemical constraints on the genesis of the Montcalm of the Montcalm Gabbroic Complex and Ni-Cu Deposit, Western Abitibi Subprovince, Ontario. Canadian Mineralogist,**28**:451-474.

Barrie,C.T., Gorton,M.P., Naldrett,A.J. and Hart,T.R. 1991. Geochemical constraints on the petrogenesis of the Kamiskotia gabbroic complex and related basalts, western Abitibi Subprovince, Ontario, Canada. Precambrian Research,**50**:173-199.

Bau,M., 1991. Rare-earth element mobility during hydrothermal and metamorphic fluid- rock interaction and the significance of the oxidation state of europium. Chemical Geology,**93**:219-230.

Beswick,A.E. and Soucie,G. 1978. A correction procedure for metasomatism in an Archean greenstone belt. Precambrian Research,**6**:235-248.

Blum,N. and Crocket,J.H. 1992. Repetitive cyclical volcanism in the Late Archean Larder Lake Group near Kirkland Lake, Ontario: implications of geochemistry on magma genesis. Precambrian Research.**54**:173-194.

Bowen,N.L. 1908. Larder Lake region, Ontario Bureau of Mines, Annual Report, vol.17,p.10-11.

Brock,R.W. 1907. The Larder Lake district, Ontario Bureau of Mines, Annual Report,vol.16, pt.1, p.202-218.

Burrows,A.G. and Hopkins,P.E. 1914. The Kirkland Lake and Swastika gold areas, Ontario Bureau of Mines, Annual Report, vol.23, pt. 2,p.1-39.

Card,K.D. and Cielsieski,A. 1986. Subdivisions of the Superior Province of the Canadian Shield. Geoscience Canada,**13**:5-13.

Card,K.D. 1990. A review of the Superior Province of the Canadian Shield, a product of Archean accretion. Precambrian Research.**48**:99-156.

Corfu,F., Krogh,T.E., Kwok,Y.Y. and Jensen,L.S. 1989. U-Pb zircon geochronology in the

southwestern Abitibi greenstone belt, Superior Province. Canadian Journal of Earth Science.**26**:1747-1763.

Corfu,F. and Nobel,S.R. 1992. Genesis of the southern Abitibi greenstone belt, Superior Province, Canada: Evidence from zircon Hf isotope analyses using a single filament technique. Geochimica et Cosmochimica Acta,**56**:2081-2097.

Cox,K.G., Bell.J.D. and Pankhurst,R.J. 1979. The Interpretation of Igneous Rocks. 5th edition. George Allen and Urwin. 450p.

Chen,C.Y., Frey,F.A., Garcia,M.O., Dalrymple,G.B. and Hart,S.R. 1991. The tholeiitic to alkalic basalt transition at Haleakala Volcano, Maui, Hawaii. Contributions to Mineralogy and Petrology,**106**:183-200.

Crow,C. and Condie,K.C. 1988. Geochemistry and origin of late Archean volcanics from the Ventersdorp Supergroup, South Africa. Precambrian Research,**42**:19-37.

DePaolo,D.J. 1981. Trace element and isotopic effects of combined wallrock assimilation and fractional crystallization. Earth and Planetary Science Letters,**53**:189-202.

Dimroth,E., Imreh,L., Rocheleau,M. and Goulet,N. 1982. Evolution of the south-central part of the Archean Abitibi Belt, Quebec. Part I: Stratigraphy and paleogeographic model. Canadian Journal of Earth Science,**19**:1729-1758.

Dimroth,E., Imreh,L., Rocheleau,M. and Goulet,N. 1983a. Evolution of the south-central part of the Archean Abitibi Belt, Quebec. Part II: Tectonic evolution and geomechanical model. Canadian Journal of Earth Science,**20**:1355-1373.

Dimroth,E., Imreh,L., Rocheleau,M. and Goulet,N. 1983b. Evolution of the south-central part of the Archean Abitibi Belt, Quebec. Part III: Plutonic and metamorphic evolution and geotectonic model. Canadian Journal of Earth Sciences,**20**:1374- 1388.

Easton,R.M. and Johns,G.W. 1986. Volcanology and Mineral Exploration: The Application of Physical Volcanology and Facies Models. *In* Volcanology and Mineral Deposits. *Edited by* J.Wood and H.Wallace. OGS Misc. Paper 129, 183p.

Flower,M. 1989. Magmatic processes in oceanic ridge and intraplate settings. *In* Oceanic Basalts. *Edited* by P.A.Floyd. Blackie.

Fowler,A.D. and Jensen,L.S. 1989. Quantitative trace-element modelling of the crystallization history of the Kinojevis and Blake River groups, Abitibi Greenstone Belt, Ontario. Canadian Journal of Earth Science,**26**:1356-1367.

Fyson,W.K. and Helmstaedt,H. 1988. Structural patterns and tectonic evolution of supracrustal domains in the Archean Slave Province, Canada. Canadian Journal of Earth Science,**25**:310-315.

Gelinas,L., Mellinger,M. and Trudel,P. 1982. Archean mafic metavolcanics from the Rouyn-Noranda district, Abitibi Greenstone Belt, Quebec. 1. Mobility of the major elements. Canadian Journal of Earth Sciences,**19**:2258-2275.

Gelinas,L. and Ludden,J.N. 1984. Rhyolitic volcanism and the geochemical evolution of an Archean central ring complex: the Blake River Group volcanics of the southern Abitibi belt, Superior Province. Physics of the Earth and Planetary Interiors,**35**:77- 88.

Hargraves,R.B. 1986. Faster spreading or greater ridge length in the Archean? Geology,**14**:750-752.

Hewitt,D.J. 1951. Geology of Skead Township, Larder Lake area, Ontario Department of Mines, vol.58, pt.6, 43p.

Hodgson,C.J. and Hamilton,J.V. 1989. Gold mineralization in the Abitibi greenstone belt: End-stage result of Archean collisional tectonics?, *In* R.R. Keays, W.R.H. Ramsay and D.I. Groves, Eds., The geology of gold deposits: The perspective in 1988: Economic Geology Monograph 6,p.80-100.

Hoffman,P.F. 1988. United Plates of America, the Birth of a Craton. Annual Review of Earth and Planetary Sciences,**16**:543-601.

Hubert,C., Gelinas,L. and Trudel,P. 1984. Archean wrench fault tectonics and volcanism related to a central ring complex in the Blake River Group, Abitibi Belt, Quebec. Canadian Journal of Earth Sciences,**22**:240-255.

Humphris,S.E. and Thompson,G. 1978a. Hydrothermal alteration of oceanic basalts by seawater. Geochimica et Cosmochimica Acta,**42**:107-125.

Humphris,S.E. and Thompson,G. 1978b. Trace element mobility during hydrothermal alteration of oceanic basalts. Geochimica et Cosmochimica Acta,**42**:127-136.

Jackson.S.L. and Harrap,R.M. 1989. Geology of Parts of Pacaud, Catharine and Southernmost Boston and McElroy Townships. Ontario Geological Survey Miscellaneous Paper **146**:125-131.

Jackson,S.L., Kimmerly,C.T., Wilkinson,L.P. and Xiangdong,J. 1990. Southern Abitibi Greenstone Belt: Structural and Stratigraphic Studies in the Larder Lake Area;*in* Summary of Field Work and Other Studies 1990, Ontario Geological Survey, Miscellaneous paper 151,78-85.

Jackson,S.L. and Sutcliffe,R.H. 1990. Central Superior Province geology: evidence for an allochthonous, ensimatic, southern Abitibi greenstone belt. Canadian Journal of Earth Science,**27**:582-589.

Jackson,S.L. and Fyon,J.A. 1991. The western Abitibi Subprovince in Ontario;*in* Geology of Ontario, Ontario Geological Survey, Special Volume 4,Part1,p.405-484.

Jackson,S.L. in press. The geology of Pacaud and Catharine Townships and portions of adjacent townships, District of Timiskaming, Ontario. Ontario Geological Survey, Open File Report.

Jensen,L.S. 1976. A new cation plot for classifying subalkalicvolcanic rocks, Ontario Division of Mines, Miscellaneous Paper 66, 22p.

Jensen,L.S. 1977. Kirkland Lake-Larder Lake Areas, District of Timiskaming; *in* Summary of Field Work. Ontario Geological Survey, Miscellaneous Paper **67:**98-101.

Jensen,L.S. 1979. Larder Lake synoptic mapping project, District of Cochrane and Timiskaming; in Summary of Field Work. Ontario Geological Survey, Miscellaneous Paper **90**:64-69.

Jensen,L.S. 1985a. Stratigraphy and petrogenesis of Archean metavolcanic sequences, southwestern Abitibi Subprovince, Ontario.*In* Evolution of Archean supracrustal sequences. *Edited by* L.D.Ayres, P.C.Thurston, K.D.Card and W.Weber. Geological Association of Canada, Special Paper 28, p.65-87.

Jensen,L.S. 1985b. Synoptic mapping in the Kirkland Lake-Larder Lake Areas, District of Timiskaming;*in* Summary of Field Work and Other Activities Ontario Geological Survey. Miscellaneous Paper,**126**:112-120.

Jensen,L.S. and Langford,F.F. 1985. Geology and Petrogenesis of the Archean Abitibi Belt in the Kirkland Lake Area, Ontario; Ontario Geological Survey, Miscellaneous Paper 123, 130p.

Jochum,K.P., Arndt,N.T. and Hofmann,A.W. 1991. Nb-Th-La in komatiites and basalts: constraints on komatiite petrogenesis and mantle evolution. Earth and Planetary Science Letters.**107**:272-289.

Jolly,W.T., 1978. Metamorphic history of the Archean Abitibi Belt: in Metamorphism in the Canadian Shield, Geological Survey of Canada, Paper 78-10, p.63-78.

Jolly,W.T., 1980. Development and Degradation of Archean Lavas, Abitibi Area, Canada, in Light of Major Element Geochemistry. Journal of Petrology,**21**:323-363.

Jolly,W.T. and Hallberg,J.A. 1990. Geochemistry of heterogeneous Archean volcanics from the Lenora-Laverton Region, Western Australia. Precambrian Research,**48**:75- 98.

Jolly,W.T., Dickin,A.P. and Wu,T.W. 1992. Geochemical stratigraphy of the Huronian continental volcanics at Thessalon, Ontario: contributions of two-stage crustal fusion. Contributions to Mineralogy and Petrology,**110**:411-428.

Lawson,A.C. 1885. On the geology of the Lake of the Woods region, with special reference to Keewatin (Huronian?) belt of the Archean rocks: Natural History Survey of Canada, Annual Report, vol.1, p.5cc-140cc.

Longerich,H.P., Jenner,G.A., Fryer,B.J. and Jackson,S.E. 1990. Inductively coupled plasma-mass spectrometric analysis of geological samples: A critical evaluation based on case studies. Chemical Geology,**83**:105-118.

Ludden,J.N., Gelinas,L. and Trudel,P. 1982. Archean metavolcanics from the Rouyn-Noranda district, Abitibi Greenstone Belt, Quebec. 2. Mobility of trace elements and petrogenetic constraints. Canadian Journal of Earth Sciences,**19**:2276-2287.

Ludden,J., Hubert,C. and Gariepy,C. 1986. The tectonic evolution of the Abitibi greenstone belt of Canada. Geological Magazine, **123**:153-166.

MacRea,N.D. 1969. Ultramafic intrusion of the Abitibi Area, Ontario. Canadian Journal of Earth Sciences, **6**:281-303.

Mandziuk,Z.L. 1980. Geology of McFadden and Rattray Townships, District of Timiskaming; Ontario Geological Survey Report 204, 49p.

Menzies,M., Seyfried,W. and Blanchard,D. 1979. Experimental evidence of rare earth element immobility in greenstones. Nature,**282**:398-399.

MERQ-OGS 1983. Lithostratigraphic map of the Abitibi Subprovince; Ontario Geological Survey/Ministere de l'Energie et des Resources, Quebec; 1:500 000: catalogued as "Map 2484" in Ontario and "DV 83-16" in Quebec.

Miller,W.G. 1902. Lake Timiskaming to the height of land: Ontario Bureau of Mines Report, vol.11, p.214-230.

Mullen,D. 1983. $MnO/TiO_2/P_2O_5$: a minor element discriminant for basaltic rocks of oceanic environments and its implications for petrogenesis. Earth and Planetary Science Letters,**62**:53-62.

Murphy,J.B. and Hynes,A.J. 1986. Contrasting secondary mobility of Ti, P, Zr, Nb and Y in two metabasaltic suites in the Appalachians. Canadian Journal of Earth Science,**23**:1138-1144.

Miyashiro,A. 1974. Volcanic rock series in island arcs and active continental margins. American Journal of Science,**274**:321-355.

Nelson,D.R., Trendall,A.F., de Laeter,J.R., Grobler,N.J. and Fletcher,I.R. 1992. A comparative study of the geochemical and isotopic systematics of late Archean flood basalts from the Pilbara and Kaapvaal Cratons. Precambrian Research,**54**:231-256.

Nisbet,E.G. and Fowler,C.M.R. 1983. Model for Archean plate tectonics. Geology.**11**:376-379.

Nystrom,J.O. 1984. Rare earth element mobility in vesicular lava during low-grade metamorphism. Contributions to Mineralogy and Petrology,**88**:328-331.

Parks,W.A. 1904. The geology of a district from Lake Timiskaming northward, Geological Survey of Canada, Summary Report for 1904,p.198-225.

Pearce,J.A. and Cann,J.R. 1973. Tectonic setting of basic volcanic rocks determined using trace element analyses. Earth and Planetary Science Letters.**19:**290-300.

Pearce,J.A. and Norry,M.J. 1979. Petrogenetic implications of Ti, Zr, Y and Nb variations in volcanic rocks. Contributions to Mineralogy and Petrology,**69:**33-47.

Pearce,J.A. 1983. Role of the sub-continental lithosphere in magma genesis at active continental margins. *In* Continental basalts and mantle xenoliths. *Edited by* C.J. Hawkesworth and M.J. Norry. Shiva Publishing Limited,p.230-249.

Saunders,A. and Tarney,J. 1989. Back-arc basins. *In* Oceanic basalts. *Edited by* P.A. Floyd. Blackie.

Shervais,J.W. 1982. Ti-V plots and the petrogenesis of modern and ophiolitic lavas. Earth and Planetary Science Letters,**59**:101-118.

Smith,I.E.M. 1980. Geochemical evolution in the Blake River Group, Abitibi Greenstone Belt, Superior Province. Canadian Journal of Earth Sciences,**17**:1292-1299.

Stern,R.J., Lin,P.N., Morris,J.D., Jackson,M.C., Fryer,P, Bloomer,S.H. and Ito,E. 1990. Enriched back-arc basin basalts from the northern Mariana Trough: implications for the magmatic evolution of back-arc basins. Earth and Planetary Science Letters,**100:**210-225.

Sun,S.S. 1982. Chemical composition and origin of the earth's primitive mantle. Geochemica et Cosmochimica.**46:**179-192.

Sun,S.S., Nesbitt,R.W. and Sharanskin,A.Y. 1978. Chemical characteristics of mid-ocean ridge basalts. Earth and Planetary Science Letters.**44:**1120-1134.

Sun,S.S. and McDonough,W.F. 1989. Chemical and isotopic systematics of oceanic basalts: implications for mantle processes. *In* Magmatism in the Ocean Basins. *Edited by* A.D. Saunders and M.J. Norry. Blackwell, Oxford, p.313-345.

Sutcliffe,R.H., Smith,A.R. and Edgar,A.D. 1991. Stratigraphy and petrology of the lower part of the Mulcahy Gabbro, northwestern Ontario: origin of reverse and normal fractionation trends and implications for tectonic setting of late Archean mafic magmatism. Canadian Journal of Earth Sciences,**28**:1753-1768.

Sylvester,P.J., Attoh,K. and Schultz,K.J. 1987. Tectonic setting of late Archean bimodal volcanism in the Michipicoten (Wawa) greenstone belt, Ontario. Canadian Journal of Earth Science. **24:**1120-1134.

Taylor,S.R. and McLennan,S.M. 1985. The Continental Crust: Its Composition and

Evolution. Blackwell, Oxford. 312p.

Thomson,J.E. 1949. Geology of Hearst and McFadden Townships, Ontario Department of Mines, Annual Report for 1947, vol.56, pt.8, p.1-34.

Thurston,P.C. 1980. Economic evaluation of Archean felsic rocks using REE geochemistry. In Archean geology. Edited by J.E. Glover and D.I. Groves. Geological Society of Australia,pp.439-450.

Thurston,P.C. 1991. Geology of Ontario:Introduction;*in* Geology of Ontario,Ontario Geological Survey, Special Volume 4,Part1,p.3-26.

Thurston,P.C. and Fryer,B.J. 1983. The geochemistry of repetitive cyclical volcanism from basalt through rhyolite in the Uchi-Confederation greenstone belt, Canada. Contributions to Mineralogy and Petrology.**83:**204-226.

Ujike,O. and Goodwin,A.M. 1987. Geochemistry and origin of Archean felsic metavolcanic rocks, central Noranda area, Quebec, Canada. Canadian Journal of Earth Sciences,**24**:2551-2567.

Wilson,M.E. 1910. Larder Lake and eastward, Geological Survey of Canada, Summary Report for 1909,p.173-179.

Winchester,J.A. and Floyd,P.A. 1977. Geochemical discrimination of different magma series and their differentiation products using immobile elements. Chemical Geology,**20**:325-34

Windley,B.F. 1984. The evolving continents (second edition): London Wiley, 385p.

Appendix I: Petrographic descriptions and UTM coordinates for samples used in geochemical analysis.

SAMPLE #	ASSEMBLAGE	EASTING	NORTHING	DESCRIPTION
90CTK045	Larder Lake			aphanitic, aphyric pillowed flow; no fabric
90CTK052	McElroy	598434	5314498	m.g. massive ultramafic flow with relict cpx and ol; accessory serp,cal,act; weak fabric
90CTK068	McElroy	598196	5314482	m.g. dendritic flow with 30% act and 60% exsolved plag, accessory chl,epi,carb,opaq,sph; relict ophitic texture
90CTK072	McElroy	598252	5314970	f.g. polygonal flow with with 75% serp and 10% trem replacement, accessory chl,sph,opaq,act; weak fabric
90CTK082	McElroy	596658	5316041	m.g. massive flow with 50% act and 30% plag, accessory epi,chl,sph,carb; rare act blastophenocrysts; no fabric
90CTK087	McElroy	596286	5315761	m.g. massive flow with serp and trem replacement; relict cpx mantled by serp, accessory epi,sph,chl,carb,opaq; no fabric
90CTK096	McElroy	597267	5315109	m.g. dendritic flow with 50% plag and 30% act, accessory opaq,epi,carb,sph,bio,chl,qtz; rare epi filled veins (3mm) wide
90CTK131	Larder Lake	597182	5319859	f.g. massive flow; 30% act and 60% epidotized plag, accessory chl,carb,qtz; no fabric
90CTK154	Larder Lake	597920	5326858	aph pillowed flow; secondary epi, carb,qtz,act; no fabric
90CTK155	Larder Lake	598430	5326505	f.g. massive flow; 50% act and 30% epidotized plag; accessory chl,carb,qtz,opaq; f.g. qtz filled veinlets
90CTK197	McElroy	598345	5315490	m.g. flow; 60% act,20% plag, accessory chl,sph,epi,opaq; blastoporphyritic act; no fabric
90CTK201	McElroy	598778	5315034	aph flow; 50% act,30% epi plag, accessory qtz,sph,carb; no fabric
90CTK209	McElroy	598391	5314591	m.g. leucogabbro; 60% plag, 15% cpx-chl, accessory epi,sph,opaq; relict ophitic texture; no fabric

90CTK210	McElroy	598487	5314651	m.g. dendritic flow; 30% plag, 40% bladed act, 15% chl, accessory epi, sph, opaq,qtz; no fabric
90CTK219	McElroy	599138	5314423	aph pillowed flow; 50% act,30% epi plag, 15% chl, accessory qtz,opaq,sph,carb; <1% amygdules qtz,chl,epi,carb filled; no fabric
90CTK245	McElroy	598127	5315354	aph pillowed flow; consists of act,chl,epi,qtz,carb; no fabric
90CTK263	Larder Lake	596224	5325890	f.g. massive flow; contains act,epi,chl,carb,qtz; strong fabric
90CTK272	Larder Lake	596719	5325151	f.g. massive flow; contains act,epi,chl, accessory opaq,qtz,carb; weak fabric
90CTK283	McElroy	587765	5319858	aph massive flow; 40% act,15% chl, 30% epi plag, accessory qtz,opaq,sph; minor microveins; no fabric
90CTK287	McElroy	588002	5319412	m.g. dendritic flow; 40% act, 40% epi plag, accessory sph,carb,qtz,chl; large bladed crystals bend
90CTK290	McElroy	587578	5319683	m.g. massive flow; 50% act, 40% epi, accessory chl,qtz,plag,sph; no fabric
90CTK294	McElroy	586639	5319884	m.g. massive flow; 30% act, 50% epi, accessory qtz,chl,plag,opaq, sph; no fabric
90CTK294D	McElroy	586639	5319884	same as above
90CTK307	McElroy	586926	5320356	f.g. massive flow; 50% act, 40% epi, accessory opaq,plag; minor veining; no fabric
90CTK309	McElroy	598285	5315715	m.g. massive flow; 30% act, 40% plag, accessory epi,opaq; blasto-ophitic texture weakly preserved
90CTK310	McElroy	585786	5321001	m.g. massive flow; 40% act, 50% epi, accessory opaq,plag,carb,qtz; ophitic texture preserved; no fabric
90CTK322	Larder Lake	603541	5324641	aph massive flow; 40% act, 50% epi, accessory opaq,chl,qtz,chl; no fabric
90CTK327	McElroy	594885	5316538	m.g. dendritic flow; 40% act, 50% epi, accessory plag,chl,sph,qtz; bladed dendrites; minor microveins; fo fabric

90CTK335	McElroy	587472	5319482	aph massive flow; 25% act, 35% epi, 20% chl, accessory qtz,carb,opaq,sph; minor microveining; no fabric
91LL01	Larder Lake	603100	5323815	f.g. to m.g. massive flow;30-40% act.; f.g. epidotized plag; minor qtz and epi microveins
91LL20	Larder Lake			aph. pillowed flow with swallow tail act. after cpx; minor plag, qtz, chl, epi
91LL20D	Larder Lake			
91LL33-2	Larder Lake	603305	5324375	f.g. to m.g. massive flow; 60% act.,30% epid plag; act 2x grain size than plag
91LL49	Larder Lake	603775	5324395	aph pillowed flow; felsic metavolcanic on Mandzuik map; actually mafic metavolcanic

Appendix II: Kinojevis assemblage geochemistry locations.

Sample #	Easting	Northing
KJ-1	597435	5332045
KJ-2	596500	5332000
KJ-3	595870	5331975
KJ-4	599015	5333535
KJ-5	598420	5333870
KJ-6	585215	5347475
KJ-7	585770	5340860
KJ-8	585765	5340845
KJ-9	584390	5348545
KJ-10	584390	5348520
KJ-11	584700	5348210
KJ-12	570720	5341875
KJ-13	570260	5341315
KJ-14	570240	5341315
KJ-15	569715	5340380
KJ-16	569675	5340410
KJ-17	593160	5336010
KJ-18	595415	5336510
KJ-19	559075	5348225
KJ-20	555720	5349620
KJ-21	555085	5341275
KJ-22	555540	5342525
KJ-23	555535	5342550
KJ-24	558390	5333920
KJ-25	606015	5336210
KJ-26	606020	5336240
KJ-27	605495	5337095
KJ-28	605550	5337080
KJ-29	602520	5336805
KJ-30	562250	5329340

Appendix III

Kinojevis assemblage

	Rock Description	SiO2	Al2O3	FeO(T)	MgO	CaO	Na2O	K2O	TiO2	P2O5	MnO	Total
KJ-1	apha. pill bas	46.88	19.67	9.83	10.14	12.78	0.77	0.02	0.56	0.04	0.14	100.84
KJ-2	aphan mass mafic volc	50.22	14.02	15.24	6.74	9.20	2.45	0.08	1.93	0.16	0.25	100.29
KJ-3	mafic to int pill volc	49.05	16.08	13.86	6.46	10.57	2.95	0.03	1.23	0.11	0.18	100.52
KJ-4	pill volc	53.17	13.65	15.55	5.28	7.50	3.02	0.28	1.72	0.18	0.26	100.62
KJ-4(D)	pill volc	52.70	13.59	15.52	5.22	7.52	3.02	0.27	1.73	0.17	0.26	100.00
KJ-6	aph pill volc	54.06	14.70	12.26	7.03	8.84	1.59	0.03	1.29	0.10	0.25	100.15
KJ-8	aph int volc	58.57	13.18	10.30	4.14	8.81	3.71	0.26	1.22	0.09	0.16	100.43
KJ-9	aph mass flow	51.68	14.03	15.51	6.06	8.46	2.02	0.15	1.89	0.17	0.20	100.18
KJ-10	f.f. mafic mass flow	52.05	13.14	16.51	5.22	7.71	3.32	0.15	1.93	0.17	0.20	100.41
KJ-11	aph pill flow	50.82	13.74	16.00	5.69	9.54	2.63	0.04	1.48	0.11	0.27	100.34
KJ-12	aph pill mafic flow	54.50	14.40	14.08	5.71	7.95	2.15	0.04	1.33	0.08	0.18	100.41
KJ-13	f.g. to m.g. mass flow	52.61	14.74	15.25	5.59	6.20	2.57	2.02	1.39	0.08	0.19	100.63
KJ-14	f.g. mafic mass flow	52.83	14.36	14.18	6.79	4.66	0.55	5.69	1.28	0.08	0.20	100.63
KJ-14(D)	f.g. mafic mass flow	52.19	14.22	14.13	6.68	4.56	0.55	5.61	1.25	0.08	0.20	99.48
KJ-15	aph to f.g. pill flow	49.96	13.74	15.70	6.25	9.06	3.38	0.18	1.81	0.24	0.26	100.58
KJ-16	aph pill flow	49.10	14.21	15.99	5.93	10.82	2.12	0.14	1.85	0.24	0.29	100.69
KJ-17	bladed mass flow (hb gabb)	53.59	14.26	11.66	7.13	8.62	2.74	0.77	1.26	0.09	0.16	100.30
KJ-18	aph mafic pill flow	49.73	13.58	15.88	5.11	9.77	4.21	0.20	1.96	0.18	0.21	100.84
KJ-19	f.g. to m.g. mass flow	52.60	15.59	11.54	7.75	8.83	2.89	0.52	0.82	0.05	0.16	100.74
KJ-20	aph to f.g. mass flow	52.97	14.60	12.87	6.33	7.93	3.38	0.92	1.40	0.10	0.18	100.69
KJ-20(D)	aph to f.g. mass flow	52.58	14.64	12.93	6.46	7.86	3.28	0.91	1.34	0.10	0.17	100.26
KJ-21	aph pill flow	49.30	15.26	11.54	8.25	12.33	1.89	0.70	0.94	0.05	0.17	100.43
KJ-22	plag phyric pill flow	51.58	14.94	10.91	7.04	12.15	2.19	0.35	0.76	0.04	0.19	100.15
KJ-23	aph pill flow	51.07	15.01	11.48	7.65	11.12	2.42	0.44	0.76	0.05	0.20	100.21
KJ-24	f.g. to m.g. mass flow	52.56	15.41	10.91	6.82	10.93	1.79	0.46	0.78	0.04	0.20	99.91
KJ-25	f.g mass mafic flow	57.98	15.14	17.36	6.33	0.30	0.13	1.19	1.78	0.15	0.06	100.40
KJ-26	aph pill flow	57.62	14.41	12.94	4.66	5.90	3.15	0.05	1.68	0.13	0.22	100.75
KJ-27	aph pill flow	54.16	13.75	13.29	5.42	8.28	3.17	0.24	1.61	0.14	0.24	100.30
KJ-27(D)	aph pill flow	53.80	13.70	13.38	5.51	8.31	3.13	0.25	1.60	0.13	0.24	100.04
KJ-28	aph pill flow	54.75	13.74	12.60	5.25	8.20	2.95	0.57	1.59	0.13	0.22	100.01
KJ-30	aph mafic to int pill flow	51.72	14.80	11.10	8.80	10.26	2.47	0.06	0.75	0.04	0.21	100.20
	average	52.47	14.53	13.56	6.37	8.55	2.47	0.73	1.38	0.11	0.20	100.37
	maximum	58.57	19.67	17.36	10.14	12.78	4.21	5.69	1.96	0.24	0.29	130.92
	minimum	46.88	13.14	9.83	4.14	0.30	0.13	0.02	0.56	0.04	0.06	75.09
	standard deviation	2.56	1.17	2.03	1.23	2.47	0.95	1.36	0.40	0.06	0.05	12.28

	Cu	Ni	Sc	V	Zn	Rb	Sr	Y	Zr
KJ-2	122	42	34	543	103	2	107	33	101
KJ-3	94	119	29	288	87	0	223	12	56
KJ-4	88	46	44	431	141	4	725	41	122
KJ-4(D)	87	47	38	433	134	4	742	42	122
KJ-6	113	105	41	369	98	0	145	34	88
KJ-8	125	40	38	377	72	3	315	44	110
KJ-9	93	47	37	399	110	2	105	36	95
KJ-10	158	45	39	422	99	1	79	41	108
KJ-11	113	61	45	415	125	1	104	33	85
KJ-12	116	34	38	453	101	1	154	29	76
KJ-13	89	30	44	498	101	31	135	29	74
KJ-14	90	30	46	439	106	83	137	27	72
KJ-14(D)	95	30	40	441	108	83	135	27	71
KJ-15	132	81	45	412	110	4	178	20	69
KJ-16	124	84	49	428	107	3	141	21	70
KJ-17	163	95	45	401	42	39	106	32	87
KJ-18	74	84	40	429	97	4	199	26	66
KJ-19	109	88	33	287	84	14	108	25	62
KJ-20	54	73	43	419	87	60	118	28	87
KJ-20(D)	61	75	49	421	94	60	116	27	83
KJ-21	111	129	45	343	64	28	163	18	44
KJ-22	110	100	40	279	61	9	82	24	60
KJ-23	114	106	42	293	71	15	105	24	58
KJ-24	107	98	38	290	68	13	135	21	57
KJ-25	76	27	64	629	159	37	10	22	122
KJ-26	120	37	40	479	116	0	153	42	118
KJ-27	131	40	46	460	105	7	101	41	115
KJ-27(D)	128	36	39	452	115	7	101	41	116
KJ-28	122	36	44	458	93	15	107	40	116
KJ-30	110	101	37	283	71	1	88	22	52
average	107.68	65.55	41.74	409.04	97.59	17.73	170.54	30.07	85.51
maximum	163.28	129.28	63.73	629.12	159.15	83.20	741.83	43.92	122.49
minimum	53.88	27.11	28.78	279.16	42.35	0.11	9.92	12.46	44.30
standard deviation	24.29	30.73	6.07	79.40	24.50	24.00	158.99	8.38	23.99